



**Victorian Coastline
Longshore Sediment
Transport Modelling**
Victorian Coastal Monitoring Program



Energy,
Environment
and Climate Action

OFFICIAL

Acknowledgements

We would like to acknowledge the support of the Victorian Coastal Monitoring Program (VCMP) and related research organizations (the University of Melbourne and Deakin University) for the efforts of developing the wave models.

Author

Jin Liu, DEECA. Email: jin.liu@delwp.vic.gov.au

Jak McCarroll, DEECA. Email: jak.mccarroll@delwp.vic.gov.au

Acknowledgment

We acknowledge and respect Victorian Traditional Owners as the original custodians of Victoria's land and waters, their unique ability to care for Country and deep spiritual connection to it. We honour Elders past and present whose knowledge and wisdom has ensured the continuation of culture and traditional practices.

We are committed to genuinely partner, and meaningfully engage, with Victoria's Traditional Owners and Aboriginal communities to support the protection of Country, the maintenance of spiritual and cultural practices and their broader aspirations in the 21st century and beyond.



© The State of Victoria Department of Energy, Environment and Climate Action 2023



This work is licensed under a Creative Commons Attribution 4.0 International licence. You are free to re-use the work under that licence, on the condition that you credit the State of Victoria as author. The licence does not apply to any images, photographs or branding, including the Victorian Coat of Arms, the Victorian Government logo and the Department of Energy, Environment and Climate Change (DEECA) logo. To view a copy of this licence, visit <http://creativecommons.org/licenses/by/4.0/>

ISBN 978-1-76136-413-6 (pdf/online/MS word)

Disclaimer

This publication may be of assistance to you but the State of Victoria and its employees do not guarantee that the publication is without flaw of any kind or is wholly appropriate for your particular purposes and therefore disclaims all liability for any error, loss or other consequence which may arise from you relying on any information in this publication.

Accessibility

If you would like to receive this publication in an alternative format, please telephone the DEECA Customer Service Centre on 136186, email customer.service@delwp.vic.gov.au or via the National Relay Service on 133 677 www.relayservice.com.au. This document is also available on the internet at www.delwp.vic.gov.au.

Contents

Executive summary	4
1 Data and methods	5
1.1 Models	5
1.1.1 Model 1: WAVEWATCH III (Liu et al., 2022a; Liu et al., 2023a)	5
1.1.2 Model 2: SCHISM-WWMIII (Tran et al., 2021)	5
1.2 Longshore sediment transport methods	6
1.2.1 Wave transformation to breakpoint	6
1.2.2 CERC formula	7
1.2.3 Van Rijn (2014) formula	7
1.3 Site descriptions	7
2 Longshore sediment transport at selected locations	9
2.1 Apollo Bay (APO) – WW3	9
2.2 Patterson River (PAT) – SCHISM-WWMIII	12
3 Longshore sediment transport at VCMP sites	16
3.1 Seaspray (SEA)	22
3.1.1 Model 1 – WW3	22
3.2 Inverloch (INV)	23
3.2.1 Model 1 – WW3	23
3.3 Cowes (COW)	24
3.3.1 Model 1 – WW3	24
3.4 Blairgowrie (BLR)	25
3.4.1 Model 1 – WW3	25
3.4.2 Model 2 – SCHISM-WWMIII	26
3.5 Dromana-McCrae (DRM)	27
3.5.1 Model 1 – WW3	27
3.5.2 Model 2 – SCHISM-WWMIII	28
3.6 Mount Martha (MAR)	29
3.6.1 Model 1 – WW3	29
3.6.2 Model 2 – SCHISM-WWMIII	30
3.7 Frankston (FRA)	31
3.7.1 Model 1 – WW3	31
3.7.2 Model 2 – SCHISM-WWMIII	32
3.8 Patterson River (PAT)	33
3.8.1 Model 1 – WW3	33
3.8.2 Model 2 – SCHISM-WWMIII	34
3.9 Sandringham (SND)	35
3.9.1 Model 1 – WW3	35
3.9.2 Model 2 – SCHISM-WWMIII	36

3.10 Altona (ALT)	37
3.10.1 Model 1 – WW3	37
3.10.2 Model 2 – SCHISM-WWMIII	38
3.11 WTP (WTP)	39
3.12 Portarlington (PAR)	40
3.12.1 Model 1 – WW3	40
3.12.2 Model 2 – SCHISM-WWMIII	41
3.13 Anderson Reserve (AND)	42
3.13.1 Model 1 – WW3	42
3.13.2 Model 2 – SCHISM-WWMIII	43
3.14 St Leonards (LEO)	44
3.14.1 Model 1 – WW3	44
3.14.2 Model 2 – SCHISM-WWMIII	45
3.15 Queenscliff (QCL)	46
3.15.1 Model 1 – WW3	46
3.15.2 Model 2 – SCHISM-WWMIII	47
3.16 Point Lonsdale (LON)	48
3.16.1 Model 1 – WW3	48
3.16.2 Model 2 – SCHISM-WWMIII	49
3.17 Ocean Grove (OGR)	50
3.17.1 Model 1 – WW3	50
3.18 Torquay (TRQ)	51
3.18.1 Model 1 – WW3	51
3.19 Jan Juc (JJU)	52
3.19.1 Model 1 – WW3	52
3.20 Demons Bluff (DMN)	53
3.20.1 Model 1 – WW3	53
3.21 Point Roadknight (RDK)	54
3.21.1 Model 1 – WW3	54
3.22 Eastern View (EVV)	55
3.22.1 Model 1 – WW3	55
3.23 Wye River (WYE)	56
3.23.1 Model 1 – WW3	56
3.24 Kennett River (KEN)	57
3.24.1 Model 1 – WW3	57
3.25 Skenes Creek (SKE)	58
3.25.1 Model 1 – WW3	58
3.26 Apollo Bay (APO)	59
3.26.1 Model 1 – WW3	59
3.27 Marengo (MGO)	60
3.27.1 Model 1 – WW3	60

2 Victorian Coastline Longshore Sediment Transport Modelling

3.28 Warrnambool (WAR)	61
3.28.1 Model 1 – WW3.....	61
3.29 Killarney (KIL)	62
3.29.1 Model 1 – WW3.....	62
3.30 Port Fairy (PTF).....	63
3.30.1 Model 1 – WW3.....	63
3.31 Portland (PLA).....	64
3.31.1 Model 1 – WW3.....	64
3.32 Point Impossible (IMP)	65
3.32.1 Model 1 – WW3.....	65
3.33 Lorne (LRN).....	66
3.33.1 Model 1 – WW3.....	66
3.34 Bells Beach (LRN)	67
3.35 Point Addis (ADD).....	67
3.36 Walkerville (WLK)	68
3.36.1 Model 1 – WW3.....	68
3.37 Flinders (FLI).....	69
3.37.1 Model 1 – WW3.....	69
3.38 Portsea (PSE).....	70
3.38.1 Model 1 – WW3.....	70
3.38.2 Model 2 – SCHISM-WWMIII.....	71
3.39 Rye (RYE)	72
3.39.1 Model 1 – WW3.....	72
3.39.2 Model 2 – SCHISM-WWMIII.....	73
3.40 Mount Eliza (ELZ).....	74
3.40.1 Model 1 – WW3.....	74
3.40.2 Model 2 – SCHISM-WWMIII.....	75
4 Longshore sediment transport across the Victorian coast	76
4.1 Model 1 - WW3 (full Victoria extent).....	76
4.2 Model 2 - SCHISM-WWMIII (full Port Phillip Bay extent).....	77
5 Data outputs, variables and access to data	78
6 Conclusions	80
References	81

Executive summary

Recently, high-resolution wave models were developed to investigate the wave climate of Victorian coastal waters and Port Phillip Bay. Longshore sediment transport, an important input of coastal facilities, is still unknown in this region. This study aims to fill the knowledge gap by developing longshore sediment transport based on long-term wave hindcast. This dataset covers all Victorian Coastal Monitoring Program (VCMP) sites and the whole Victorian coast. The datasets are generated by following the below steps (Figure E1),

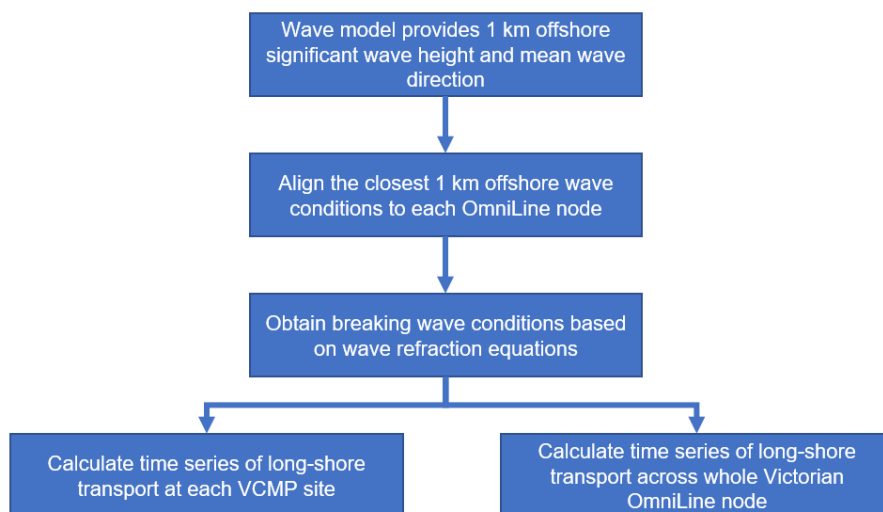


Figure E1: Flow chart of the present study.

The results indicate the powerful long-period Southern Ocean swell propagating towards western Victoria and Great Ocean Road. Significant wave height and longshore sediment transport in these regions show large amplitudes. The semi-closed Port Phillip Bay shows the least longshore sediment transport due to its closure. Eastern Port Phillip Bay also marks apparent beach rotation.

The following variables and data are available via the Victorian Coastal Data portal (<https://viccoastdata.quatrix.it/>). Please feel free to contact vcmp@delwp.vic.gov.au for access.

	1 km offshore and breaking wave conditions and longshore sediment transport	
Wave model	Hourly data	Annual mean and seasonal values
WW3	All VCMP sites	Victorian coast
SCHISM-WWMIII	VCMP sites of Port Phillip Bay	Port Phillip Bay coast

1 Data and methods

1.1 Models

High-resolution wave hindcasts of Victorian coastal regions are available from two regional ocean wave models: the WAVEWATCH III (WW3) model of Liu et al. (2022a) and the SCHISM-WWMIII model of Tran et al. (2021). The model outputs are extracted at nodes located 1 km offshore and include significant wave height (H_s), peak wave period (T_p), mean wave direction (Dir) and peak wave direction (D_p). The wave variables are transformed to the breaking point and are then used to estimate potential longshore sediment transport (LST) rates (Section 1.2).

In this study, we estimate longshore sediment transport rates for different sections of the VIC coast for each of the two regional models:

- Model 1 – WW3 (Liu et al., 2022a; Liu et al., 2023a) applied to the full Victorian coastline, including the open coast and Port Phillip Bay.
- Model 2 – SCHISM-WWMIII (Tran et al., 2021) applied to Port Phillip Bay and nearby areas of the open coast.

1.1.1 Model 1: WAVEWATCH III (Liu et al., 2022a; Liu et al., 2023a)

The WW3 hindcast model of south-east Australia is a third-generation wave model developed by the University of Melbourne, which solves the random phase spectral action balance equation. The wave physics of WW3 includes ST6 source term package (wind input, white-cap dissipation, swell dissipation and negative wind input), nonlinear quadruplet wave-wave interactions, JONSWAP bottom friction and depth-induced wave breaking. A high-resolution unstructured grid was adopted (Figure 1.1), which has been successfully employed by three wave models of south-east Australia (Liu et al., 2022a; Liu et al., 2022b; Liu et al., 2023a; Liu et al., 2023b). The WW3 model was driven by ERA5 reanalysis winds and the boundary conditions were provided by the global wave hindcast of Liu et al. (2021). The model covers the period from 1981 to 2020. 10 integrated wave parameters of the domain were generated. Please read Liu et al. (2022a) and Liu et al. (2023a) for details.

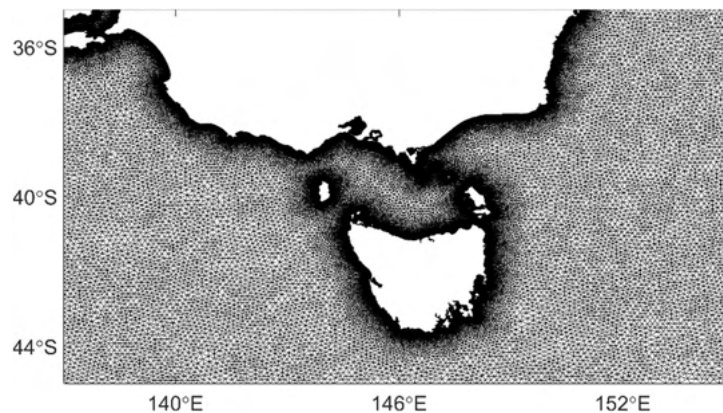


Figure 1.1: WW3 grid.

1.1.2 Model 2: SCHISM-WWMIII (Tran et al., 2021)

The SCHISM-WWMIII is a coupled circulation-wave system, which was implemented in Port Phillip Bay (Figure 1.2). The SCHISM model solves current advection in the momentum terms using semi-implicit schemes. The open boundary conditions of the SCHISM model were from 10 tidal constituents that used the latest global finite element solution tide model (FES2014). CFSR winds and HYCOM non-tidal signals were used to drive the SCHISM model. The WWMIII model is a third-generation phase-average wave model that solves the wave action balance equation. The open boundary conditions were from the IFREMER WW3 hindcast. Both the SCHISM and WWMIII models adopted an unstructured grid, which has 54,432 nodes and 103,543 elements. The grid resolution is up to 20 m at the coastal regions and ~3 km in the center of Port Phillip Bay.

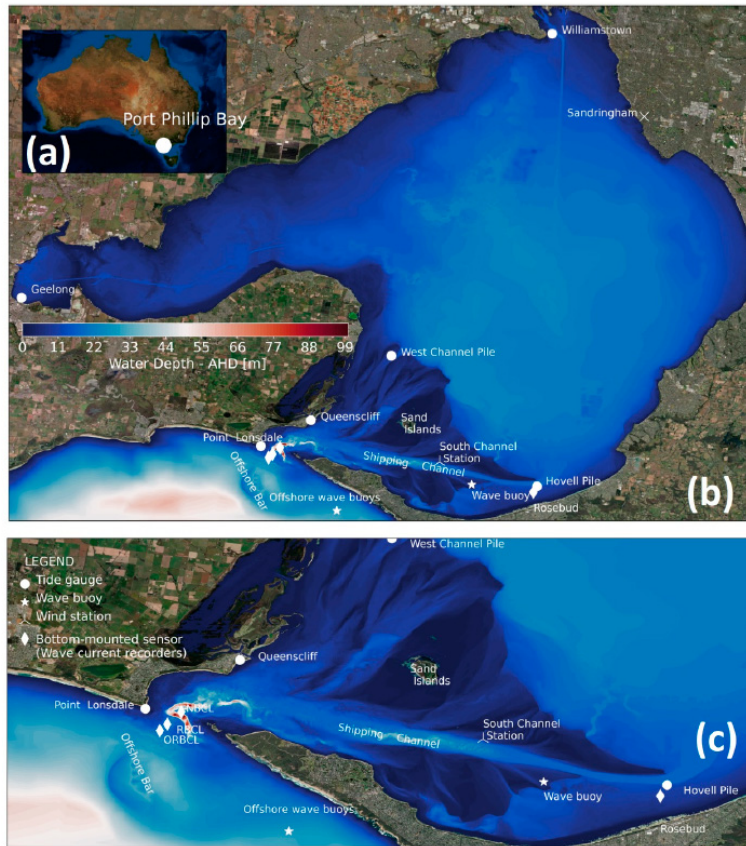


Figure 1.2: SCHISM-WWMIll domain.

1.2 Longshore sediment transport methods

The workflow for the longshore sediment transport model is:

Step 1 - wave transformation: convert regional wave model outputs to the breakpoint based on Van Rijn (2014) approach (Section 1.2.1).

Step 2 – calculate potential longshore sediment transport: CERC formula (Section 1.2.2) and Van Rijn (2014) longshore sediment transport formula (Section 1.2.3).

1.2.1 Wave transformation to breakpoint

The wave parameters at the breaker line can be estimated by Van Rijn (2014) as,

$$H_{s,br} = \gamma h_{br}, \quad (1.1)$$

$$\sin\theta_{br} = (c_{br}/c_o)\sin\theta_o, \quad (1.2)$$

$$h_{br} = [(H_{s,o}^2 c_o \cos\theta_o)/(\alpha\gamma^2 g^{0.5})]^{0.4}, \quad (1.3)$$

where $\gamma = 0.6$ is a constant (0.6-0.8), $H_{s,br}$, h_{br} and c_{br} are significant wave height, wave depth and phase speed at breaker line, $H_{s,o}$, c_o and θ_o are significant wave height, phase speed, and wave incidence angle at 1 km offshore regions, respectively, $\alpha = 1.8$ is the calibration coefficient, and $g = 9.81 \text{ m/s}^2$ is the acceleration of gravity.

1.2.2 CERC formula

The most commonly used equation to quantify longshore transport is the CERC formula (Shore Protection Manual, 1984; Bayram et al., 2007), which assumes the rate of total longshore sediment transport is proportional to the wave energy flux.

$$Q_{LST} = \frac{\rho K \sqrt{g/\gamma_b}}{16(\rho_s - \rho)(1-a)} \rho g^{3/2} H_{s,br}^{5/2} \sin(2\theta_{br}) \cdot \quad (1.4)$$

Where Q_{LST} is longshore sediment transport rate (m^3/s), $\rho=1025 \text{ kg/m}^3$ is water density, $K=0.39$ is an empirical coefficient (Shore Protection Manual, 1984; Bayram et al., 2007), $g=9.81 \text{ m/s}^2$ is acceleration of gravity, $\gamma_b=0.78$ is breaker index (Smith et al., 2009; Bosboom & Stive, 2021), $\rho_s=2650 \text{ kg/m}^3$ is sediment density, $a=0.4$ is porosity index (Bayram et al., 2007), $H_{s,br}$ is significant wave height at the breaker line, θ is wave incidence angle at the breaker line.

1.2.3 Van Rijn (2014) formula

One of the more sophisticated and advanced representations of longshore sediment transport ($Q_{t, \text{mass}}$, kg/s) is the following equation (Van Rijn, 2014),

$$Q_{t, \text{mass}} = 0.00018 K_{\text{swell}} \rho_s g^{0.5} (\tan \beta)^{0.4} (d_{50})^{-0.6} (H_{s,br})^{3.1} \sin(2\theta_{br}), \quad (1.5)$$

where $K_{\text{swell}}=1$ (default) is the swell factor, $\rho_s=2,650 \text{ kg/m}^3$ is sediment density, $g=9.81 \text{ m/s}^2$ is acceleration of gravity, $\tan \beta=0.02$ is surface zone slope, $d_{50}=0.0005 \text{ m}$ is sediment size, $H_{s,br}$ and θ_{br} are significant wave height and wave incidence angle at the breaker line.

1.3 Site descriptions

We have selected 39 VCMP sites (Figure 1.3) to conduct detailed longshore sediment transport analysis as these sites match up with the locations of drone surveys. The VCMP sites mainly cover Port Phillip Bay, Great Ocean Road and western and eastern Victoria. Furthermore, longshore sediment transports across the whole Victorian coast have been estimated as an extension.



Figure 1.3: VCMP sites.

2 Longshore sediment transport at selected locations

2.1 Apollo Bay (APO) – WW3

The WW3 model (Liu et al., 2022a) output included 10 wave parameters. In this study, we estimated the longshore sediment transport based on the Hs and Dir. We have aligned the 1 km offshore Hs (Figure 2.1) and mean wave direction to each node of the OmniLine. However, the WW3 model has a resolution of ~400-900 m in the nearshore regions of south-east Australia, which is lower than the resolution of the OmniLine (~50 m). Therefore, wave parameters at some OmniLine nodes have an identical value (Figure 2.1). The offshore wave conditions indicate energetic ocean waves around the northern part of Apollo Bay (Figure 2.1), which mainly originated from the Southern Ocean swell. In the middle of Apollo Bay OmniLine, however, it is protected by the cape in the south, which largely reduces the amplitude of offshore Hs.

The shoreline direction at each OmniLine node can be obtained from two neighboring OmniLine nodes. The wave incidence angle is the difference between the mean wave direction from the model and the shoreline normal. At each OmniLine node, we have offshore Hs and wave incidence angle which can be used to calculate Hs and wave incidence angle at the breaker line based on equations (1.1)-(1.3). The wave conditions at the breaker line show similar patterns as the offshore wave conditions, the major differences are the dramatically reduced Hs amplitude around the cape and middle part of Apollo Bay.

The longshore sediment transports (Figure 2.1) at each OmniLine node can be determined by equation (1.5). Figure 2.2 shows the time series of the involved wave parameters at a selected OmniLine node (the middle point of the OmniLine of Apollo Bay) over the period 1981-2020, which include Hs, mean wave direction, wave incidence angle, longshore sediment transport and cumulative longshore sediment transport. Figure 2.3 is the zoom-in results of 2015-2016, which is more visible compared with Figure 2.2. The longshore sediment transport results at the selected OmniLine node indicate northeastward transports (negative values) for most of the time over the period 1981-2020. The occurrence of southwestward movement, however, is relatively minor. The cumulative longshore sediment transport further verifies this point, which shows the decreasing trend over the 1981-2020 and 2015-2016 periods.

The estimated annual mean and seasonal longshore sediment transports across Apollo Bay are shown in Figure 2.1. The results indicate that Apollo Bay is a non-balanced system, which shows northeastward transport in the northern parts of Apollo Bay and Mounts Bay over the last 40 years (1981-2020). Longshore sediment transport of central Apollo Bay, however, marks a small number of transports. Another feature of the longshore sediment transport of Apollo Bay is that it shows a small seasonal amplitude (Figure 2.1) due to its identical mean wave direction (Figure 2.4) and unchanging Hs (Figure 2.1). It is worth noting that this is an empirical estimation based on wave model results, which is of large uncertainty. However, the estimated magnitudes of longshore sediment transport in this region are generally consistent with BMT (2022).

The major difference between the present study and BMT (2022) or observations is that the present hasn't captured the beach rotation at Apollo Bay or the reversal of longshore sediment transport during the period 2020-2021. This could be associated with the identical seasonal mean wave direction (Figure 2.4) simulated by the WW3 model. The wave direction roses at selected OmniLine nodes of Apollo Bay show southwesterly-southerly waves for both winter (May-Oct) and summer (Nov-Apr) seasons. The two half-year seasons show very minor changes. The other possibilities are the different time coverage involved, e.g., 1981-2020 (present study), 2005-2019 and 2020-2021 (BMT, 2022), or the limitation of model resolution.

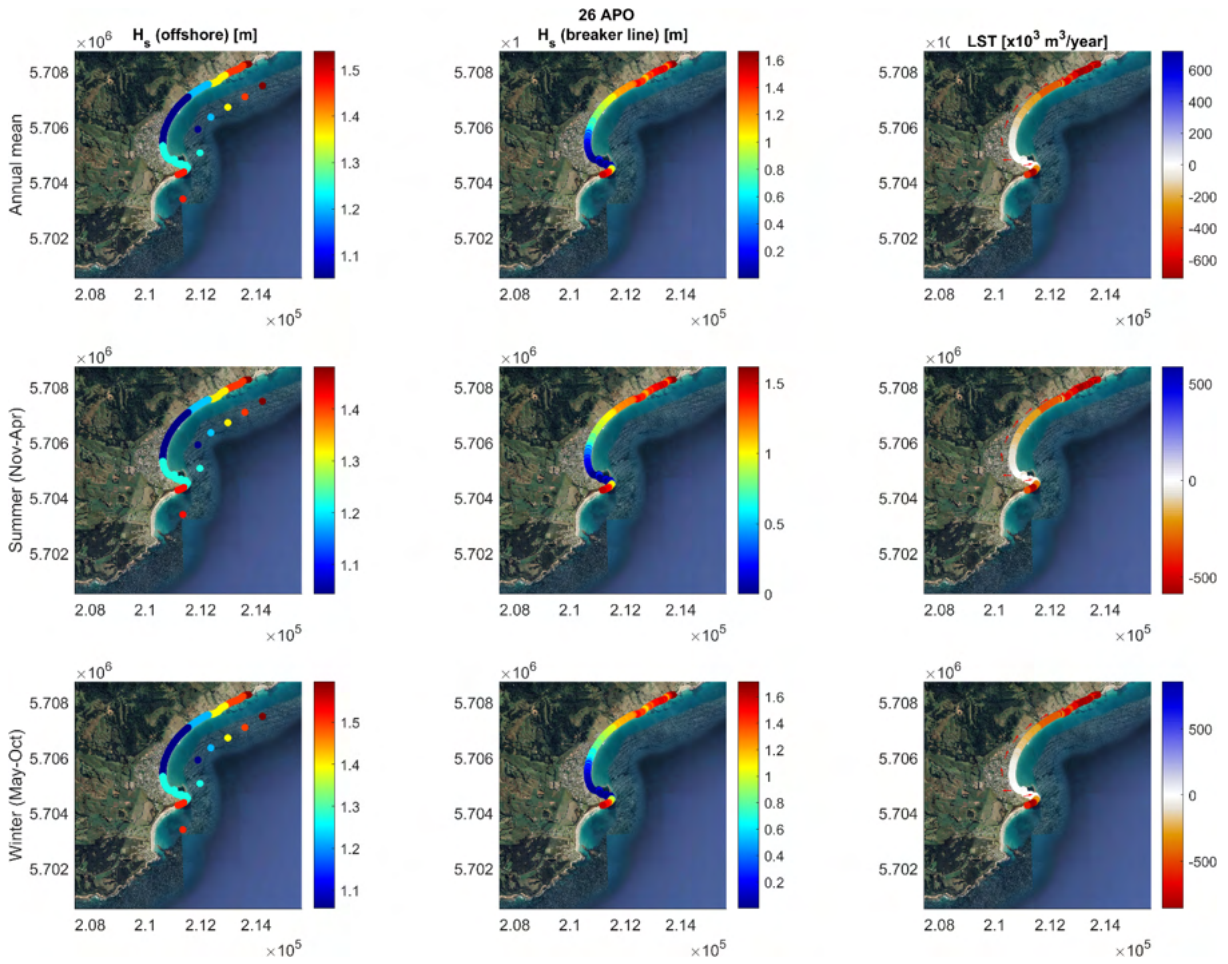


Figure 2.1: Annual mean and seasonal values of 1 km offshore H_s (left column) adopted from the closest WW3 model nodes (dots), the H_s at the breaker line (middle column) and longshore sediment transport (right column). The arrows mark the transport directions. H_s =significant wave height, LST=longshore sediment transport.

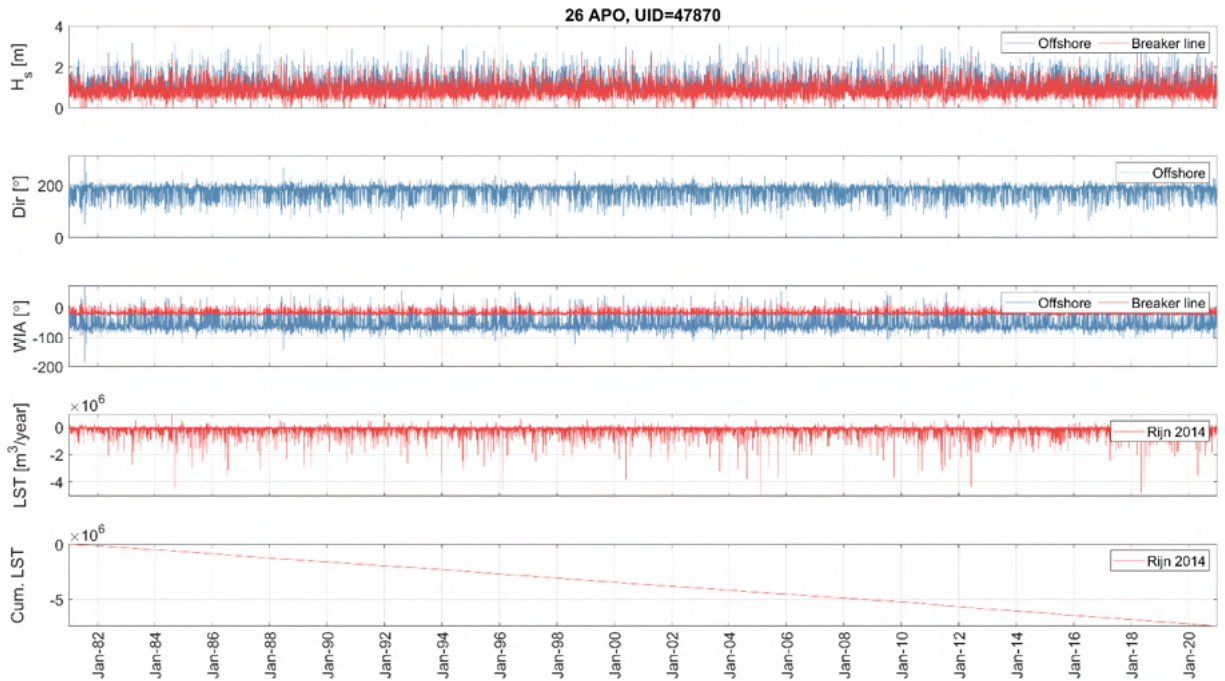


Figure 2.2: Time series at a selected OmniLine node (UID=47870) of Apollo Bay. H_s =significant wave height, Dir=mean wave direction, WIA=wave incidence angle, LST=longshore sediment transport, Cum. LST=cumulative longshore sediment transport.

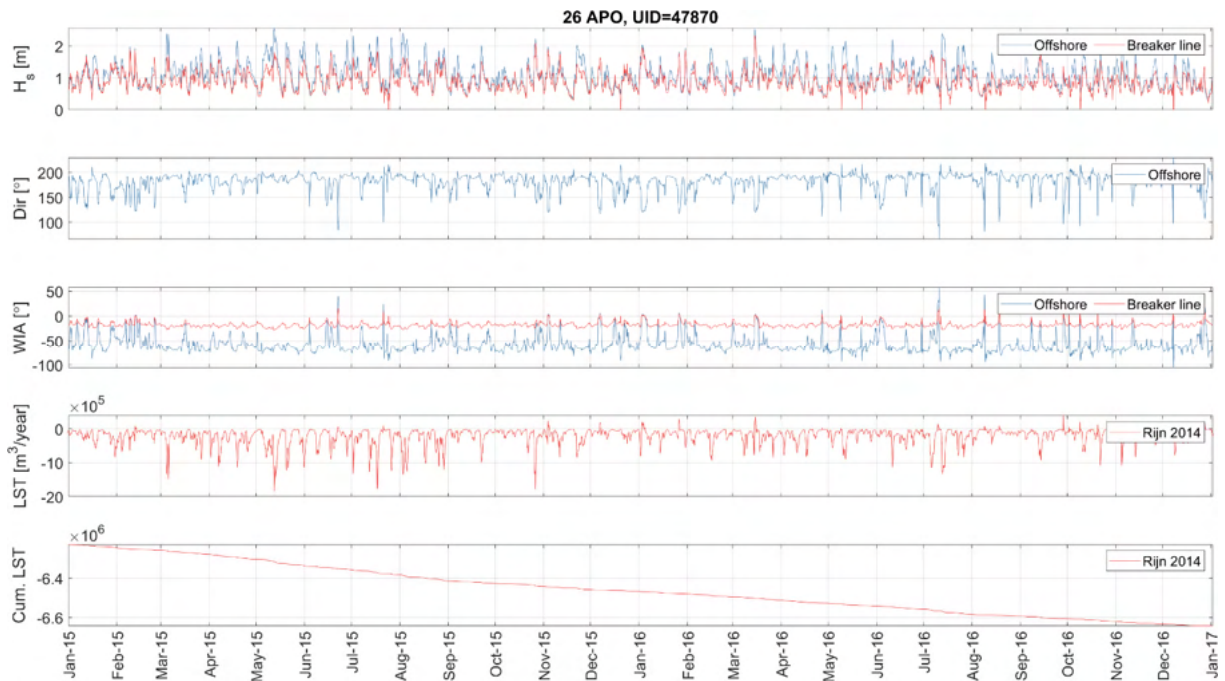


Figure 2.3: Same as Figure 2.2 but for 2015-2016.

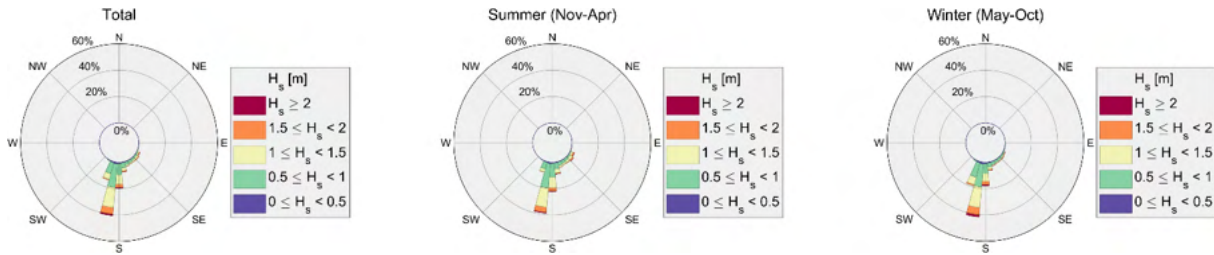


Figure 2.4: Wave roses at Apollo Bay.

2.2 Patterson River (PAT) – SCHISM-WWMIII

We also selected another VCMP site, Patterson River at eastern Port Phillip Bay, for detailed analysis. Figure 2.5 shows the wave conditions at 1 km offshore and the breaker line at Patterson River. Not surprisingly, the H_s of Patterson River is much lower than of Apollo Bay, since Apollo Bay directly opposes to the Southern Ocean, while Port Phillip Bay is well-protected. The H_s amplitudes of Patterson River are generally lower than 0.5 m, which also introduces the relatively small magnitude of longshore sediment transport. Characteristics of annual mean longshore sediment transport of Patterson River, however, show different patterns that are mostly northward transport (Figure 2.5). The seasonal values of longshore sediment transport mark apparent changes in Figure 2.7, which indicate northward transport in summer and southward transport in winter. Such seasonality is associated with wave direction changes.

The results at the middle OmniLine node of Patterson River are also tested (Figures 2.6 and 2.7). The cumulative longshore sediment transport marks the increasing trend over the period 1990-2016. Another feature of Patterson River is the seasonal changes of longshore sediment transport, e.g., northward transport during summer (Nov-Apr) and southward transport during winter (May-Oct) (Figure 2.7). The 2 years of cumulative longshore sediment transports also show the same results, which are mainly caused by the seasonal changes in mean wave direction (Figure 2.8). The wave roses in Figure 2.8 show southwesterly-westerly waves in summer (Nov-Apr), whilst the directions in winter (May-Oct) are broader and shifted clockwise.

Noteworthy, these seasonal characteristics derived from the SCHISM-WWMIII model are consistent with WW3-based results (not shown).

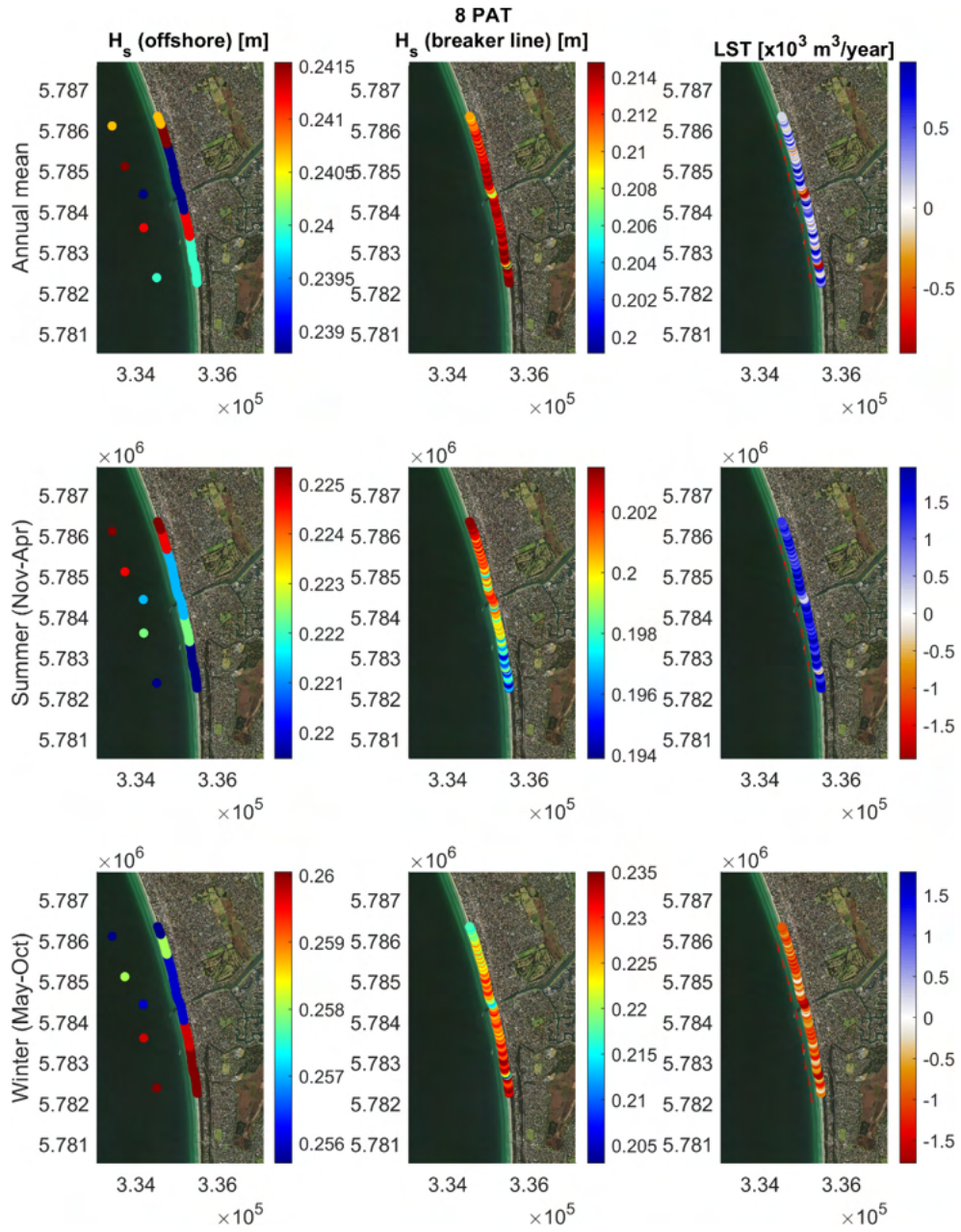


Figure 2.5: Same as Figure 2.1 but for Patterson River.

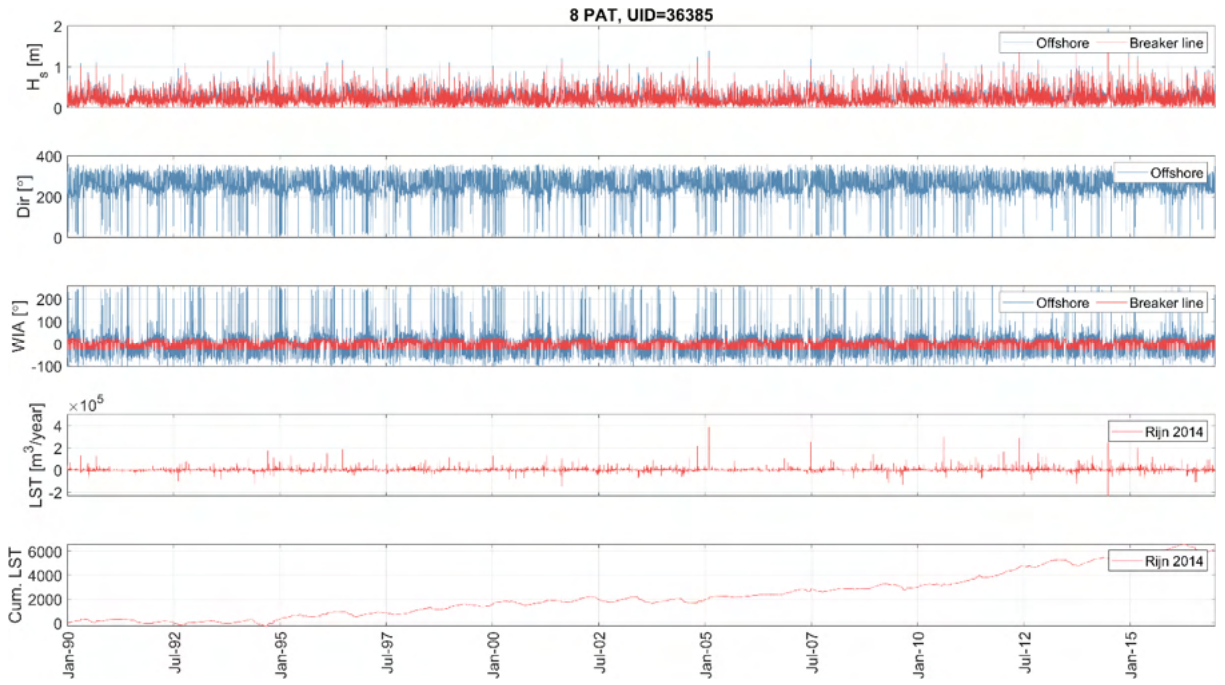


Figure 2.6: Same as Figure 2.2 but for Patterson River.

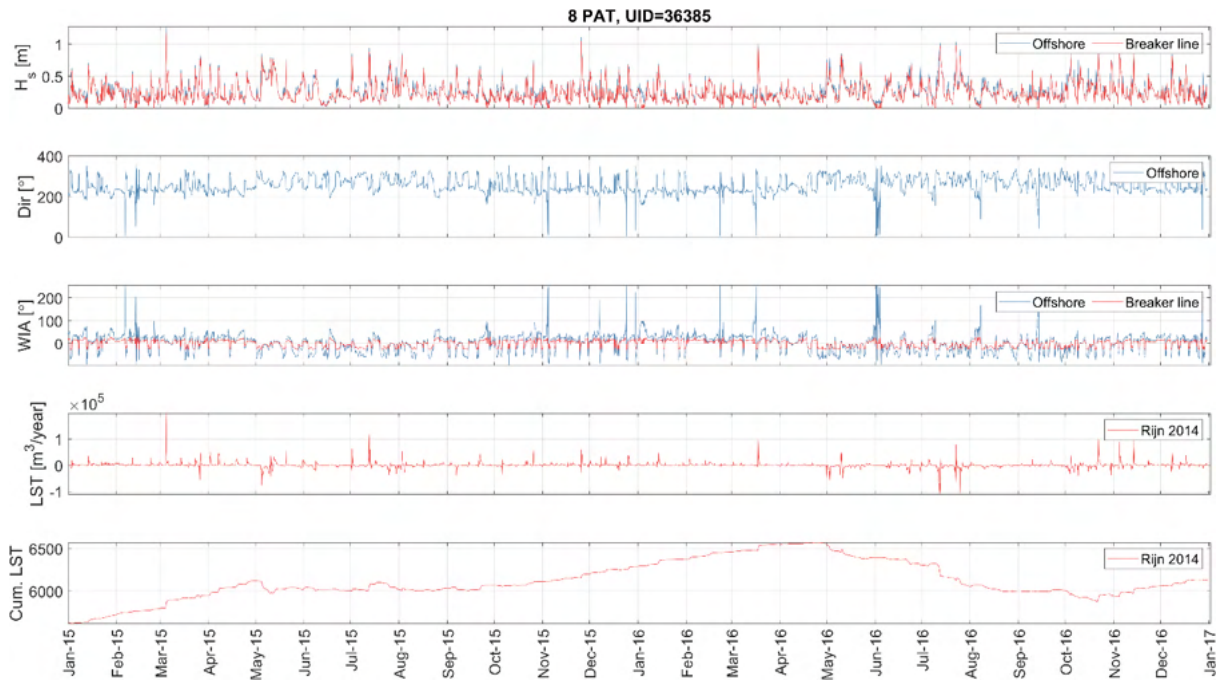


Figure 2.7: Same as Figure 2.3 but for Patterson River.

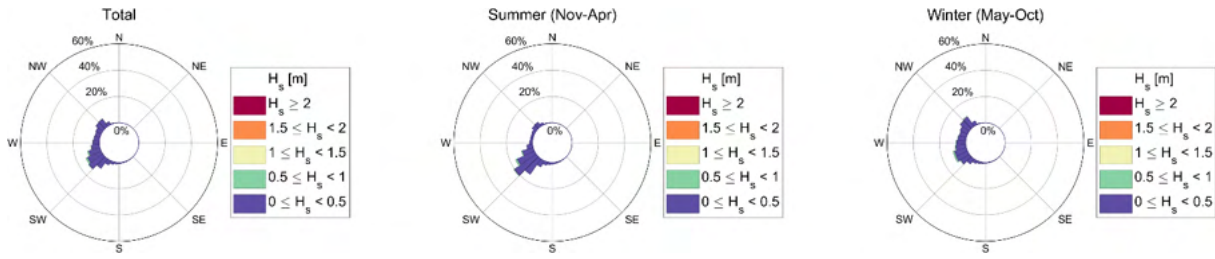


Figure 2.8: Same as Figure 2.4 but for Patterson River.

3 Longshore sediment transport at VCMP sites

Section 2 describes the computation processes of longshore sediment transport at a selected OmniLine node and all OmniLine nodes of Apollo Bay and Patterson River based on offshore wave conditions. Following the approach in Section 2, the statistics of estimated longshore sediment transports at each VCMP site are shown in Figure 3.1. Noting that the VCMP sites of western Victoria are receiving energetic Southern Ocean swell, while the VCMP sites of eastern Victoria are protected by Tasmania and thus show much calm wave status (Liu et al., 2022a). The wave conditions at VCMP sites of Port Phillip Bay are also marked by relatively low Hs as it is a semi-closed bay. Table 3.1 listed the Hs at the offshore and breaker line and gross/net longshore sediment transport at each VCMP site. The results also indicate the impacts of capes on Hs and longshore sediment transport, e.g., Port Fairy and Portland. The results show that western Victoria and Great Ocean Road experienced robust longshore sediment transport.

It is worth noting that the longshore sediment transports in Figures 3.1 and Figure 3.2 are integers, the readers are recommended to look at Table 3.1 and Table 3.2 for more accurate Hs and longshore sediment transport estimation. The differences between net and gross longshore sediment transports of Patterson are caused by the seasonal variations of mean wave direction indicated in Figure 2.8.

Net and gross longshore sediment transports of Apollo Bay, however, are identical. This means the longshore sediment transports of Apollo Bay are always northward. As indicated in Section 2, these results could be associated with the simulated identical wave directions and Hs in the WW3 model.

The annual mean values and seasonal variations of wave conditions and longshore sediment transport of all VCMP sites are included below.

O’Grady et al. (2019) estimated the longshore sediment transport at Ninty Mile Beach (a little bit further northeast of Seaspray) based on three empirical approaches. Their CERC-based on longshore sediment transport is consistent with the present study. The differences between the present study and O’Grady et al. (2019) could be associated with the locations.

Noteworthy, the longshore sediment transports in Tables 3.1 and Table 3.2 and Figures 3.1 and 3.2 are annual mean values. The longshore sediment transport could be quite different when an extreme storm occurs. McCarroll et al. (2019) indicate that extreme longshore sediment transports during a storm are comparable with the annual rate.

Table 3.1: Statistics over the period 1981-2020 (WW3).

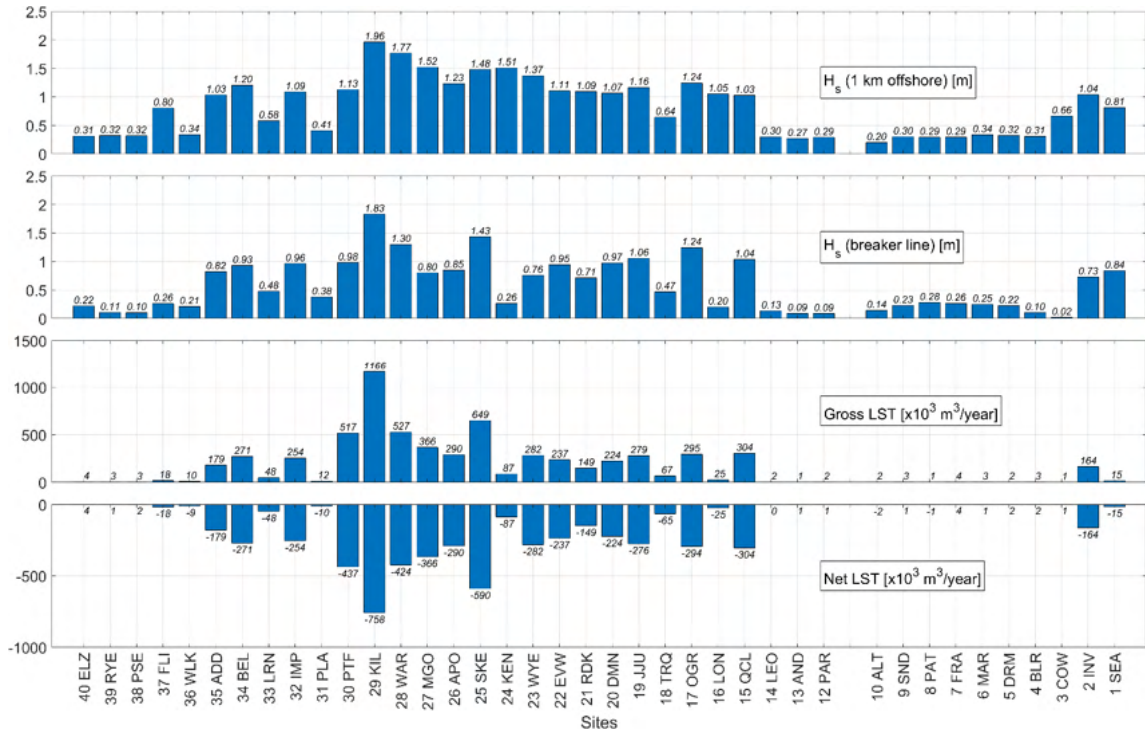
Sites	Abbr.	Site ID	Hs (offshore)	Hs (breaker line)	Gross LST (x1000 m ³ /year)	Net LST (x1000 m ³ /year)	Rank by offshore Hs
Seaspray	SEA	1	0.81	0.84	15.15	-15.15	20
Inverloch	INV	2	1.04	0.73	164.12	-164.12	17
Cowes	COW	3	0.66	0.02	1.24	1.24	22
Blairgowrie	BLR	4	0.31	0.10	2.55	1.91	32
Dromana-McCrae	DRM	5	0.32	0.22	1.86	1.84	28
Mount Martha	MAR	6	0.34	0.25	2.54	1.34	27
Frankston	FRA	7	0.29	0.26	3.50	3.50	35
Patterson River	PAT	8	0.29	0.28	1.46	-1.09	36
Sandringham	SND	9	0.30	0.23	2.61	1.38	33
Altona	ALT	10	0.20	0.14	1.83	-1.61	39
Portarlington	PAR	12	0.29	0.09	2.23	1.28	37
Anderson Reserve	AND	13	0.27	0.09	1.48	1.38	38
St Leonards	LEO	14	0.30	0.13	1.70	0.47	34
Queenscliff	QCL	15	1.03	1.04	304.33	-304.33	19

Point Lonsdale	LON	16	1.05	0.20	24.70	-24.70	16
Ocean Grove	OGR	17	1.24	1.24	294.98	-294.34	7
Torquay	TRQ	18	0.64	0.47	66.55	-65.10	23
Jan Juc	JJU	19	1.16	1.06	279.35	-275.88	10
Demons Bluff	DMN	20	1.07	0.97	223.87	-223.87	15
Point Roadknight	RDK	21	1.09	0.71	148.84	-148.84	13
Eastern View	EVW	22	1.11	0.95	236.63	-236.63	12
Wye River	WYE	23	1.37	0.76	282.38	-282.38	6
Kennett River	KEN	24	1.51	0.26	87.43	-87.43	4
Skenes Creek	SKE	25	1.48	1.43	648.60	-589.76	5
Apollo Bay	APO	26	1.23	0.85	290.16	-290.16	8
Marengo	MGO	27	1.52	0.80	366.43	-366.43	3
Warmambool	WAR	28	1.77	1.30	527.36	-424.17	2
Killarney	KIL	29	1.96	1.83	1165.72	-758.48	1
Port Fairy	PTF	30	1.13	0.98	517.48	-437.40	11
Portland	PLA	31	0.41	0.38	11.84	-9.98	25
Point Impossible	IMP	32	1.09	0.96	254.08	-254.08	14
Lorne	LRN	33	0.58	0.48	48.15	-47.92	24
Bells Beach	BEL	34	1.20	0.93	270.92	-270.92	9
Point Addis	ADD	35	1.03	0.82	179.46	-179.46	18
Walkerville	WLK	36	0.34	0.21	10.41	-9.49	26
Flinders	FLI	37	0.80	0.26	17.91	-17.90	21
Portsea	PSE	38	0.32	0.10	2.83	2.09	30
Rye	RYE	39	0.32	0.11	2.85	1.41	29
Mount Eliza	ELZ	40	0.31	0.22	4.45	3.88	31

Table 3.2: Statistics over the period 1990-2016 (SCHISM-WWMIII).

Sites	Abbr.	Site ID	Hs (offshore)	Hs (breaker line)	Gross LST (x1000 m ³ /year)	Net LST (x1000 m ³ /year)	Rank by offshore Hs
Seaspray	SEA	1					
Inverloch	INV	2					
Cowes	COW	3					
Blairgowrie	BLR	4	0.24	0.07	0.35	0.24	
Dromana-McCrae	DRM	5	0.27	0.19	1.73	1.73	
Mount Martha	MAR	6	0.27	0.20	1.49	1.26	
Frankston	FRA	7	0.24	0.20	0.96	0.96	
Patterson River	PAT	8	0.24	0.21	0.39	0.22	
Sandringham	SND	9	0.24	0.17	0.90	0.81	
Altona	ALT	10	0.17	0.11	0.60	-0.52	
Portarlington	PAR	12	0.21	0.07	0.43	0.23	
Anderson Reserve	AND	13	0.22	0.08	0.75	0.71	

St Leonards	LEO	14	0.23	0.11	0.54	0.23	
Queenscliff	QCL	15	0.96	0.93	87.05	-57.70	
Point Lonsdale	LON	16	1.25	0.66	198.56	-198.56	
Ocean Grove	OGR	17					
Torquay	TRQ	18					
Jan Juc	JJU	19					
Demons Bluff	DMN	20					
Point Roadknight	RDK	21					
Eastern View	EVW	22					
Wye River	WYE	23					
Kennett River	KEN	24					
Skenes Creek	SKE	25					
Apollo Bay	APO	26					
Marengo	MGO	27					
Warrnambool	WAR	28					
Killarney	KIL	29					
Port Fairy	PTF	30					
Portland	PLA	31					
Point Impossible	IMP	32					
Lorne	LRN	33					
Bells Beach	BEL	34					
Point Addis	ADD	35					
Walkerville	WLK	36					
Flinders	FLI	37					
Portsea	PSE	38	0.33	0.06	0.77	0.67	0.33
Rye	RYE	39	0.26	0.08	0.81	0.56	0.26
Mount Eliza	ELZ	40	0.25	0.16	1.33	1.16	0.25



Figure

3.1: WW3-based annual mean values of H_s (1 km offshore), H_s (breaker line), gross and net longshore sediment transport at VCMP sites. The integer values are indicated above/below each bar, the more accurate values are indicated in Table 3.1.

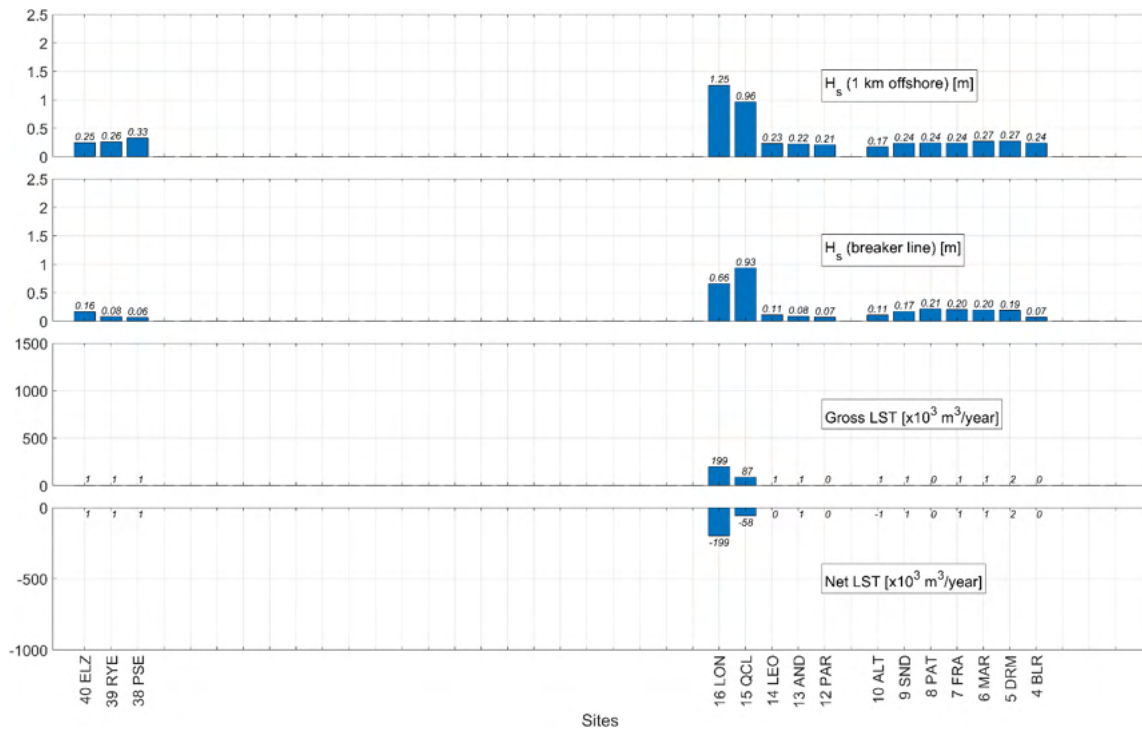


Figure 3.2: SCHISM-WWIII-based annual mean values of H_s (1 km offshore), H_s (breaker line), gross and net longshore sediment transport at VCMP sites. The integer values are indicated above/below each bar, the more accurate values are indicated in Table 3.2.

- Eastern Victoria - WW3

In terms of eastern Victoria, we refer to the following VCMP sites: 1 Seaspray, 2 Inverloch, 3 Cowes, 36 Walkerville and 37 Flinders.

Annual mean Hs in these locations is generally below 1 m and the longshore sediment transports are directed to the north/east. Inverloch shows the largest longshore sediment transport among them due to the influence of Southern Ocean swell intrusion. Seaspray experiences large seasonality in longshore sediment transport due to seasonal changes in wave directions. The wave directions are southerly in winter and south-easterly in summer in Gippsland (Liu et al., 2022a). Therefore, the longshore sediment transport of Seaspray shows north-eastward transport in winter. The other three sites, Inverloch, Walkerville and Flinders show uni-directional seasonal longshore transport.

- Port Phillip Bay – SCHISM-WWMIII

Here, the VCMP sites of Port Phillip Bay mainly include four segments: southern (4 Blairgowrie, 5 Dromana-McCrae, 38 Portsea, 39 Rye), eastern (6 Mount Martha, 7 Frankston, 8 Patterson River, 40 Mount Eliza), northern (9 Sandringham, 10 Altona) and southwestern (12 Portarlington, 13 Anderson Reserve, 14 St Leonards, 15 Queenscliff, 16 Point Lonsdale) parts.

In the southern part of Port Phillip Bay, the offshore Hs and breaking Hs are generally below 0.5 m. The seasonality of longshore sediment transports at these locations indicates winter magnitude of longshore sediment transport is comparable to the summer magnitude.

In the eastern portion of Port Phillip Bay, the annual mean magnitudes of longshore sediment transports at Mount Martha, Frankston and Mount Eliza are comparable. However, the annual mean values of longshore sediment transport at Patterson River are smaller than the other three sites as it has large seasonality with different directions in winter and in summer (details shown in Section 2).

In the northern part of Port Phillip Bay, Sandringham shows southward and northward longshore sediment transports in the north and south parts, respectively, while Altona shows northward transport. But the longshore sediment transport of Sandringham is approximately 1.5 times as Altona due to its bigger amplitude of offshore Hs. These results indicate the larger longshore sediment transport in the north-eastern part of Port Phillip Bay than the north-western part of Port Phillip Bay.

In the southwestern part of Port Phillip Bay, the longshore sediment transport of Portarlington, Anderson Reserve and St Leonards are relatively small (~500-1,500) m³/year. At the entrance of Port Phillip Bay (Queenscliff and Point Lonsdale), the longshore sediment transports show much bigger amplitude due to the influence of the Southern Ocean swell and its interaction with topography.

- Great Ocean Road - WW3

In terms of Great Ocean Road, we refer to the following VCMP sites: 18 Torquay, 19 Jan Juc, 20 Demons Bluff, 21 Point Roadknight, 22 Eastern View, 23 Wye River, 24 Kennett River, 25 Skenes Creek, 26 Apollo Bay, 27 Marengo, 32 Point Impossible, 33 Lorne, 34 Bells Beach and 35 Point Addis. The shoreline directions at these sites are consistently pointing northeast.

The annual mean values indicate gradually decreasing offshore Hs from Marengo to Torquay with amplitude generally below 1.5 m. The most important feature of Hs at the breaker line (<0.5 m) is the dramatically reduce Hs amplitudes behind the capes, e.g., Torquay, Point Roadknight, Lorne, Wye River, Kennett River, Apollo Bay and Marengo. The maximum annual mean longshore sediment transports at each VCMP are generally northward or northeastward with magnitude of 200,000-600,000 m³/year. However, longshore sediment transports behind the capes decrease as breaking Hs decreases.

The seasonal changes in offshore and breaking Hs and longshore sediment transport are very small, as energetic Southern Ocean swell approaches Great Ocean Road across the whole year.

- Western Victoria – WW3

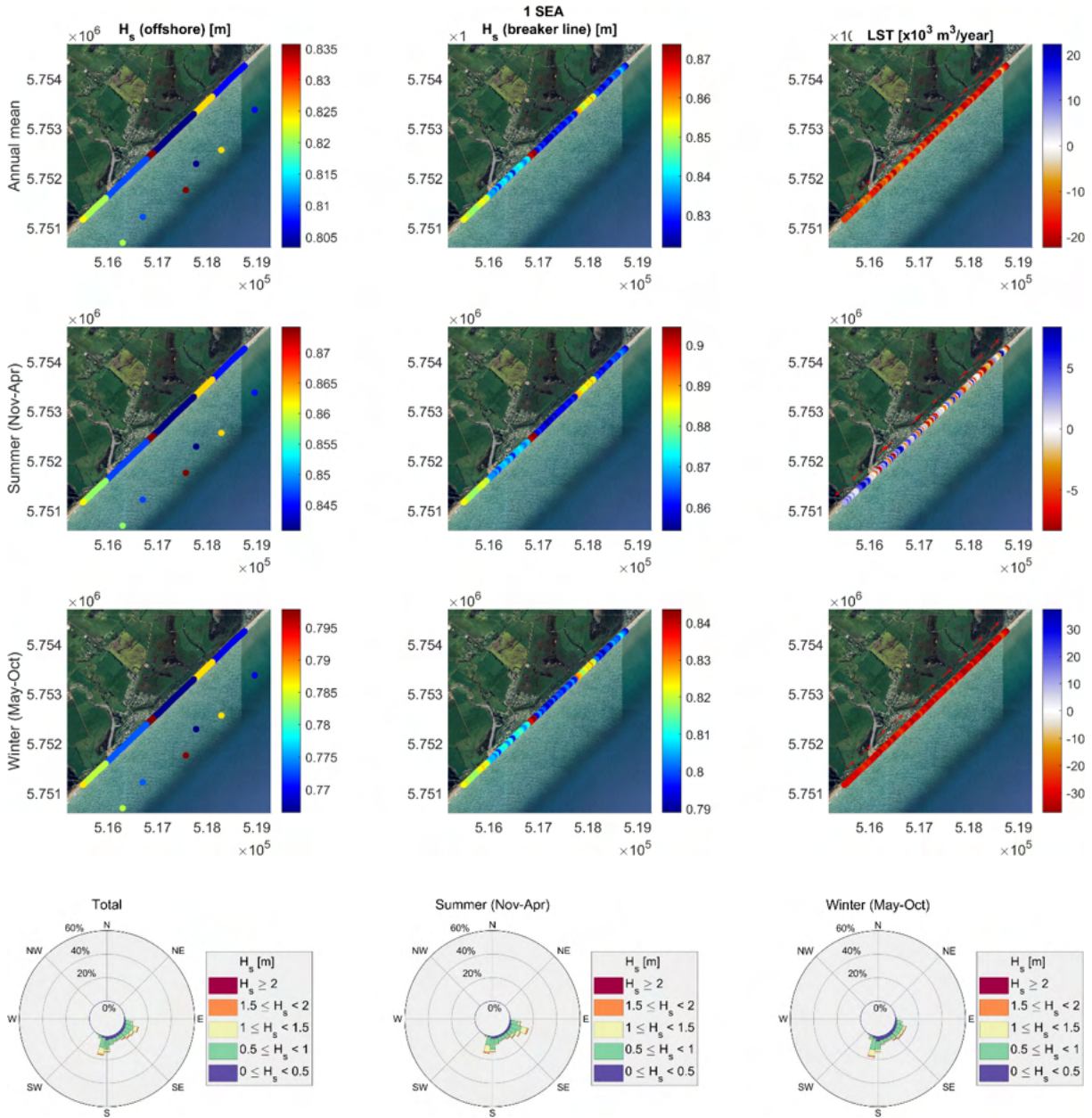
In this study, western Victoria involves the following VCMP sites: 28 Warrnambool, 29 Killarney, 30 Port Fairy and 31 Portland.

Similar to other VCMP sites, breaking Hs behind the capes decreases dramatically and largely reduces the longshore transport magnitude, e.g., Warrnambool and Port Fairy. Although the longshore sediment transports are generally eastward, longshore sediments transport at some OmniLine nodes, however, are westward due to the orientations of shoreline and wave directions.

Seasonal changes of longshore sediment transport are apparent in the center of Warrnambool and Portland, while other sites indicate relatively small changes.

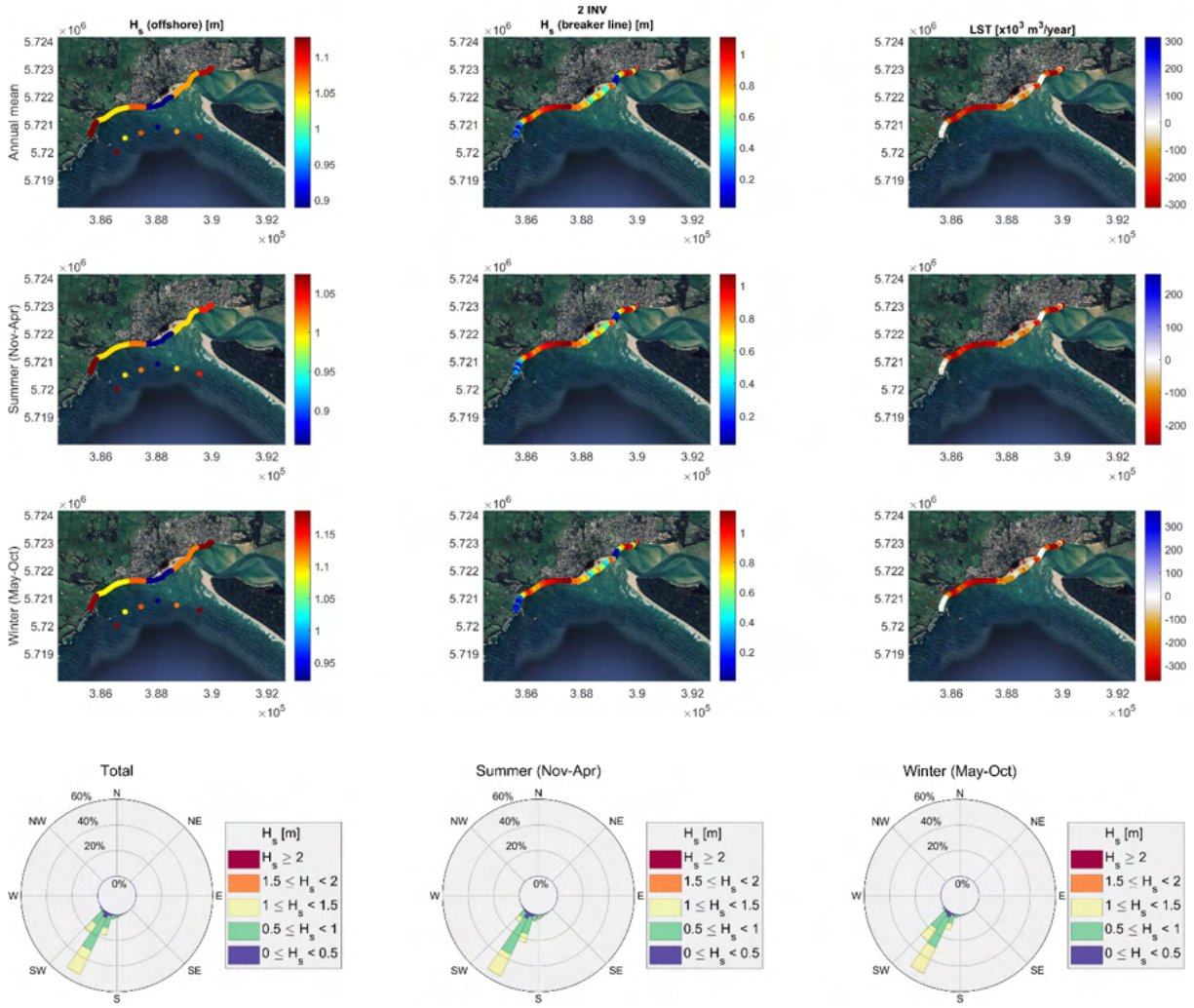
3.1 Seaspray (SEA)

3.1.1 Model 1 – WW3



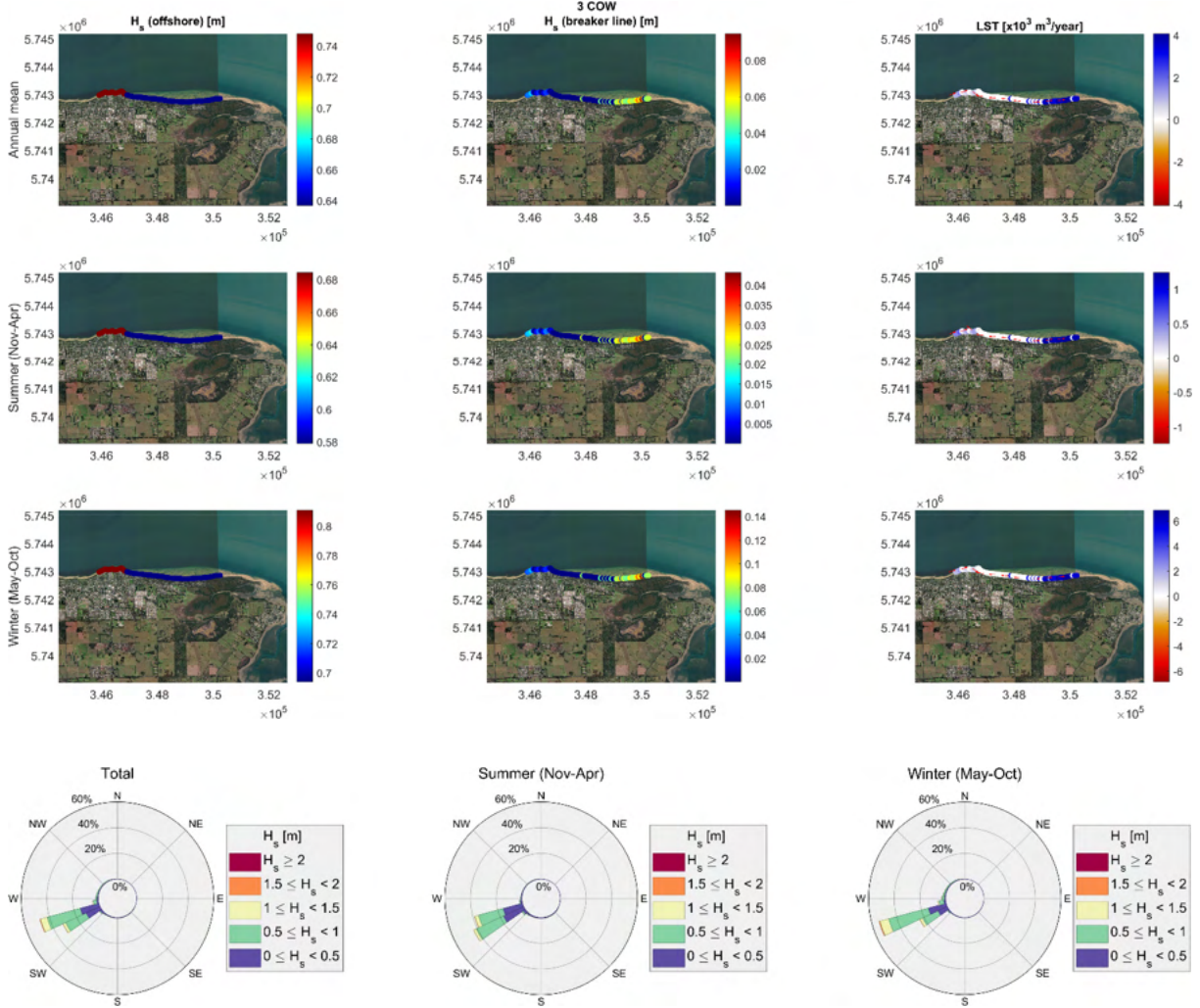
3.2 Inverloch (INV)

3.2.1 Model 1 – WW3



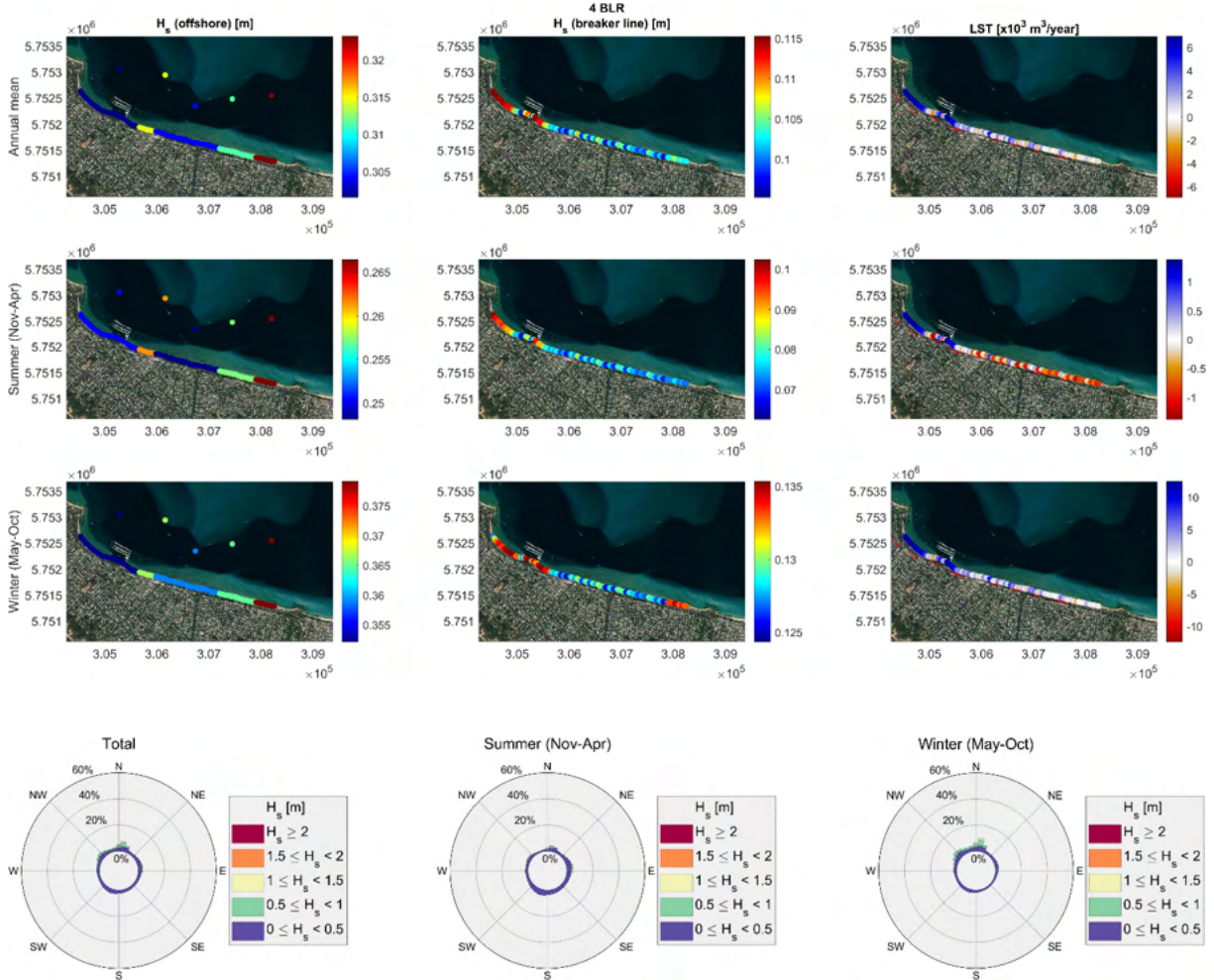
3.3 Cowes (COW)

3.3.1 Model 1 – WW3

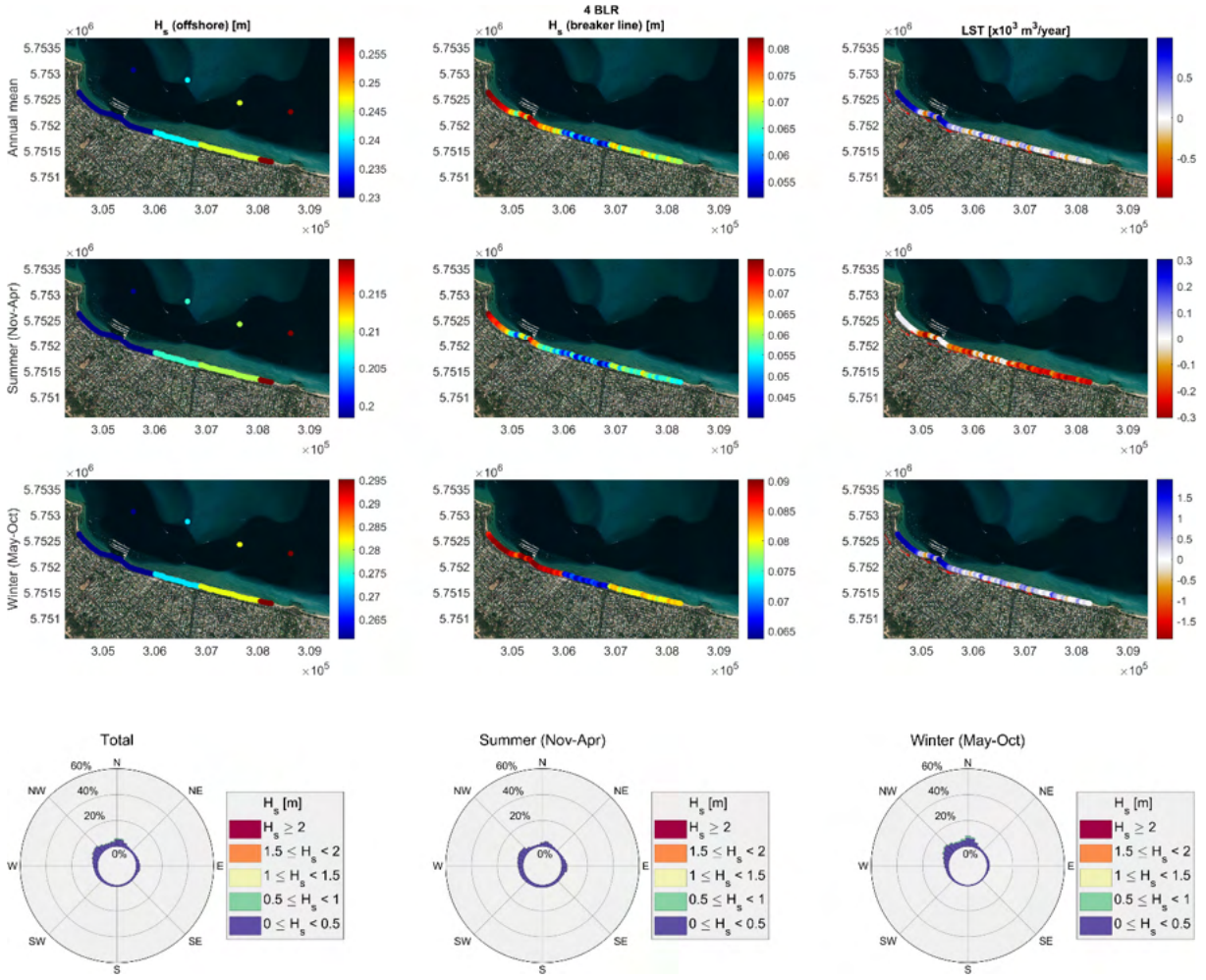


3.4 Blairgowrie (BLR)

3.4.1 Model 1 – WW3

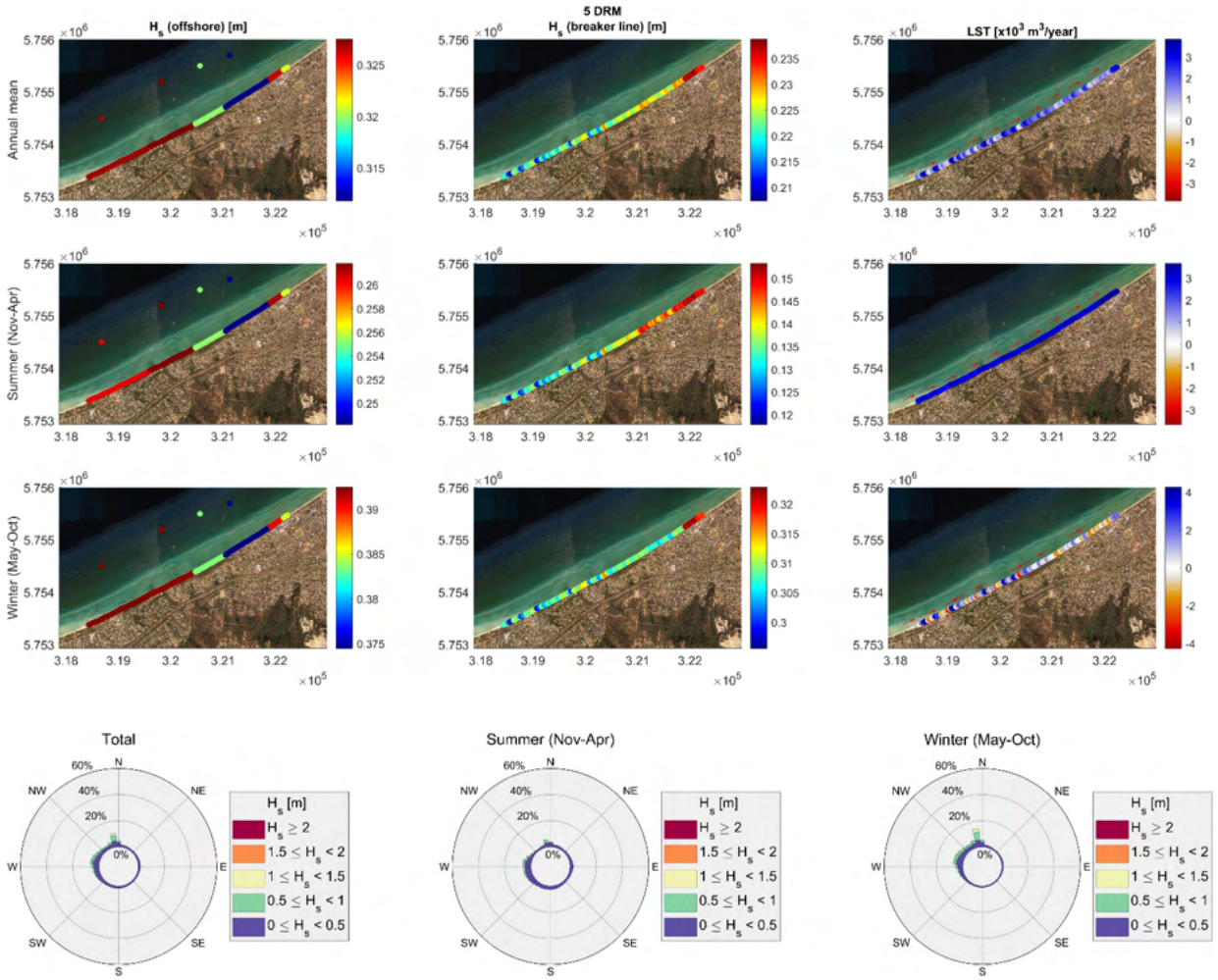


3.4.2 Model 2 – SCHISM-WWMIII

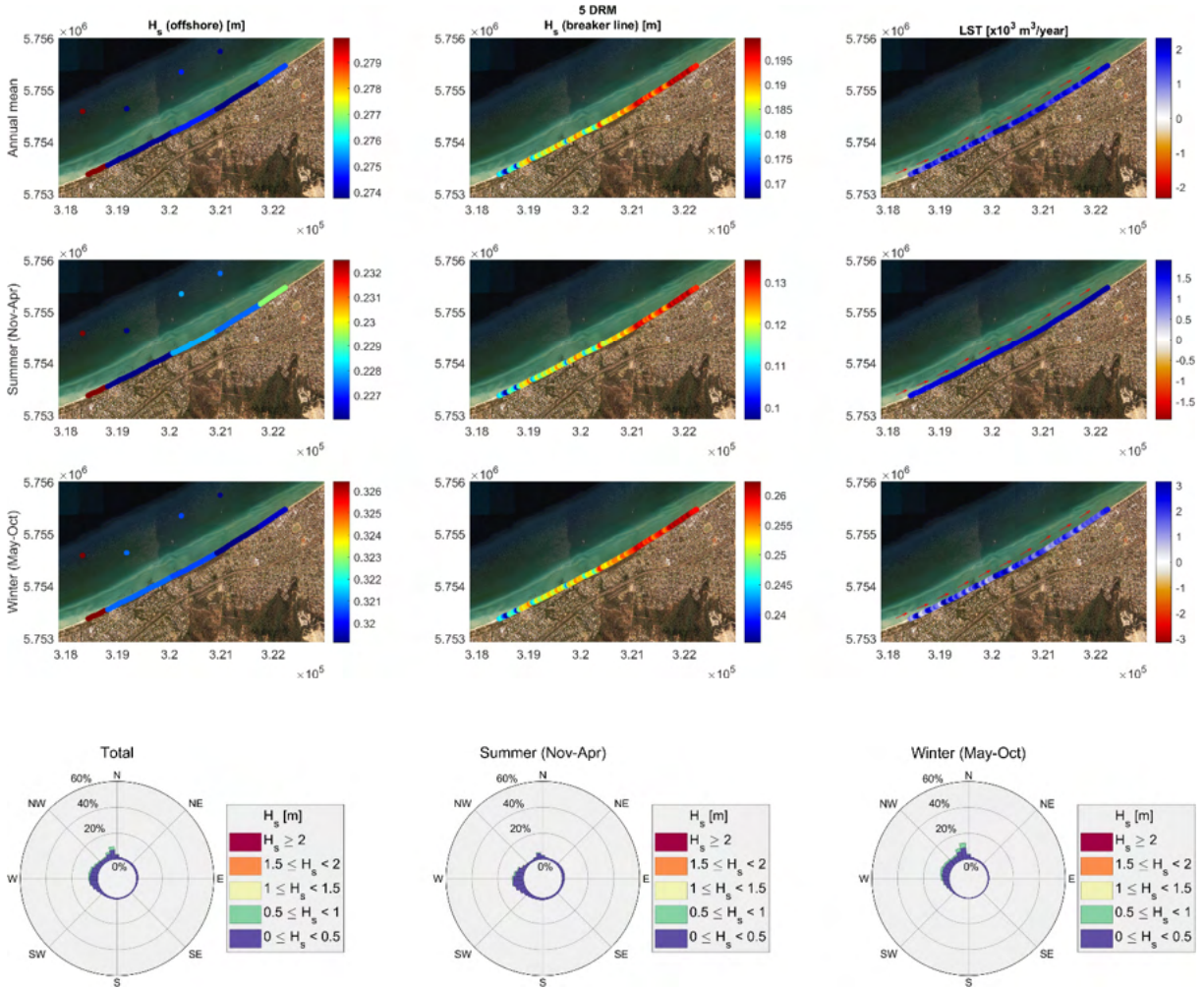


3.5 Dromana-McCrae (DRM)

3.5.1 Model 1 – WW3

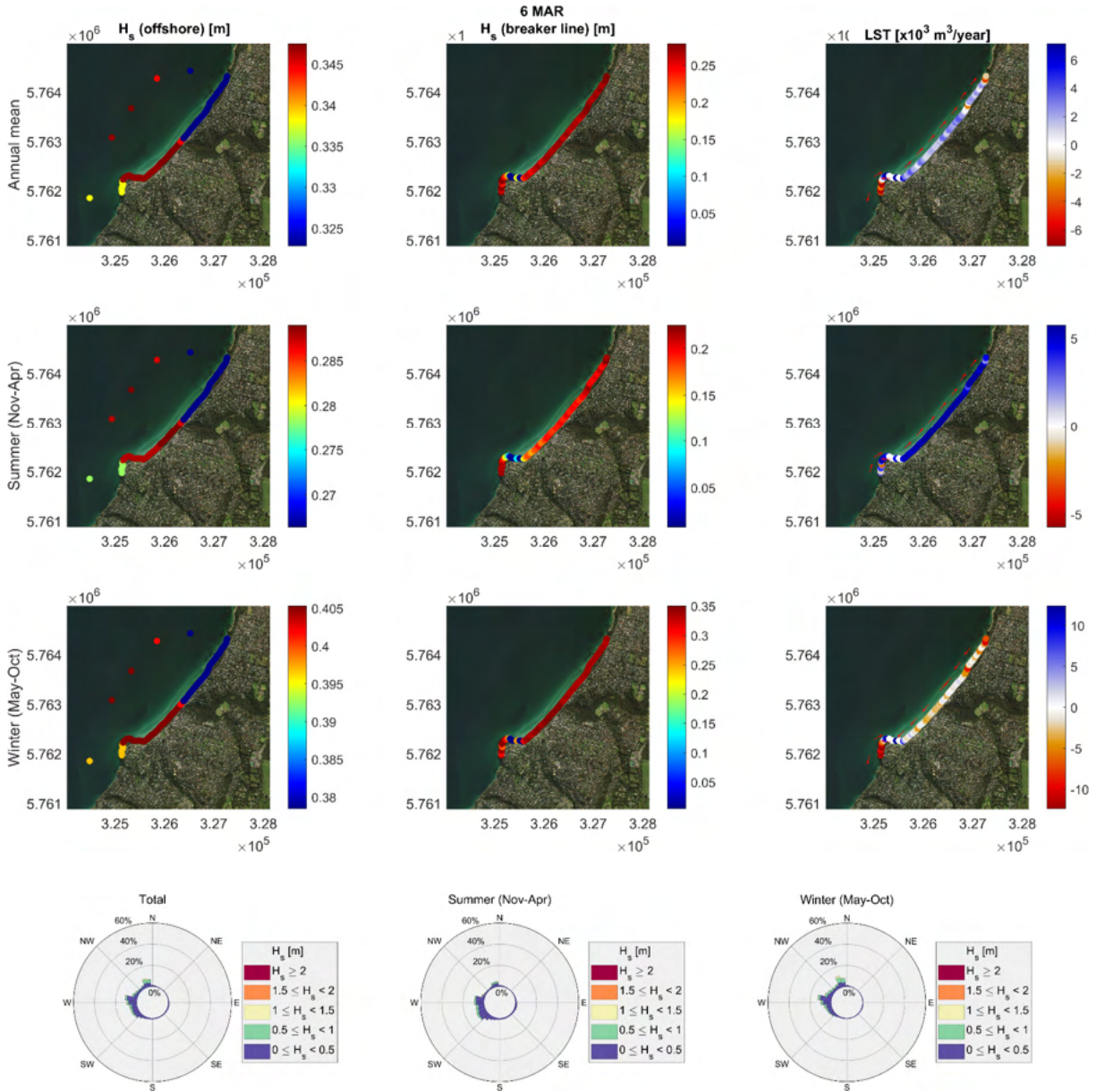


3.5.2 Model 2 – SCHISM-WWMIII

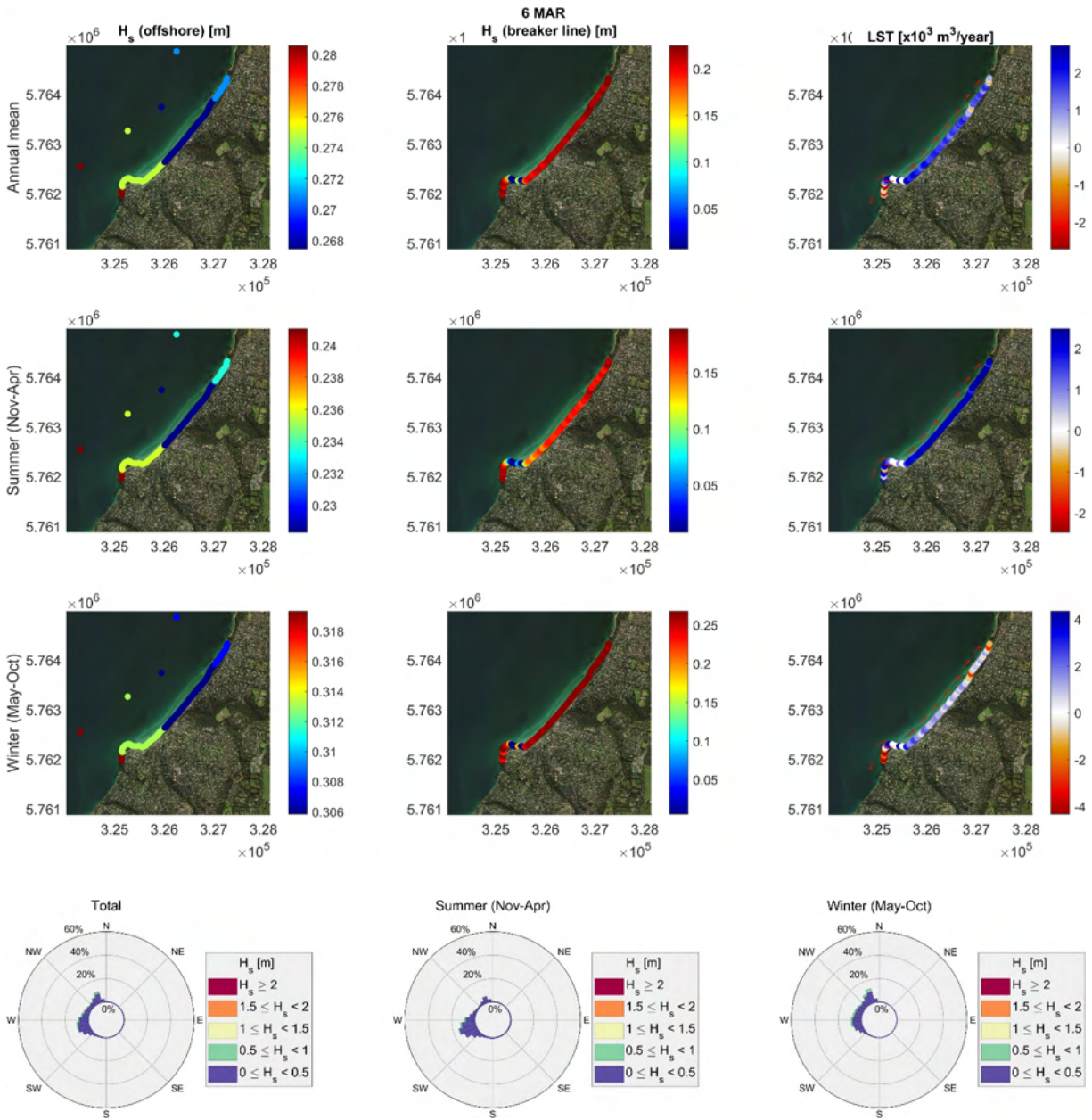


3.6 Mount Martha (MAR)

3.6.1 Model 1 – WW3

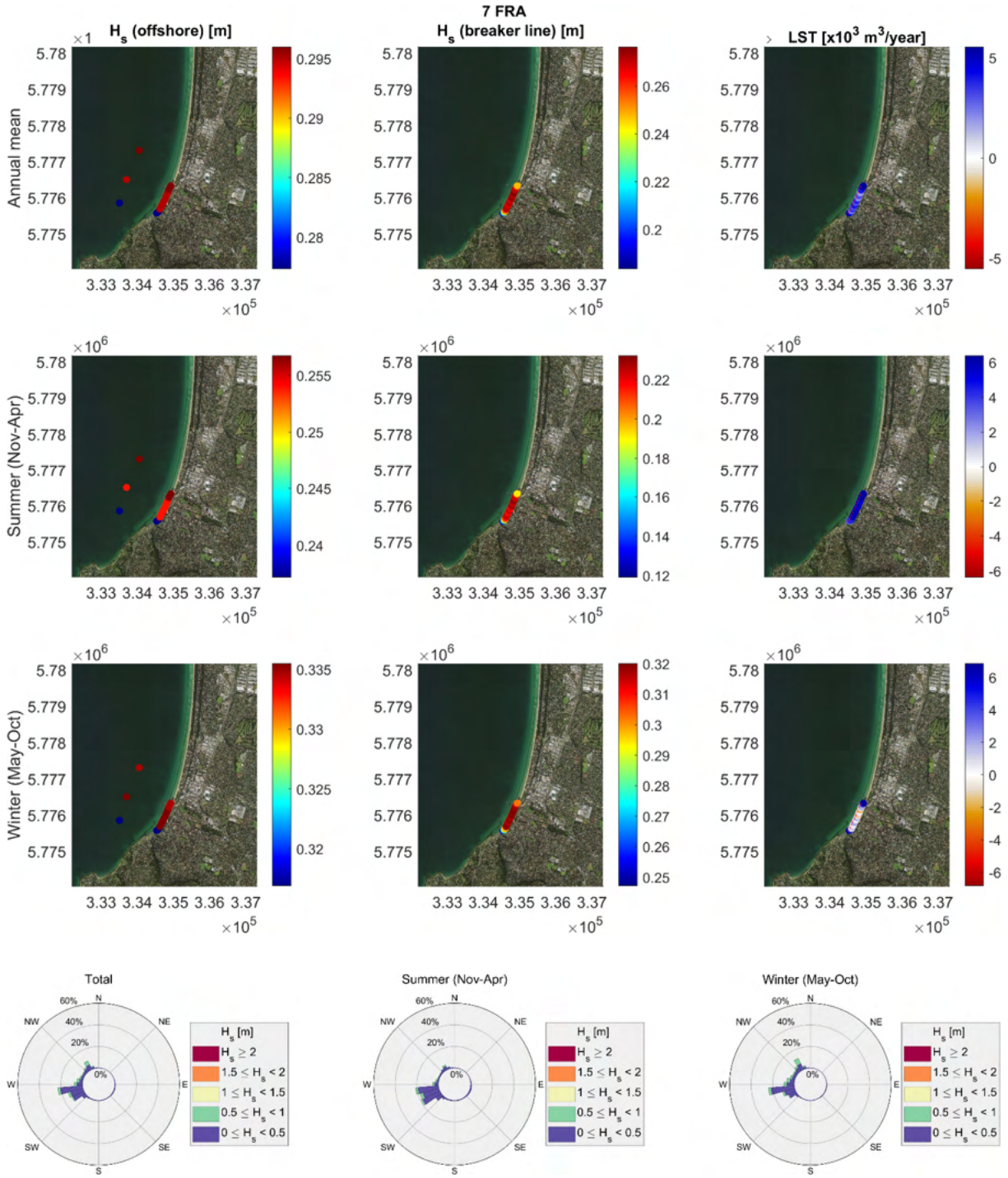


3.6.2 Model 2 – SCHISM-WWMIII

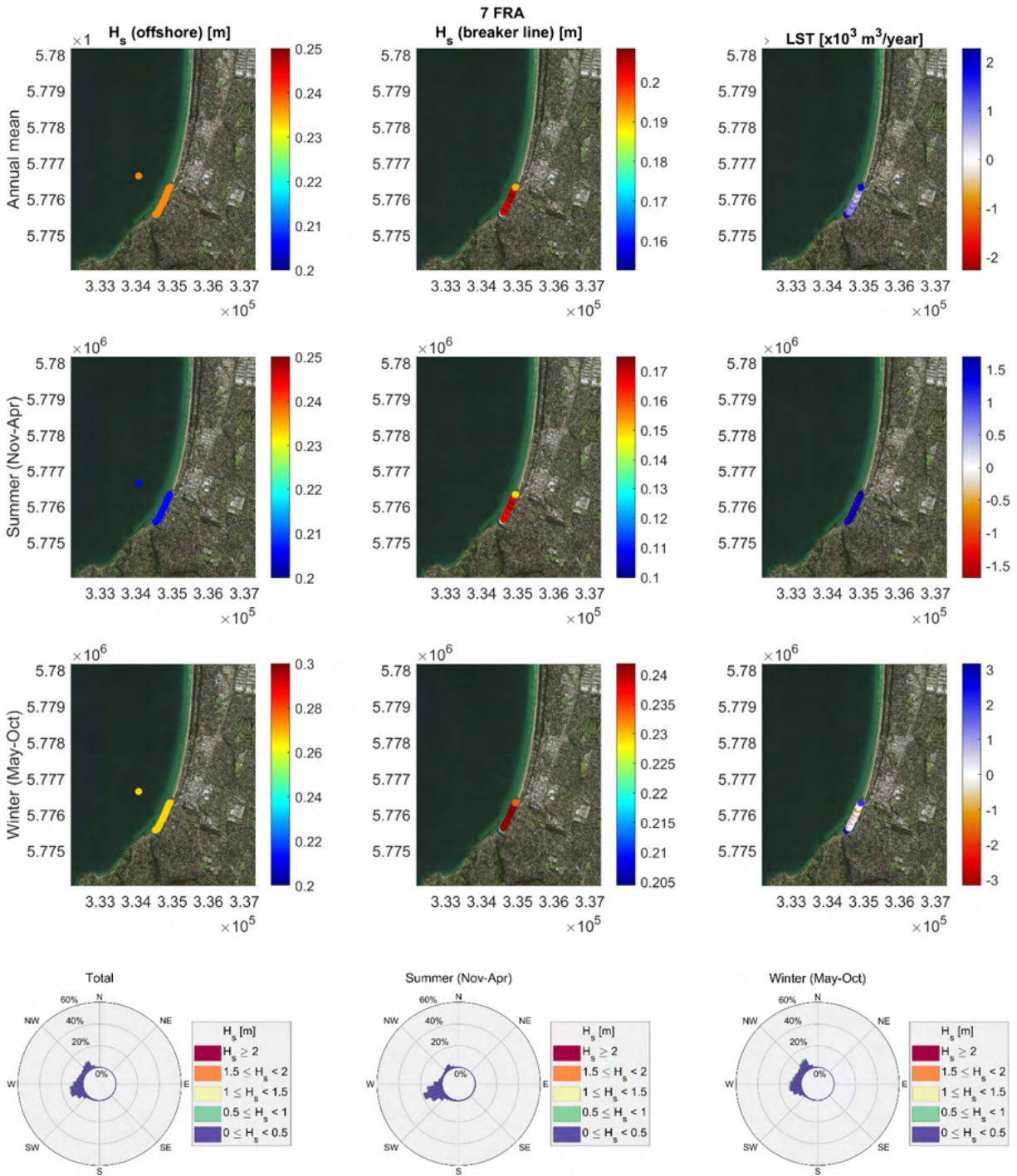


3.7 Frankston (FRA)

3.7.1 Model 1 – WW3

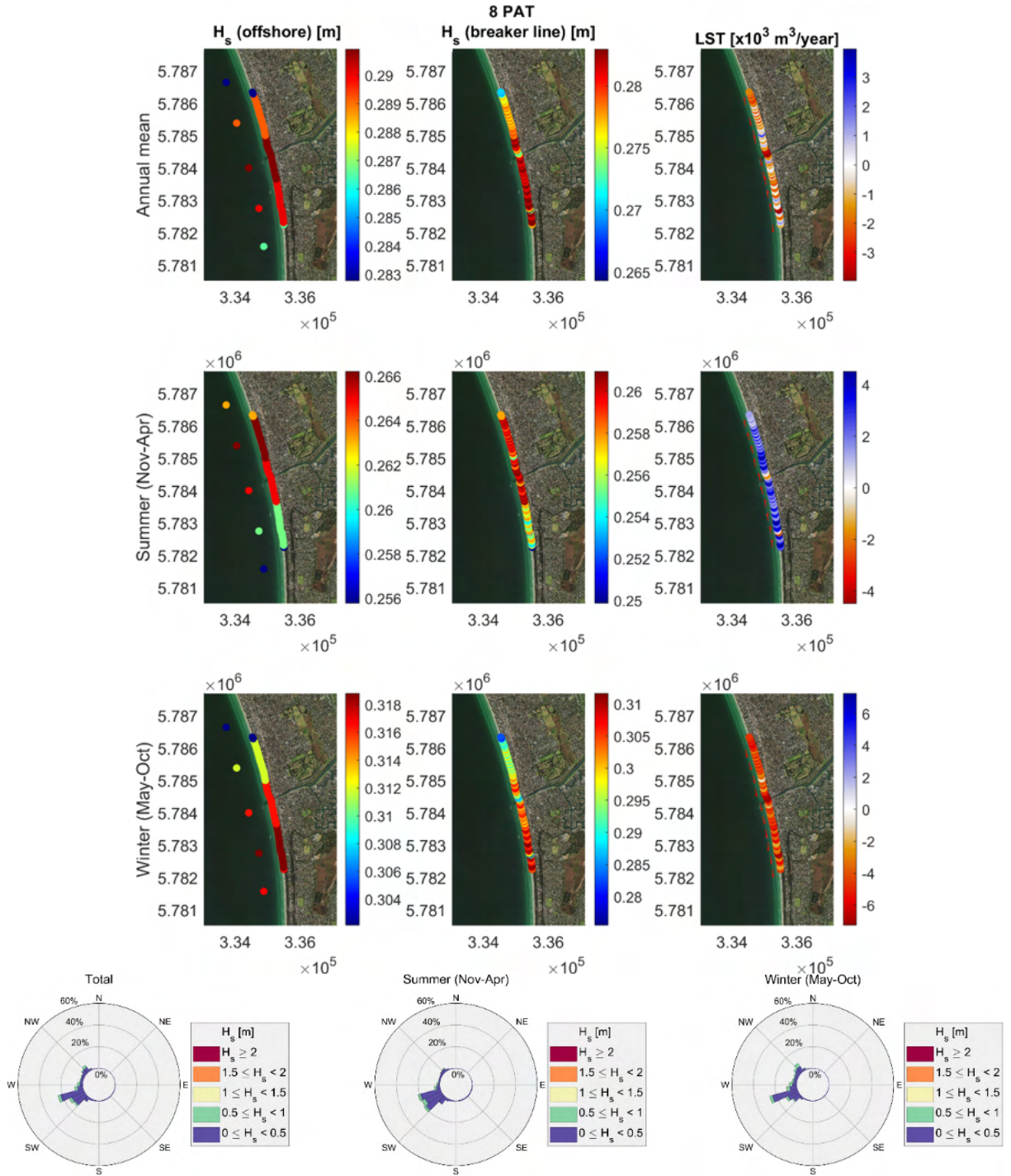


3.7.2 Model 2 – SCHISM-WWMIII

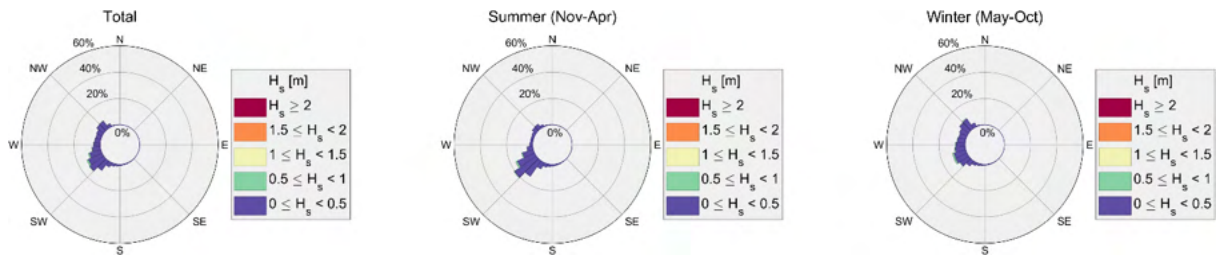
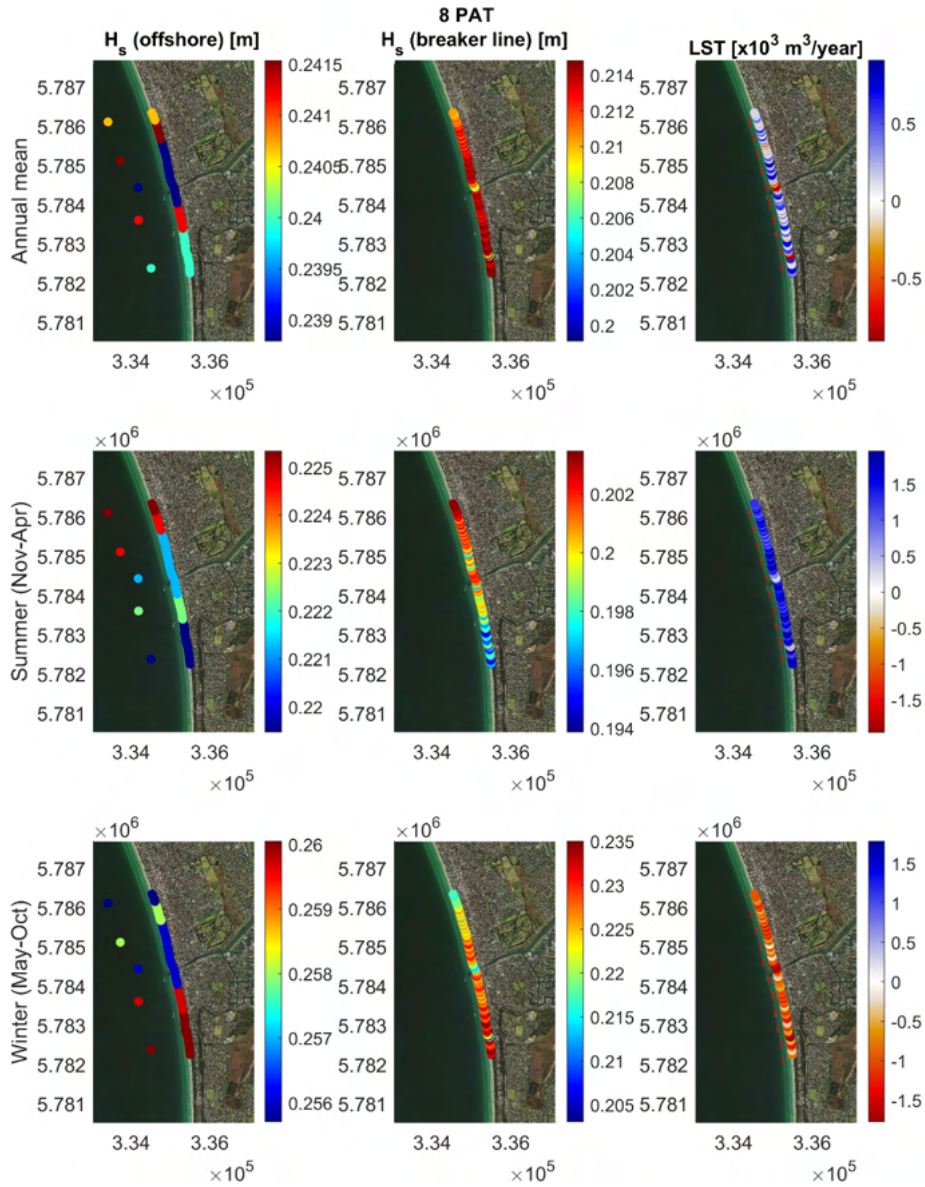


3.8 Patterson River (PAT)

3.8.1 Model 1 – WW3

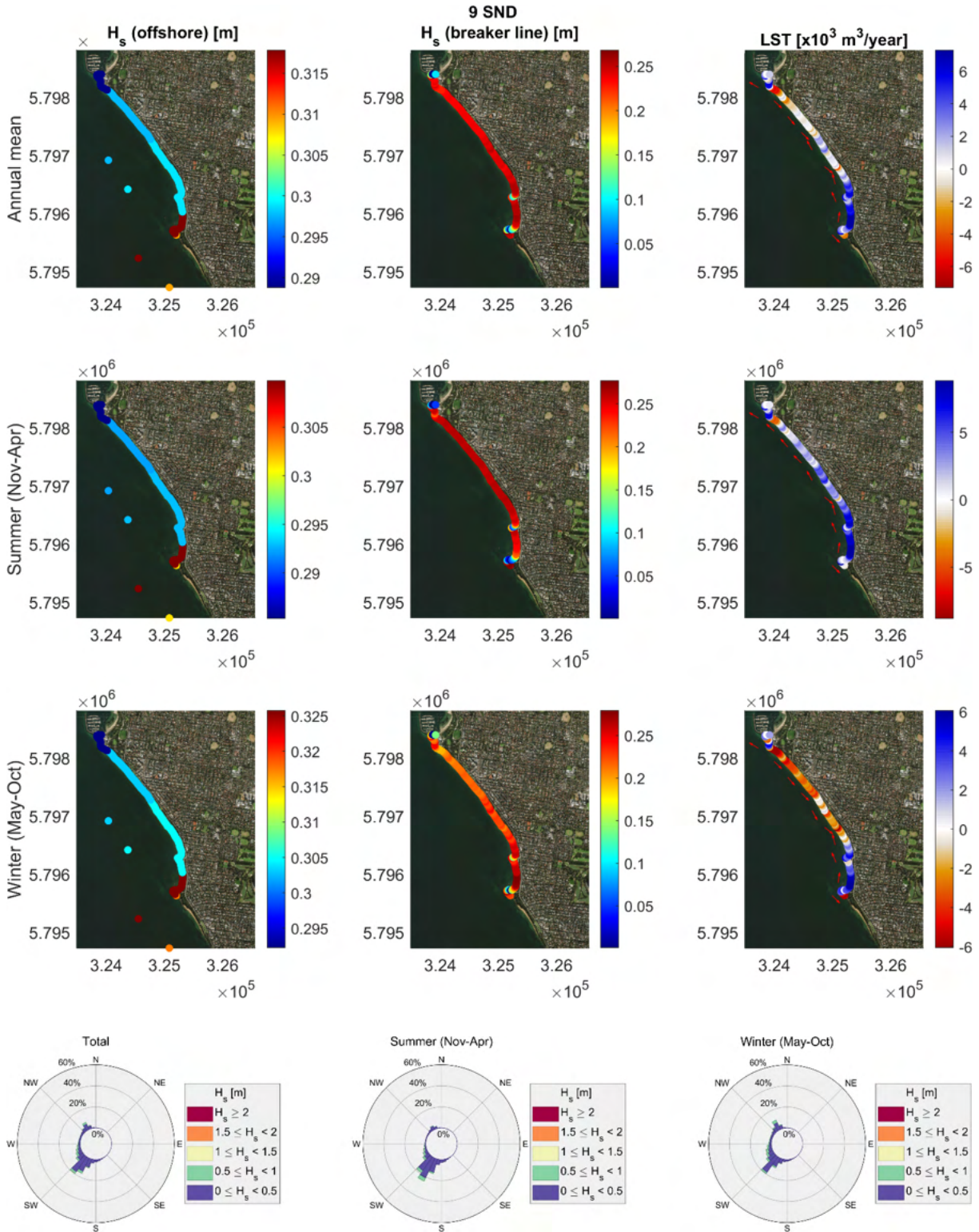


3.8.2 Model 2 – SCHISM-WWMIII

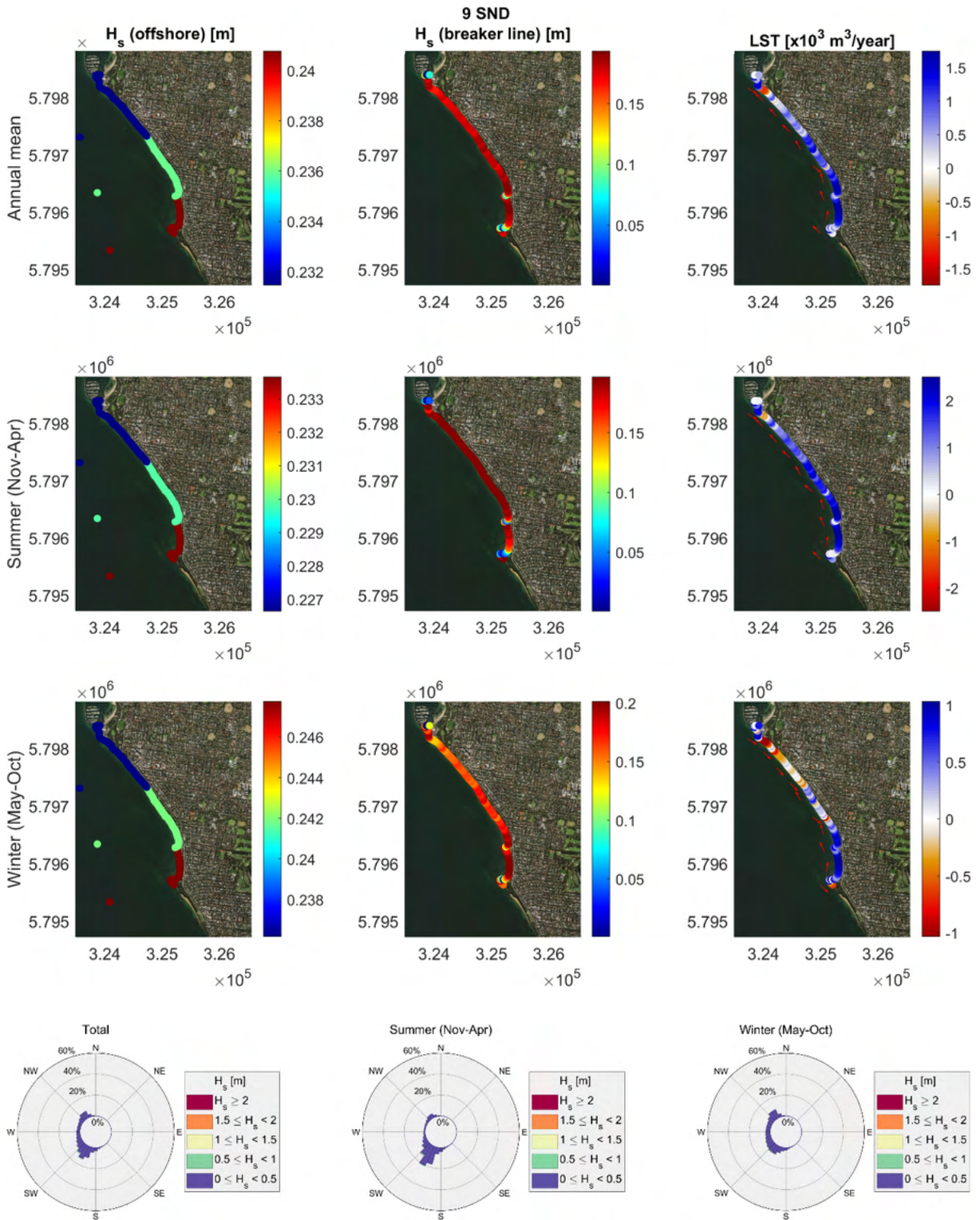


3.9 Sandringham (SND)

3.9.1 Model 1 – WW3

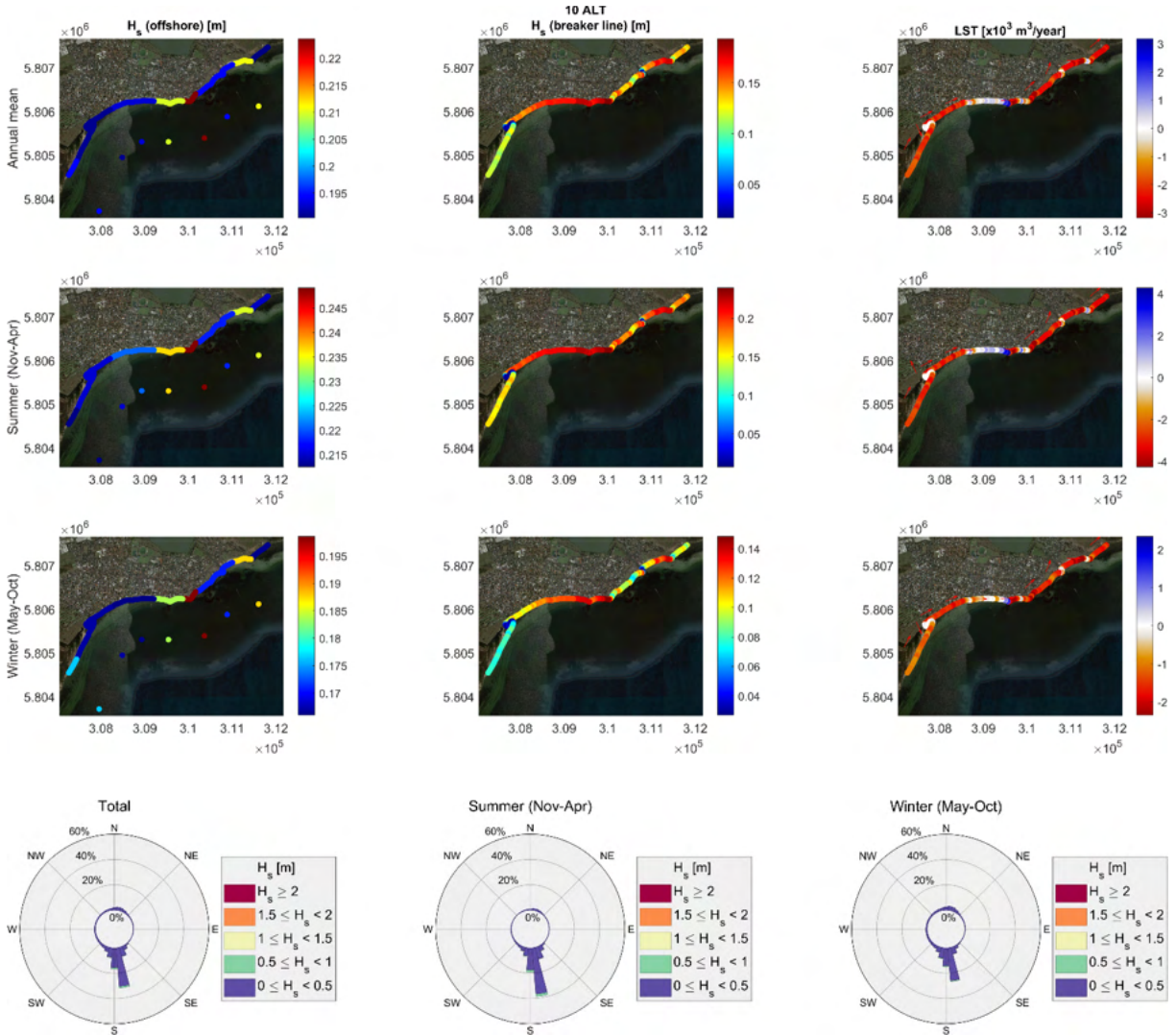


3.9.2 Model 2 – SCHISM-WWMIII

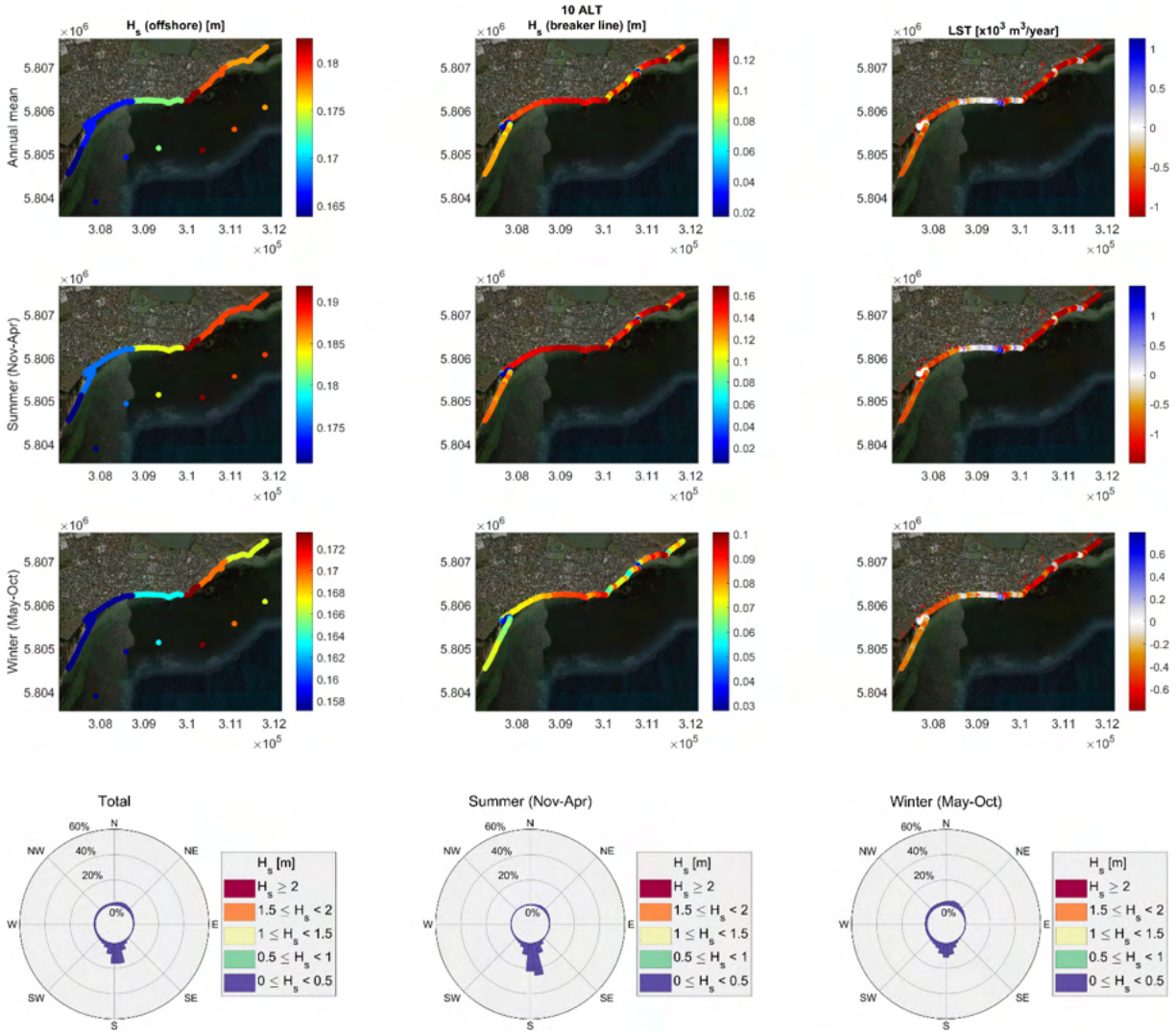


3.10 Altona (ALT)

3.10.1 Model 1 – WW3



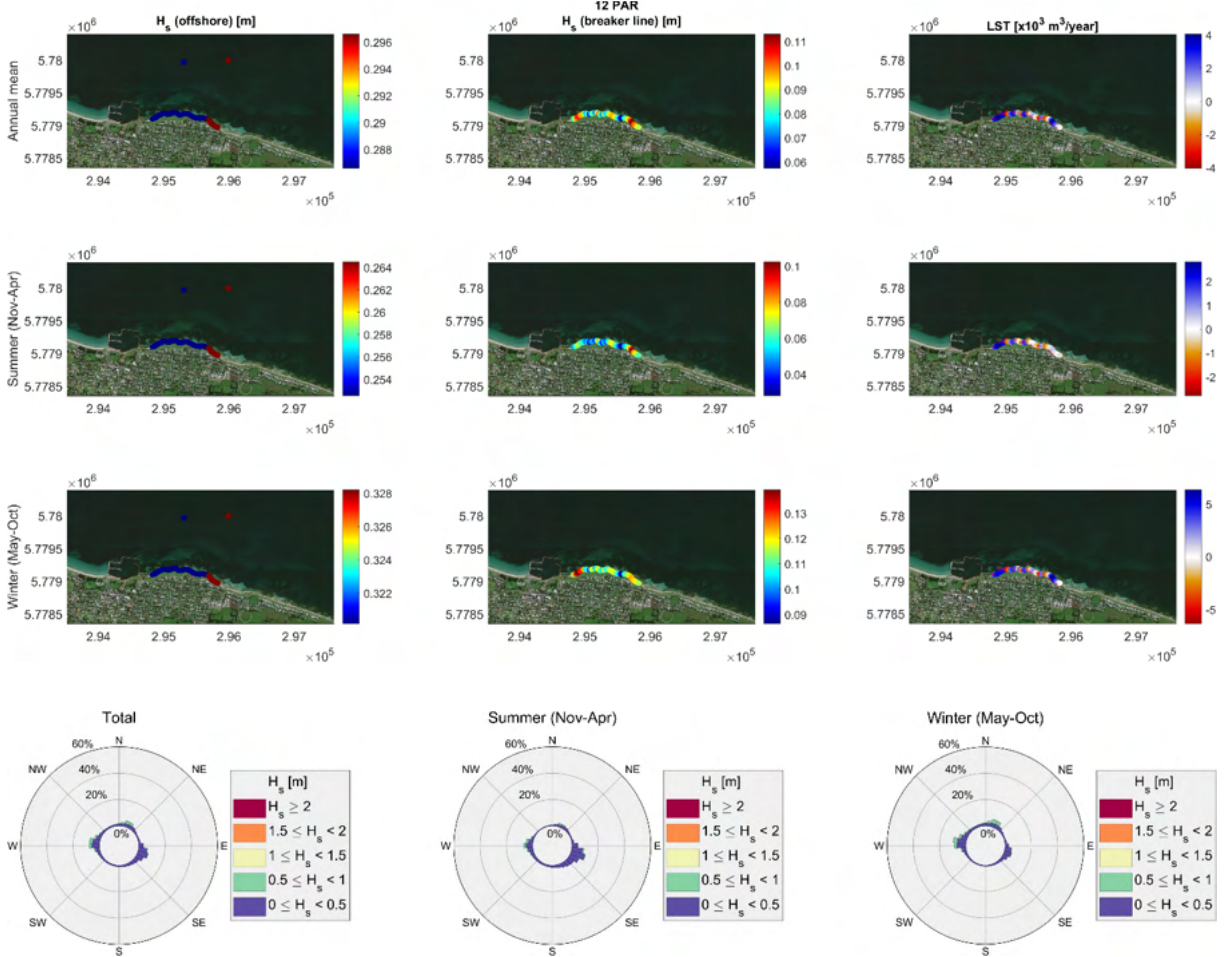
3.10.2 Model 2 – SCHISM-WWMIII



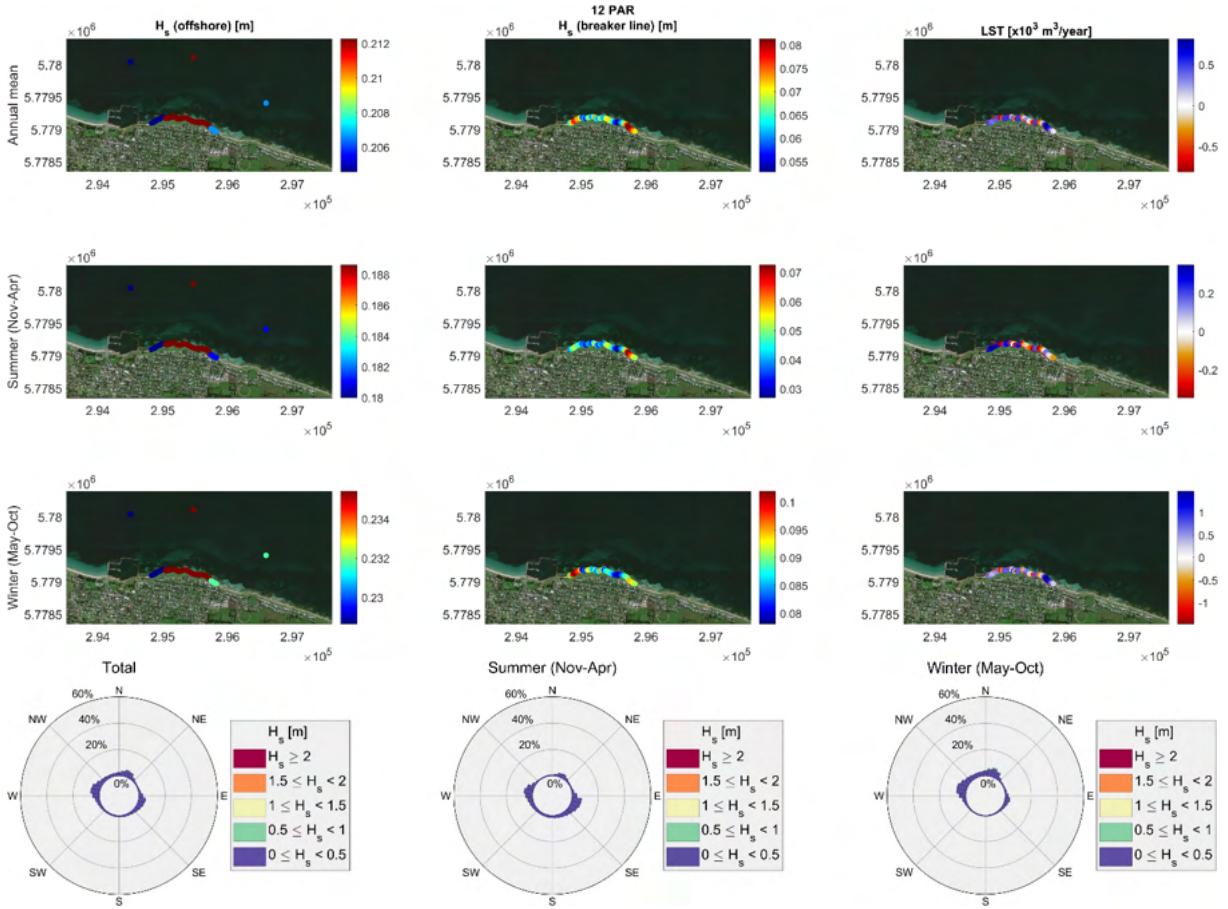
3.11 WTP (WTP)

3.12 Portarlington (PAR)

3.12.1 Model 1 – WW3

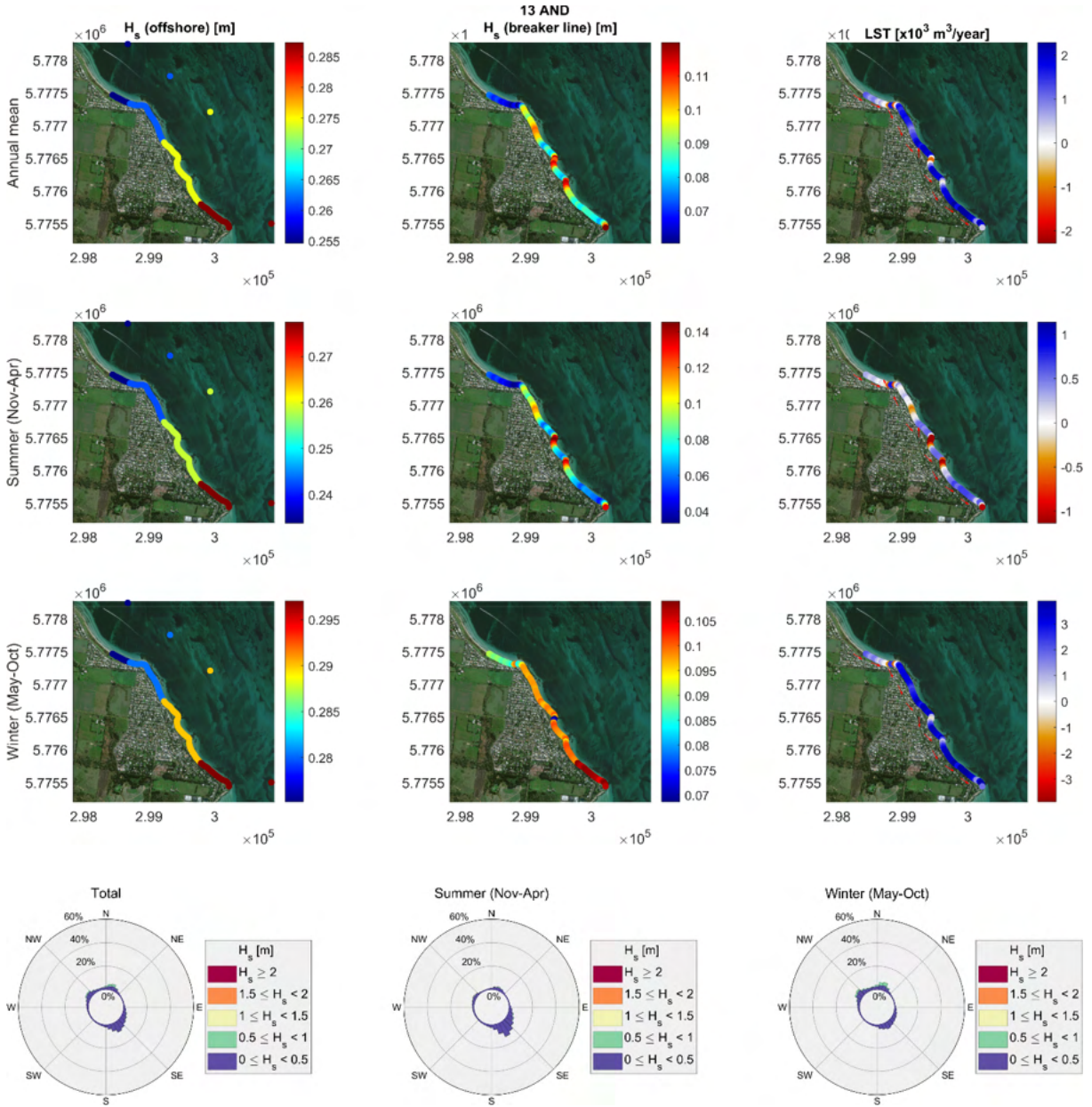


3.12.2 Model 2 – SCHISM-WWMIII

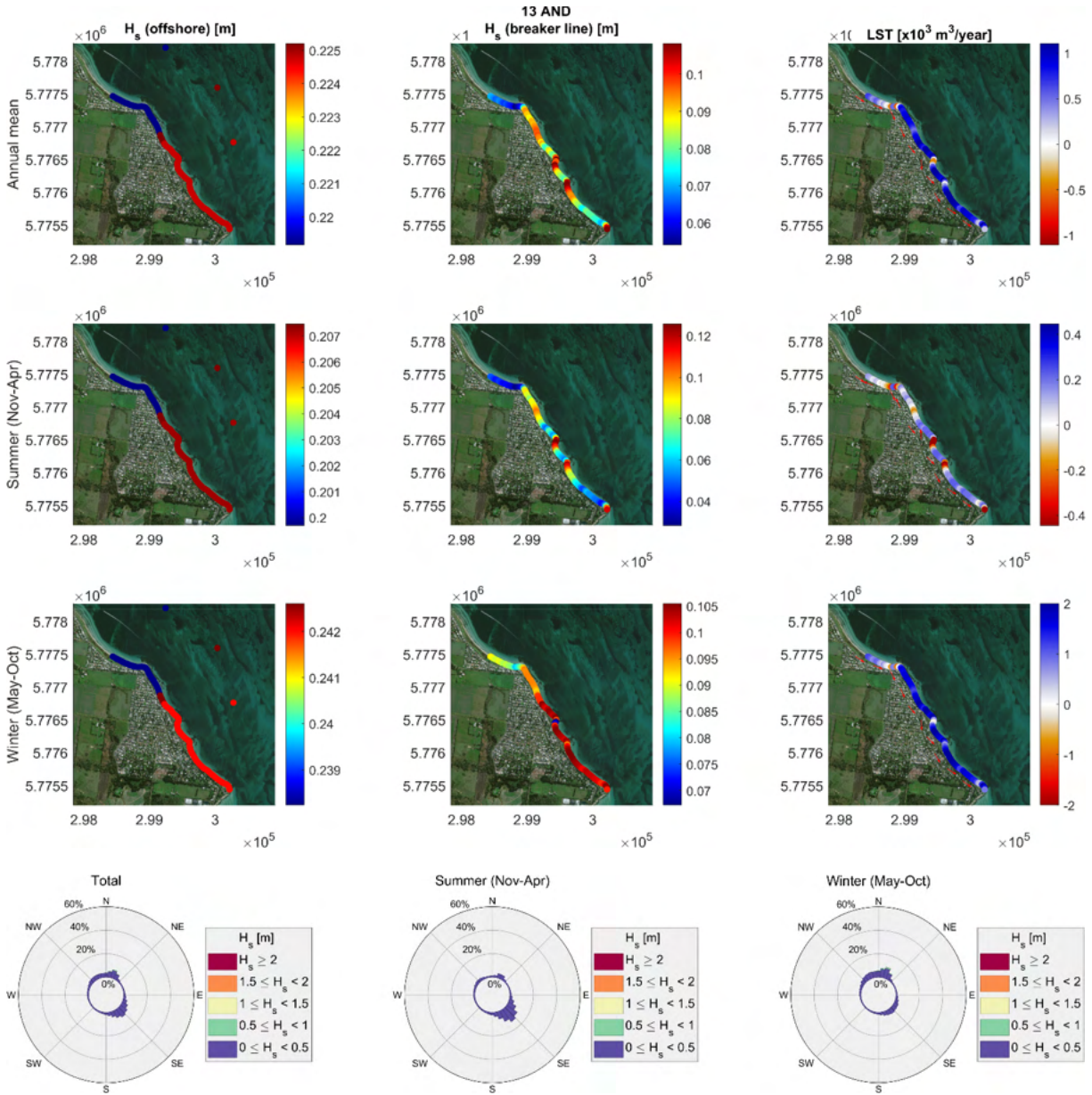


3.13 Anderson Reserve (AND)

3.13.1 Model 1 – WW3

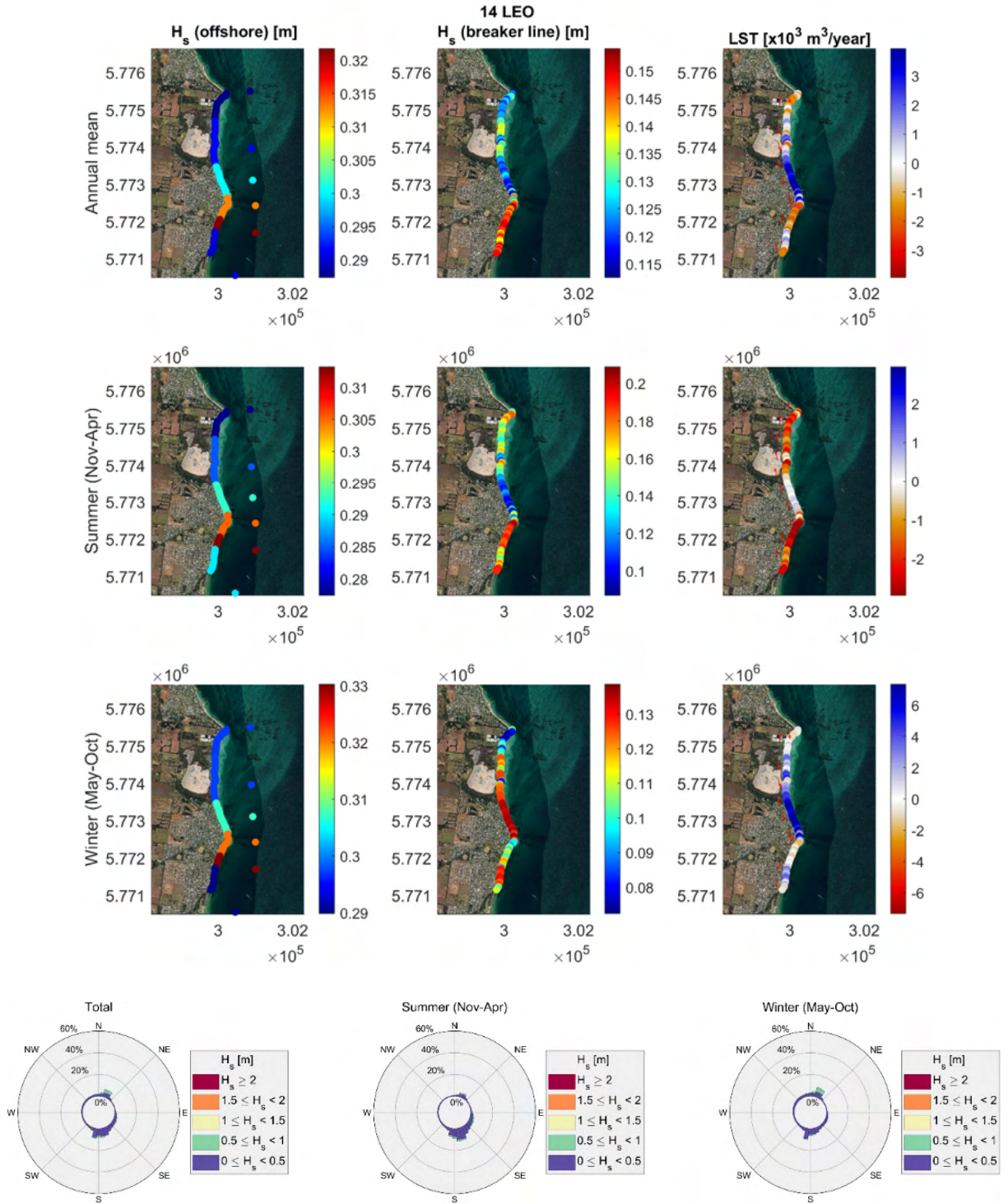


3.13.2 Model 2 – SCHISM-WWMIII

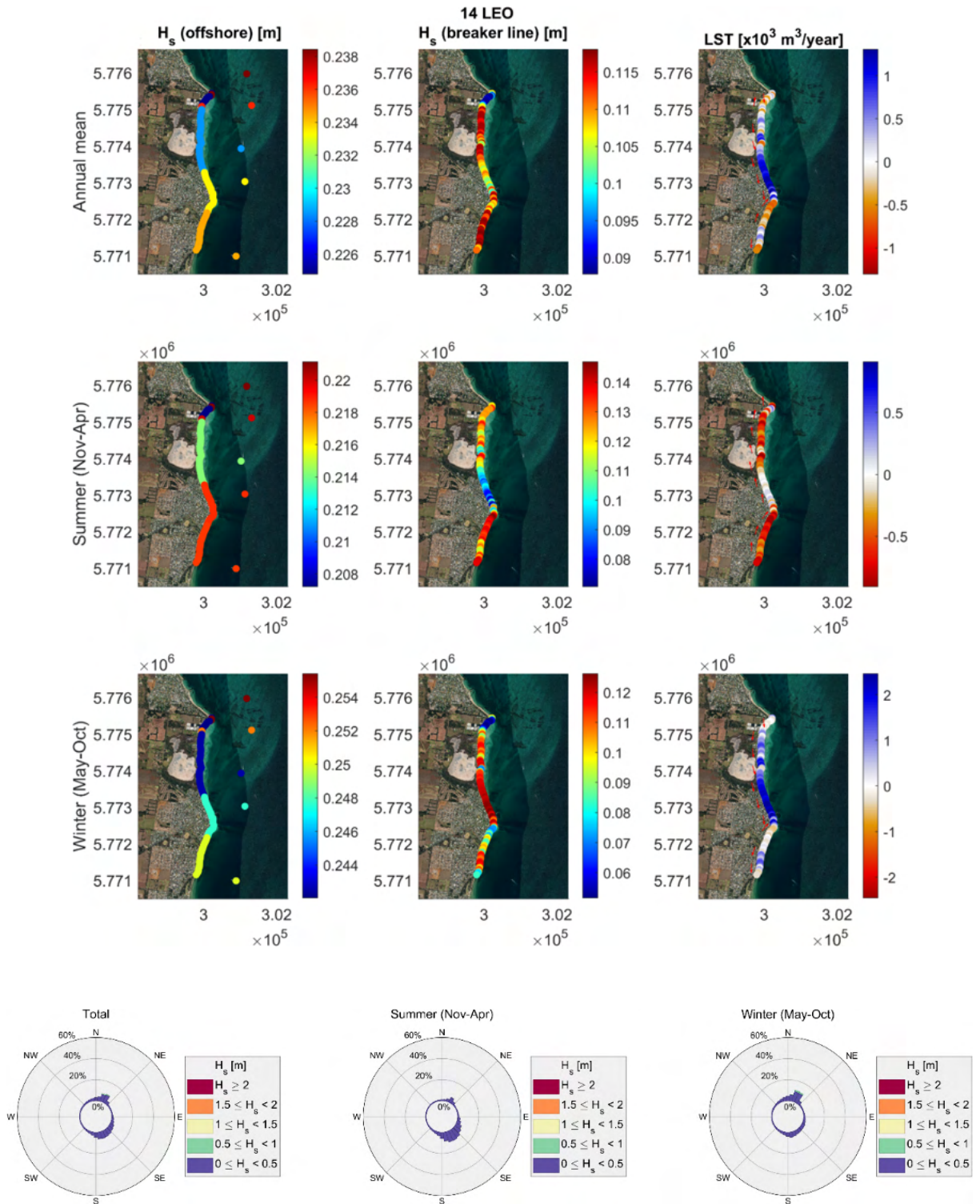


3.14 St Leonards (LEO)

3.14.1 Model 1 – WW3

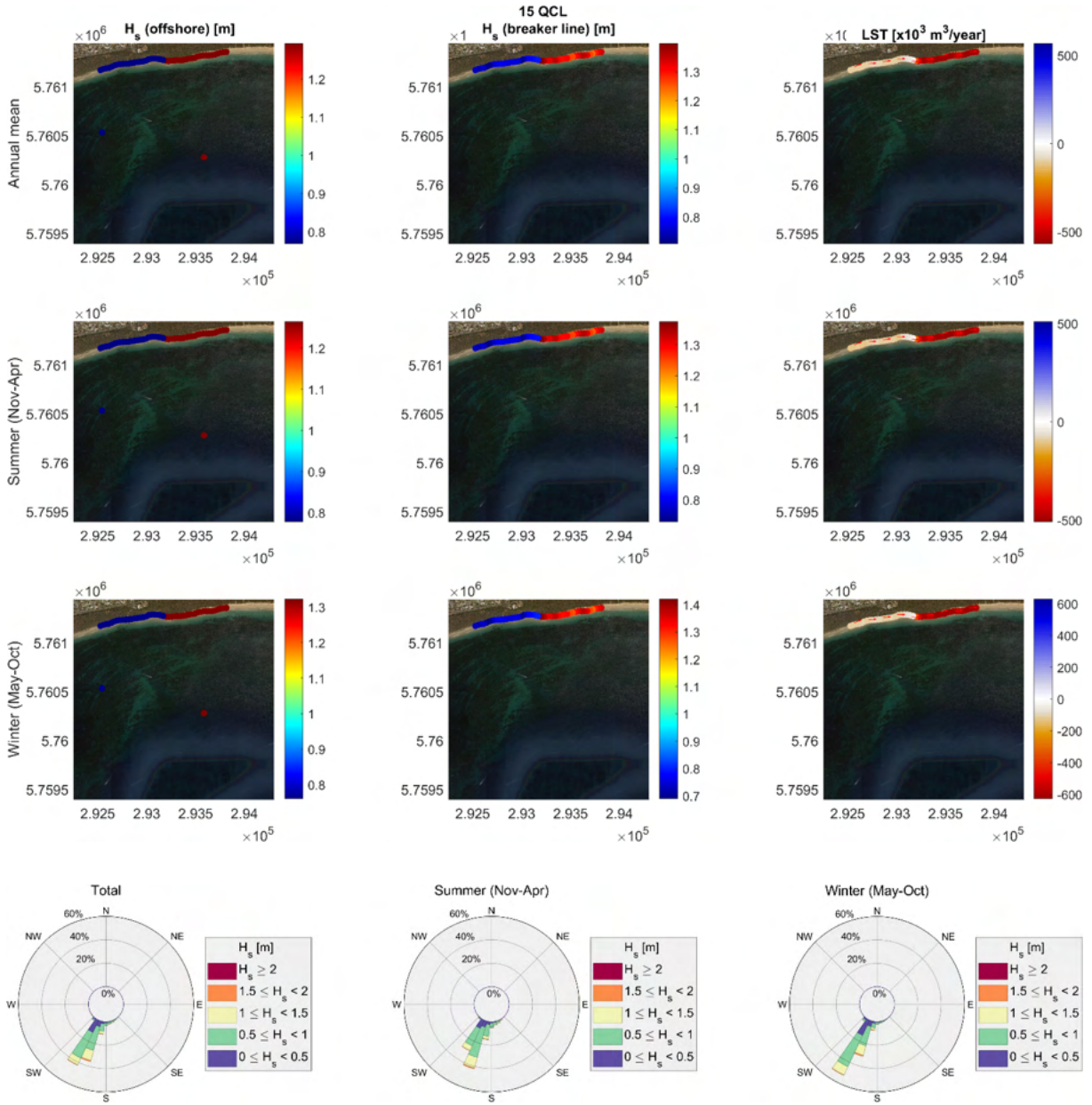


3.14.2 Model 2 – SCHISM-WWMIII

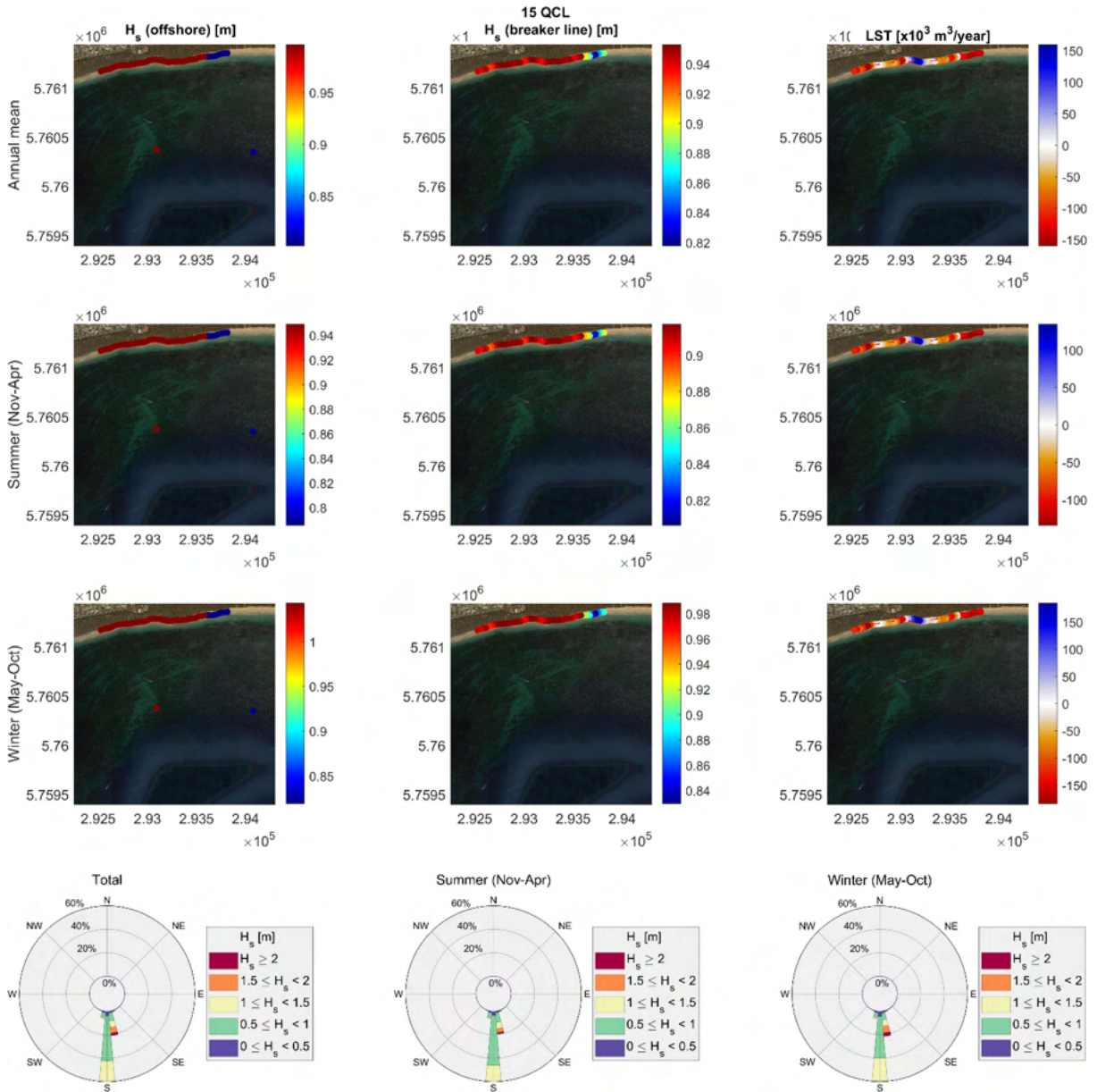


3.15 Queenscliff (QCL)

3.15.1 Model 1 – WW3

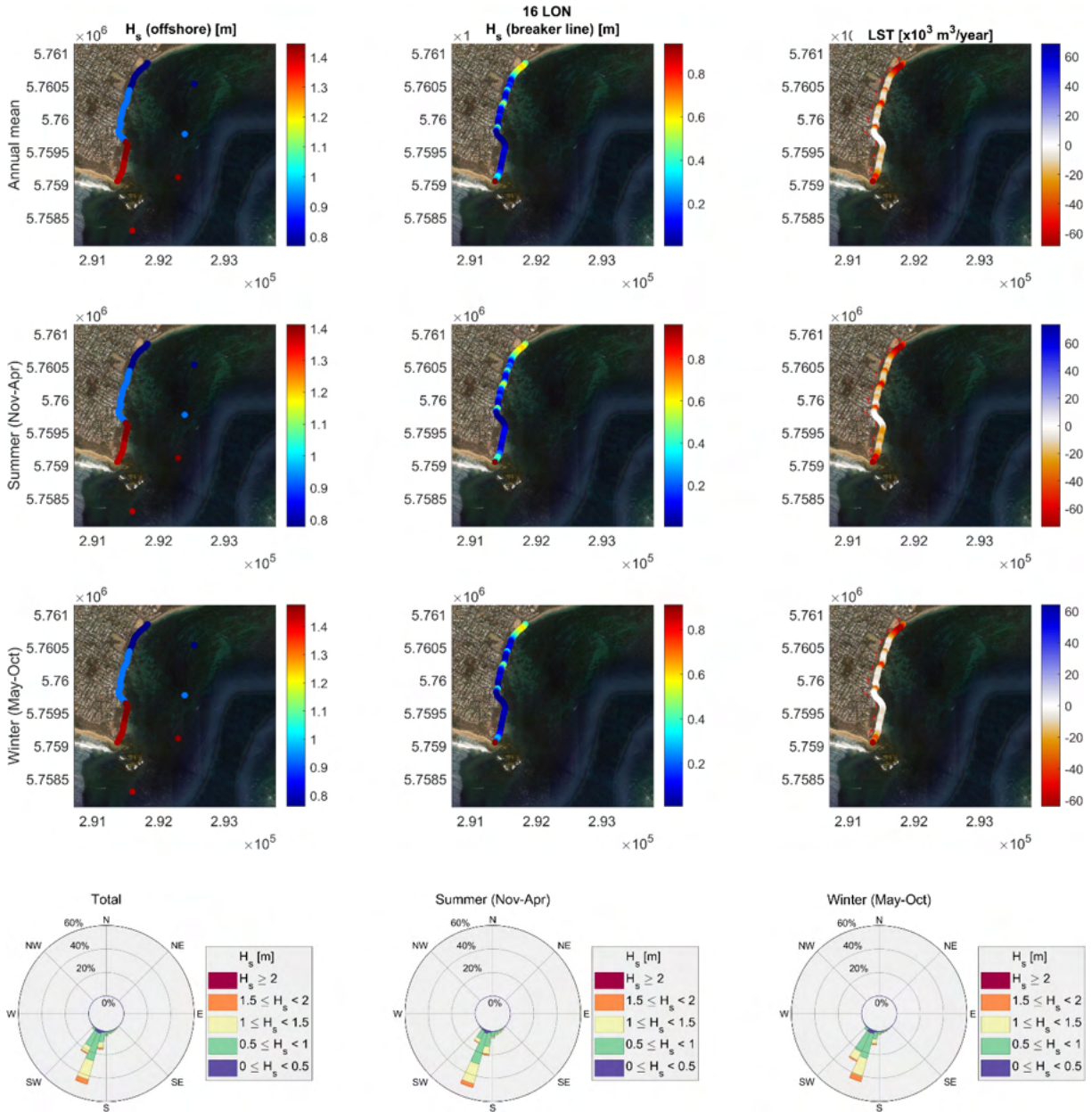


3.15.2 Model 2 – SCHISM-WWMIII

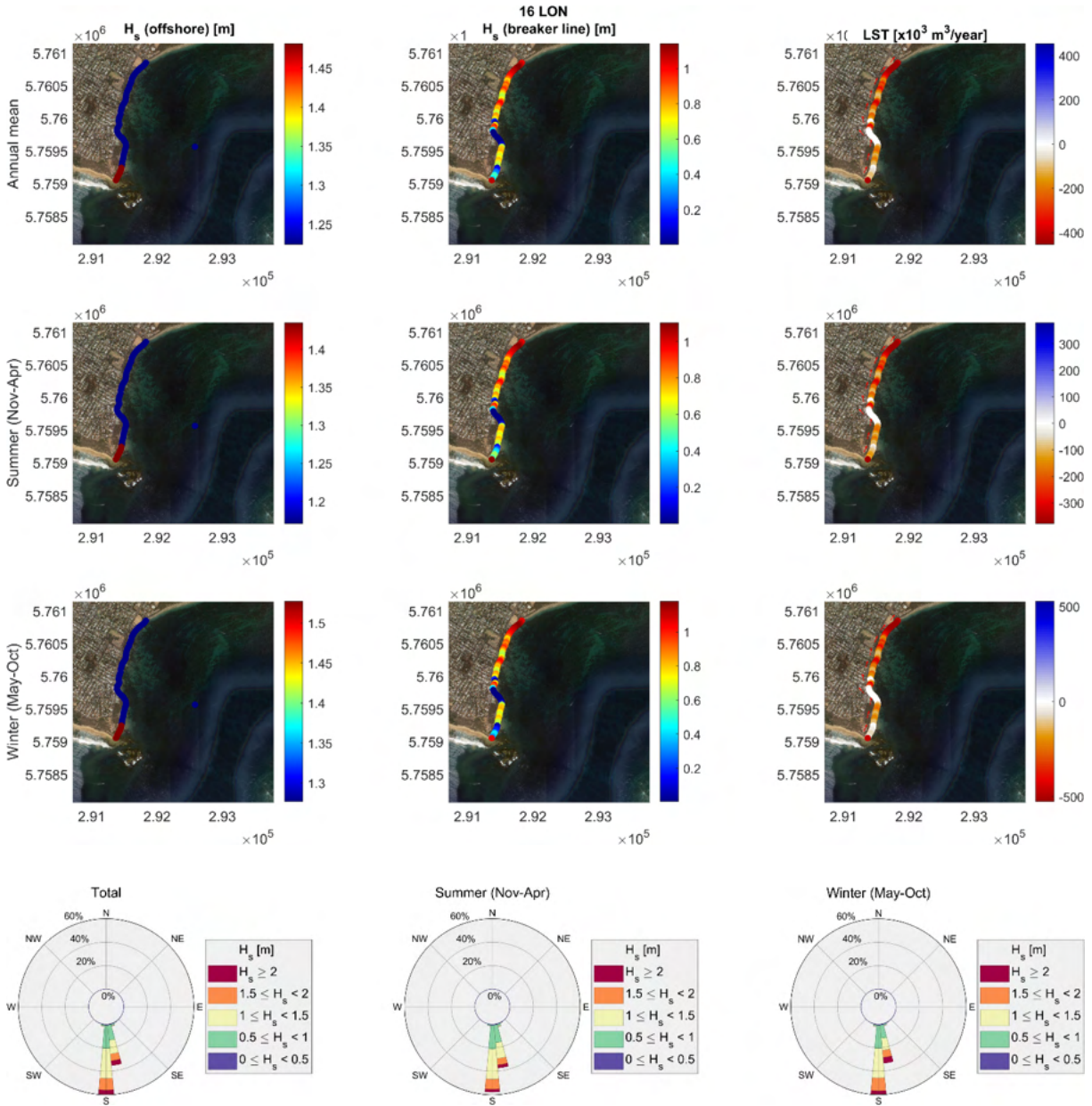


3.16 Point Lonsdale (LON)

3.16.1 Model 1 – WW3

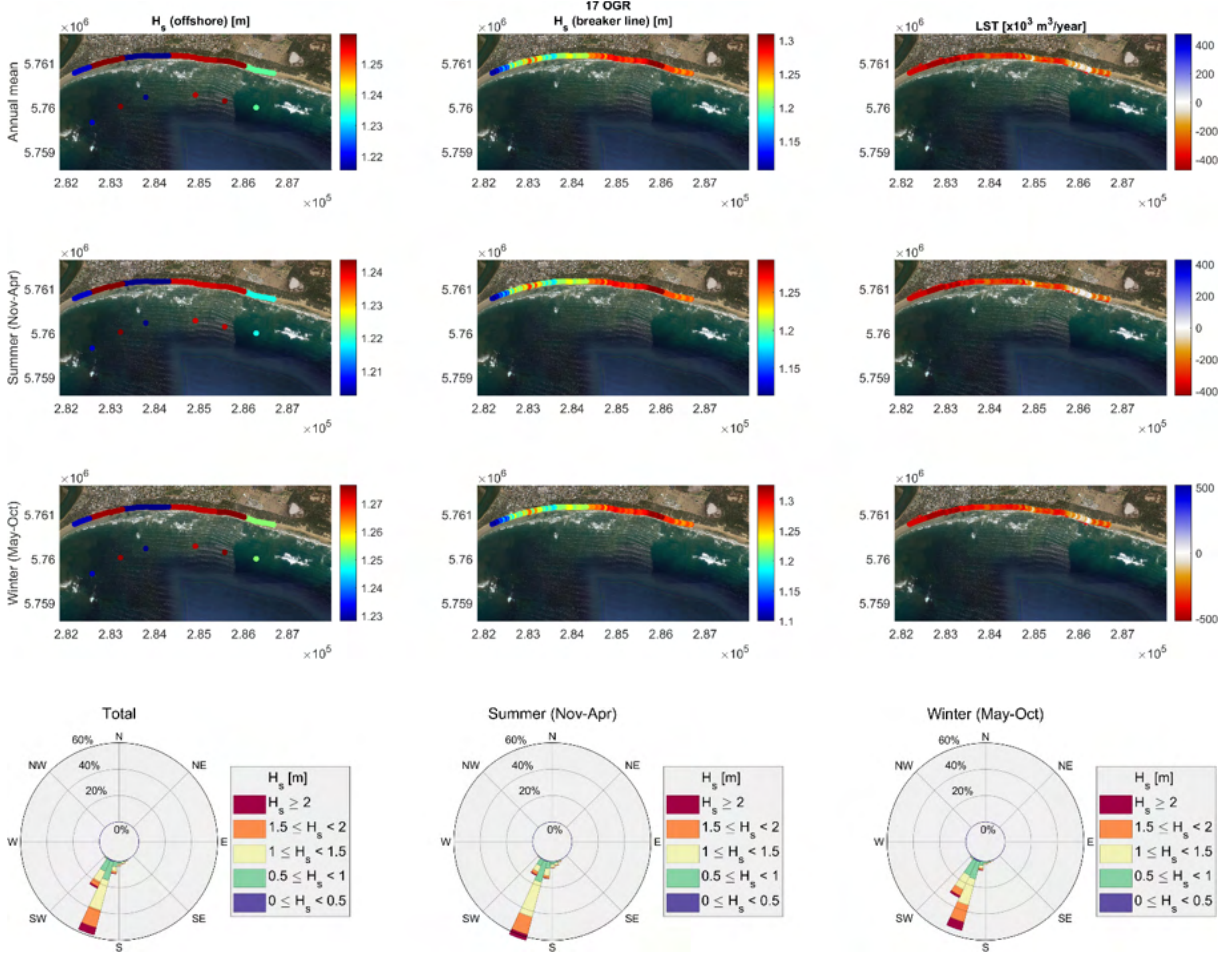


3.16.2 Model 2 – SCHISM-WWMIII



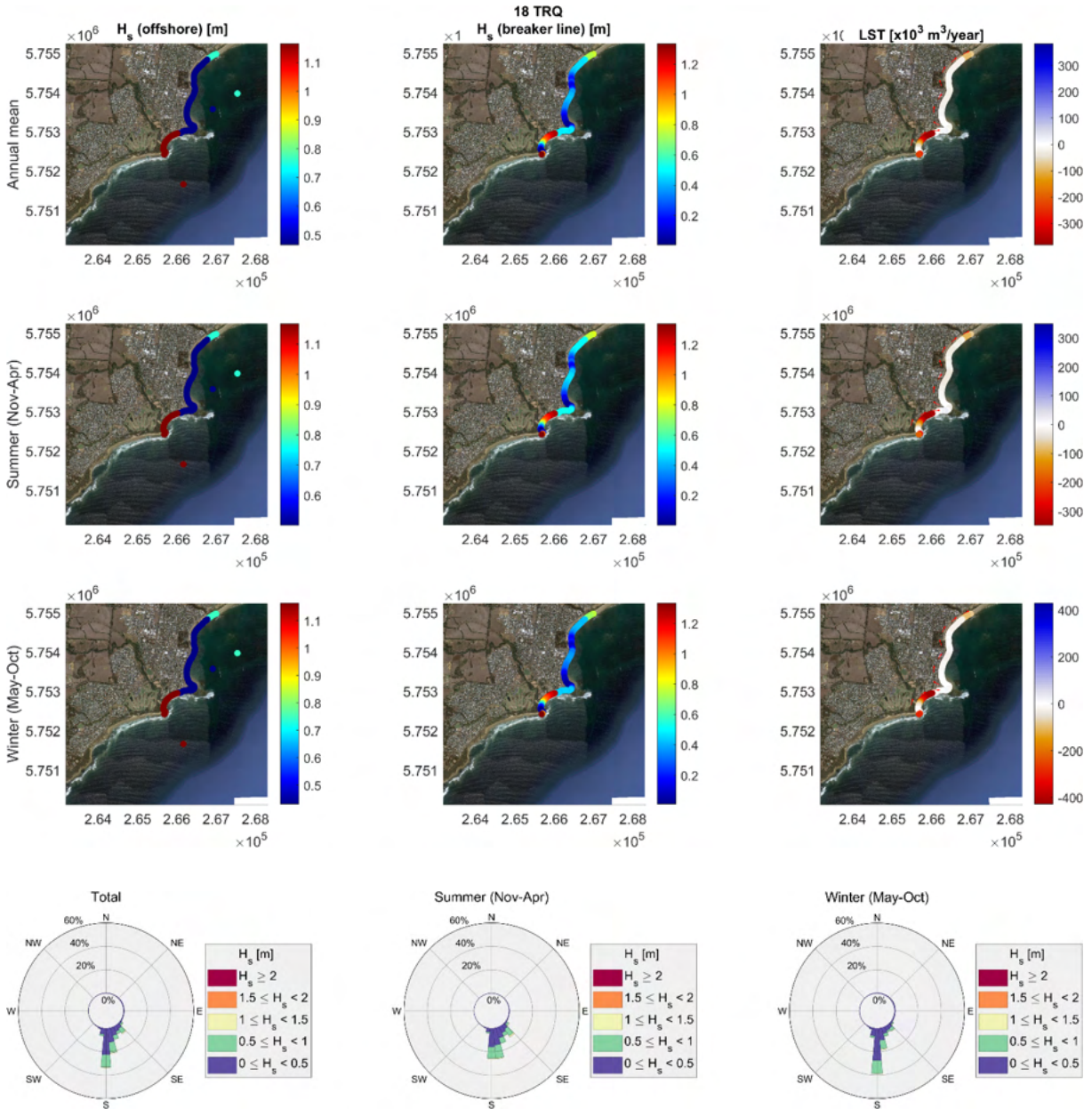
3.17 Ocean Grove (OGR)

3.17.1 Model 1 – WW3



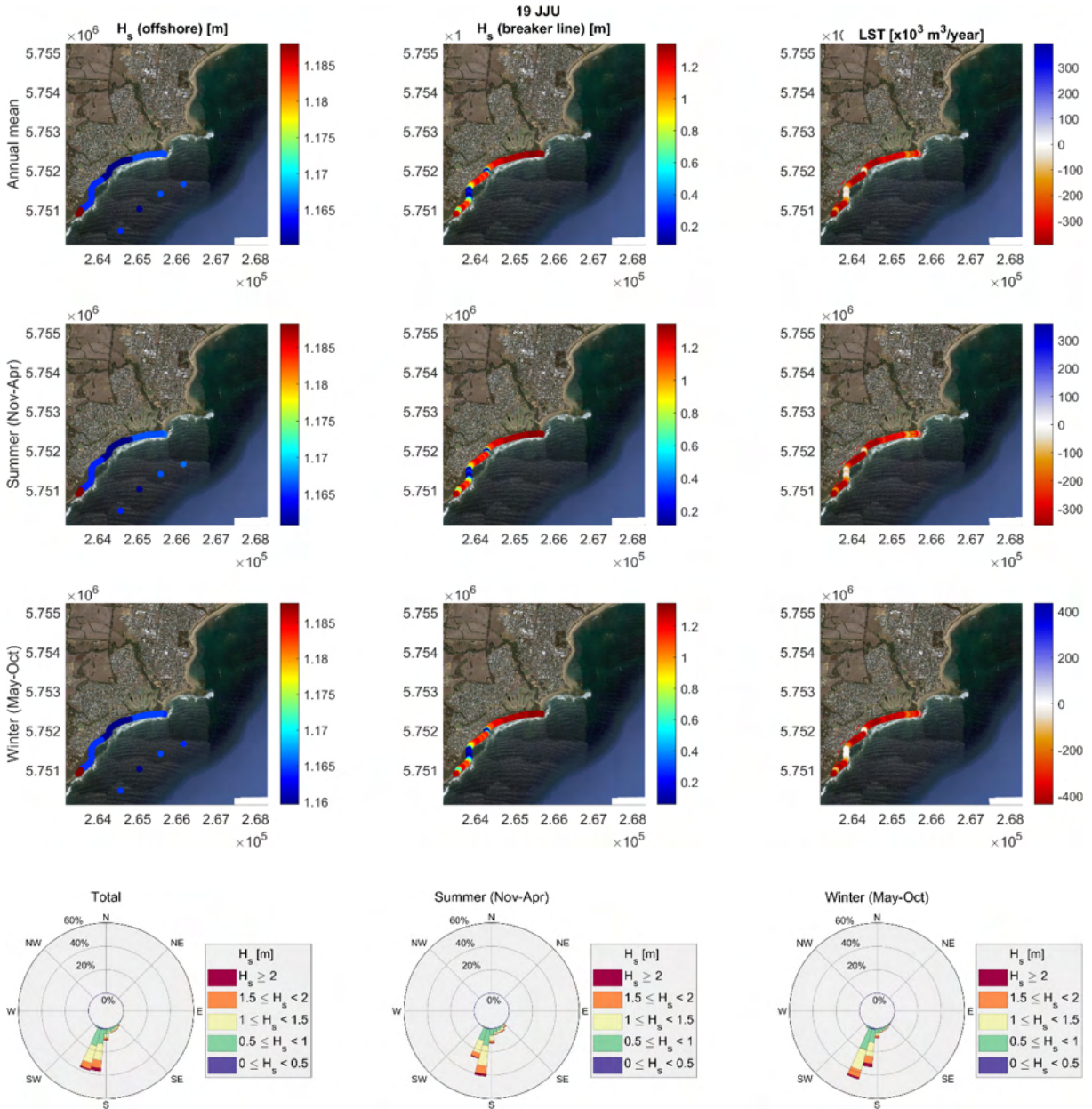
3.18 Torquay (TRQ)

3.18.1 Model 1 – WW3



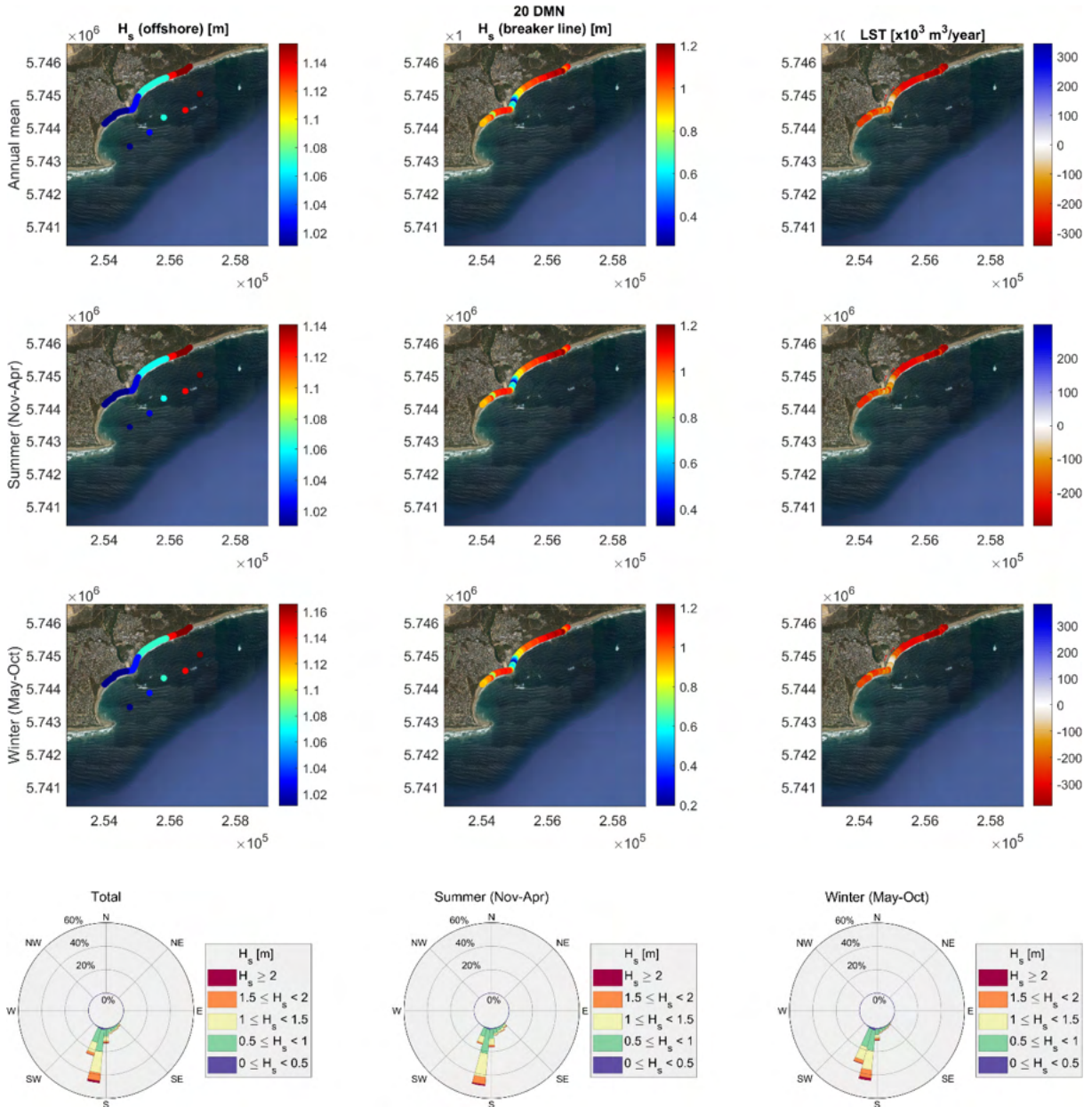
3.19 Jan Juc (JJU)

3.19.1 Model 1 – WW3



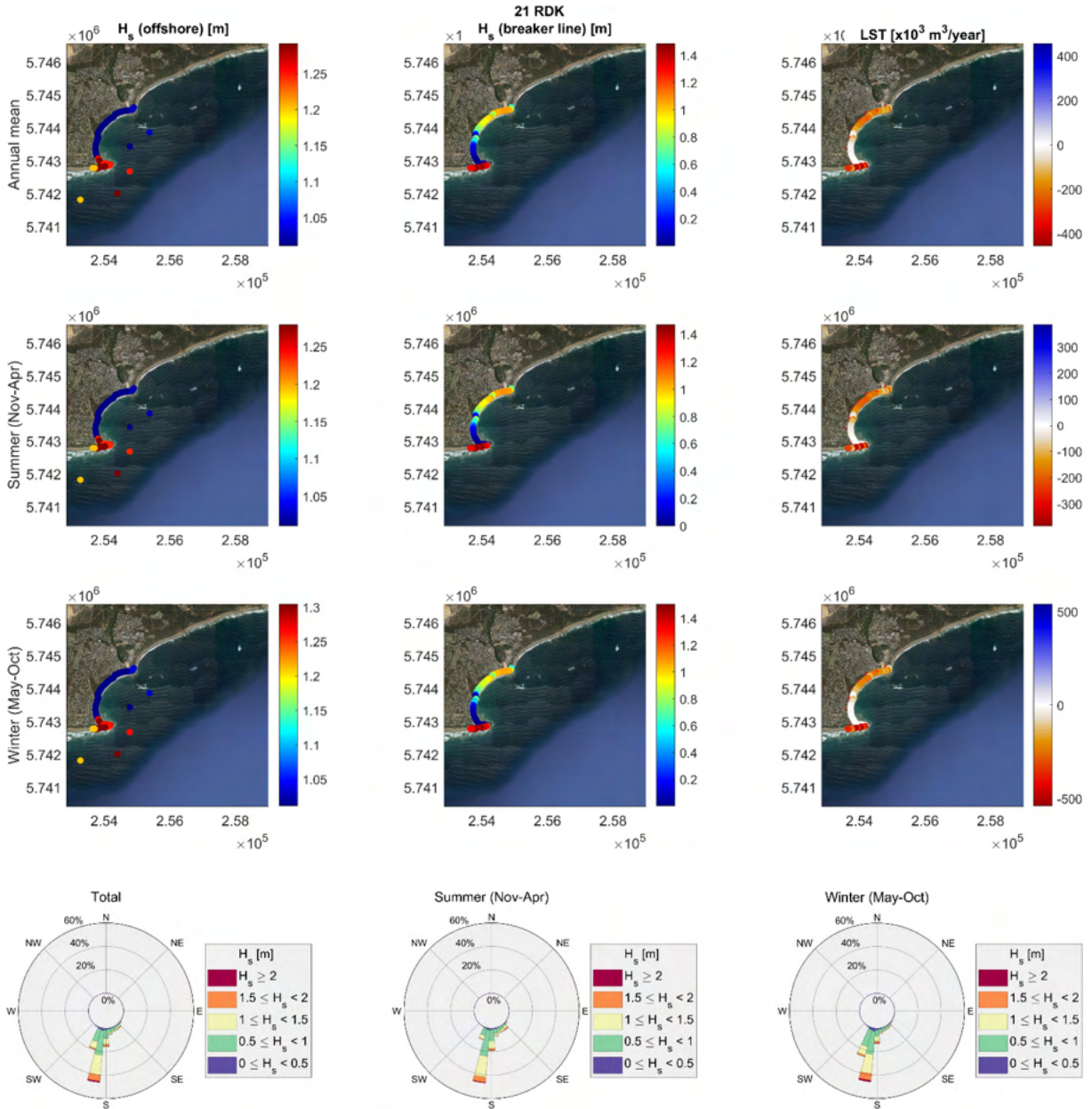
3.20 Demons Bluff (DMN)

3.20.1 Model 1 – WW3



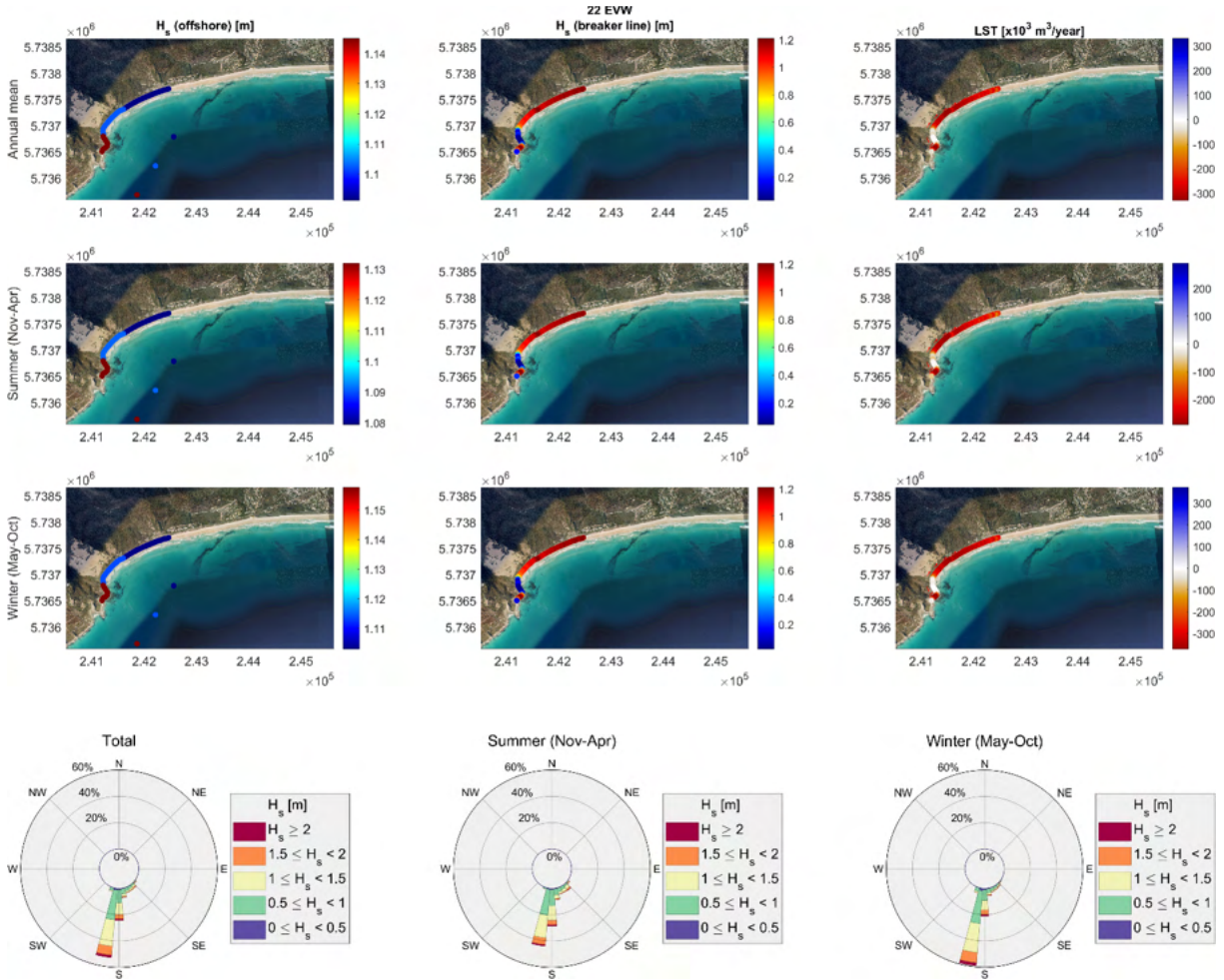
3.21 Point Roadknight (RDK)

3.21.1 Model 1 – WW3



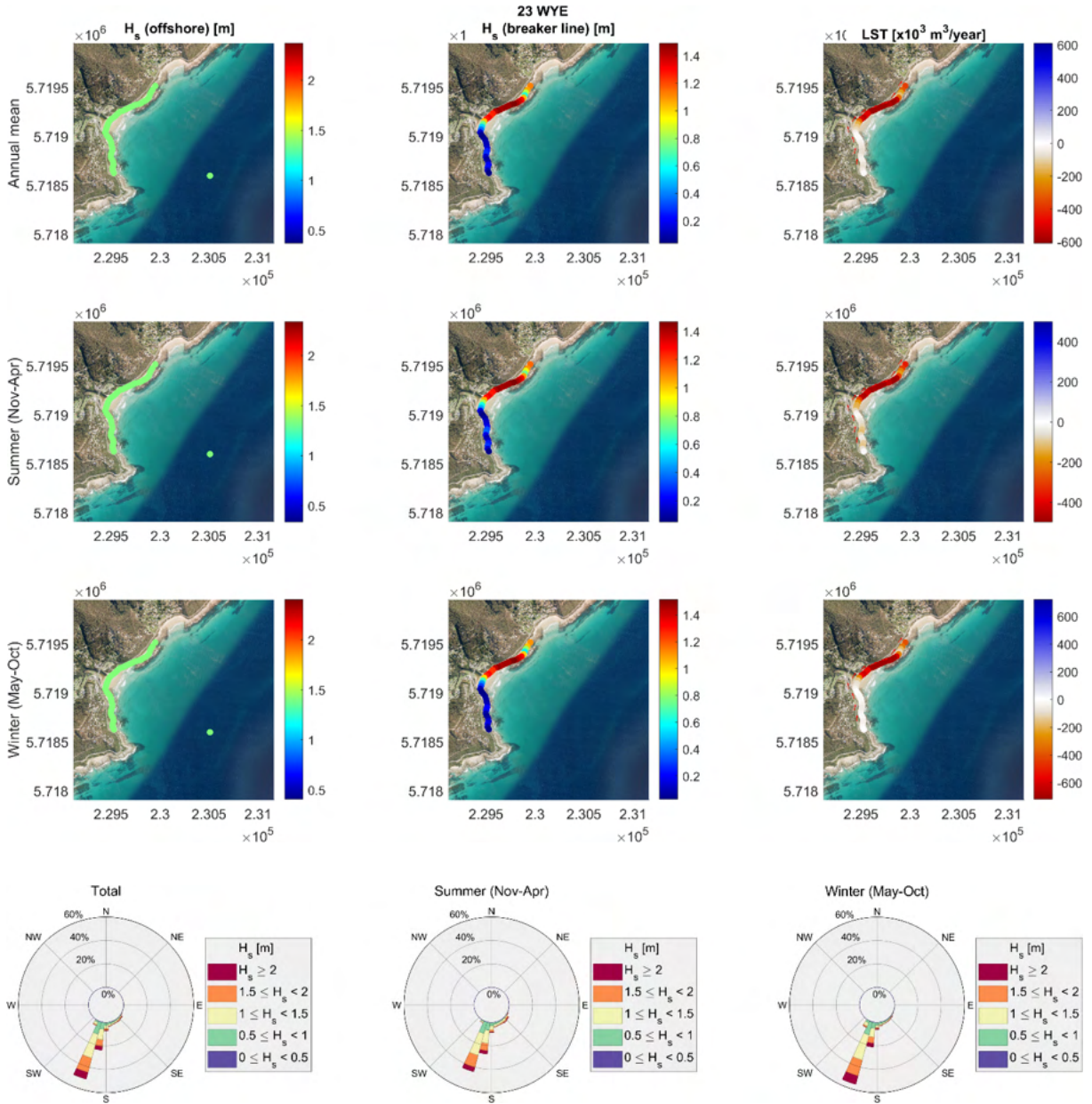
3.22 Eastern View (EVW)

3.22.1 Model 1 – WW3



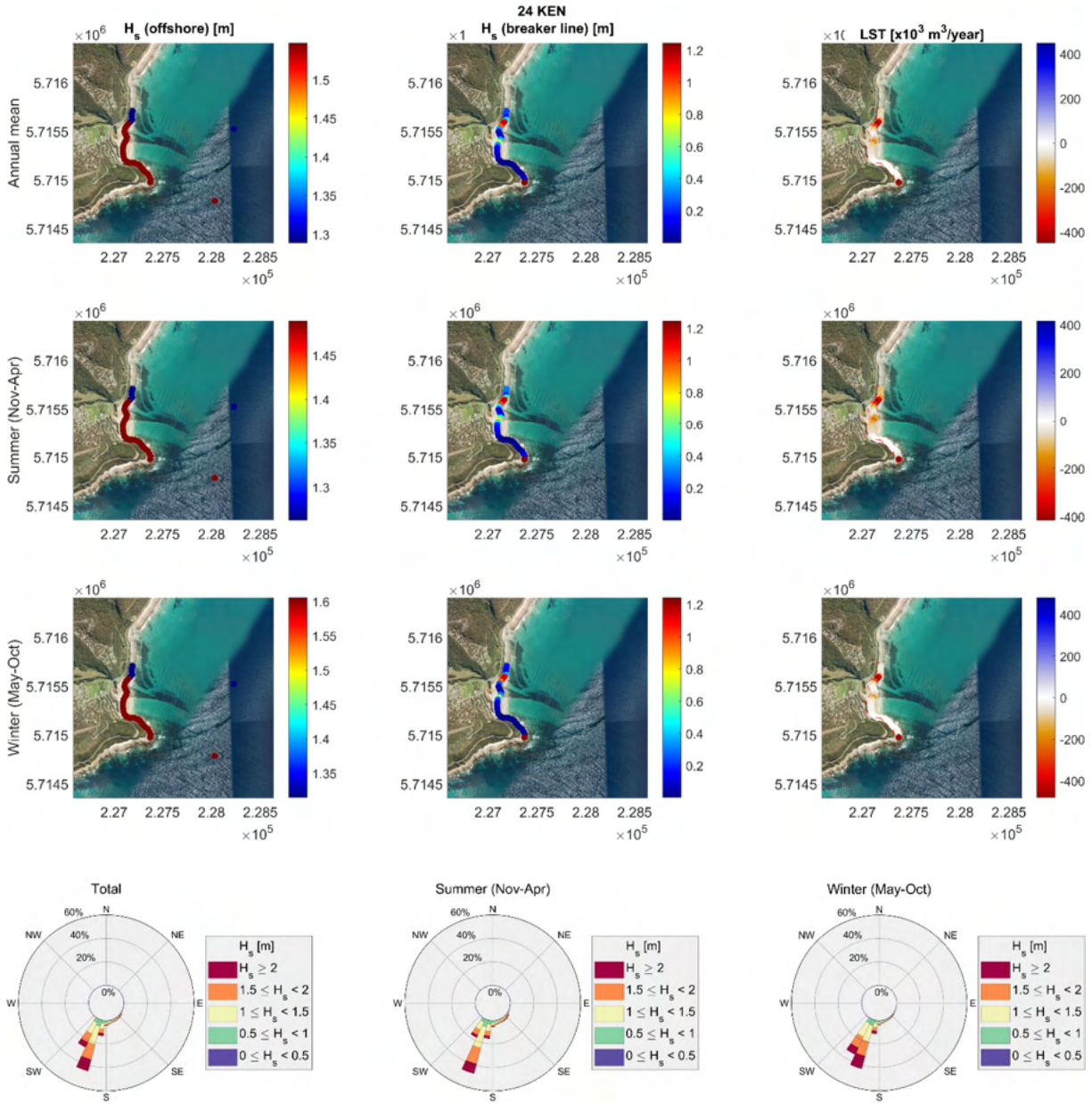
3.23 Wye River (WYE)

3.23.1 Model 1 – WW3



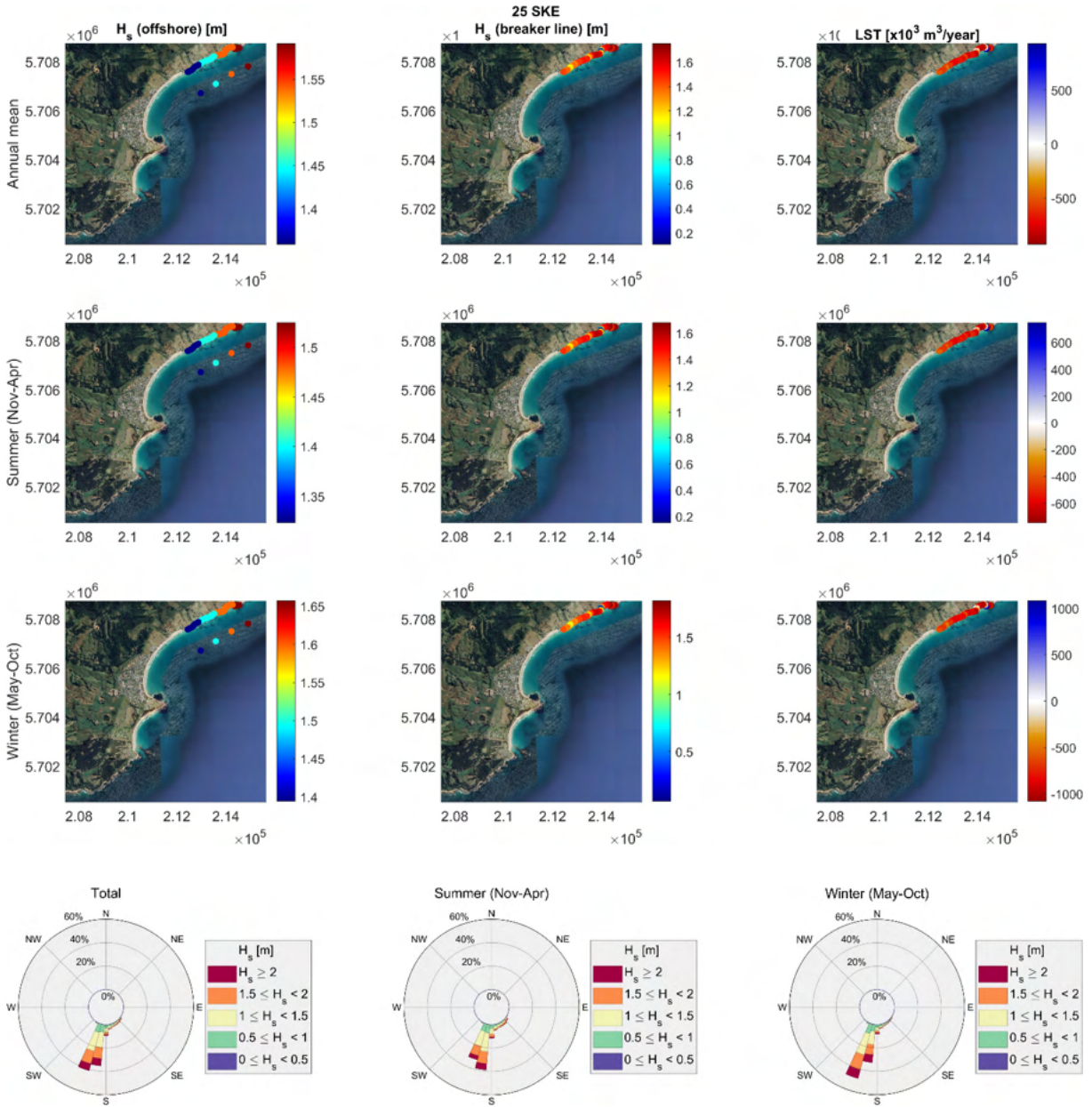
3.24 Kennett River (KEN)

3.24.1 Model 1 – WW3



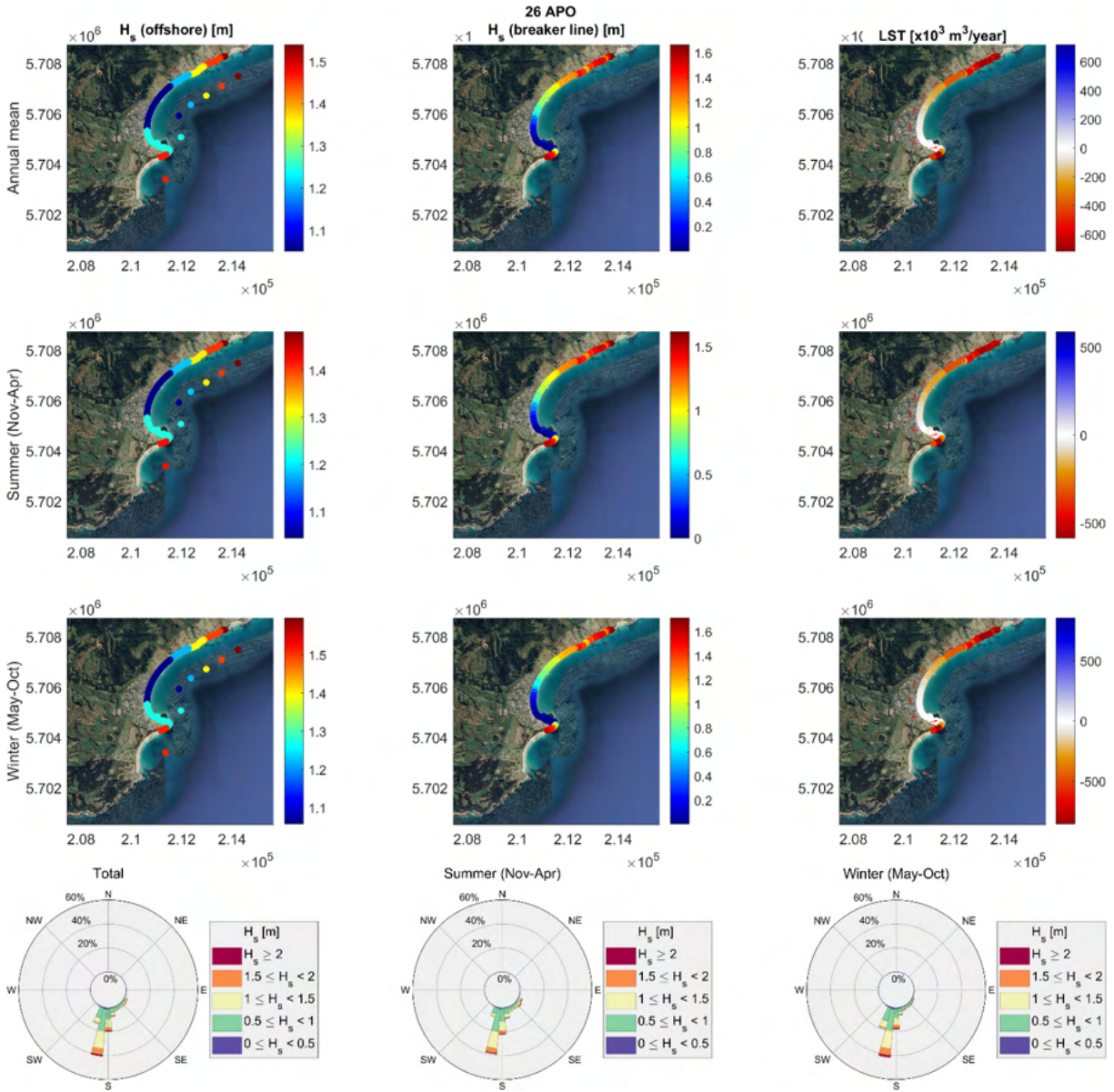
3.25 Skenes Creek (SKE)

3.25.1 Model 1 – WW3



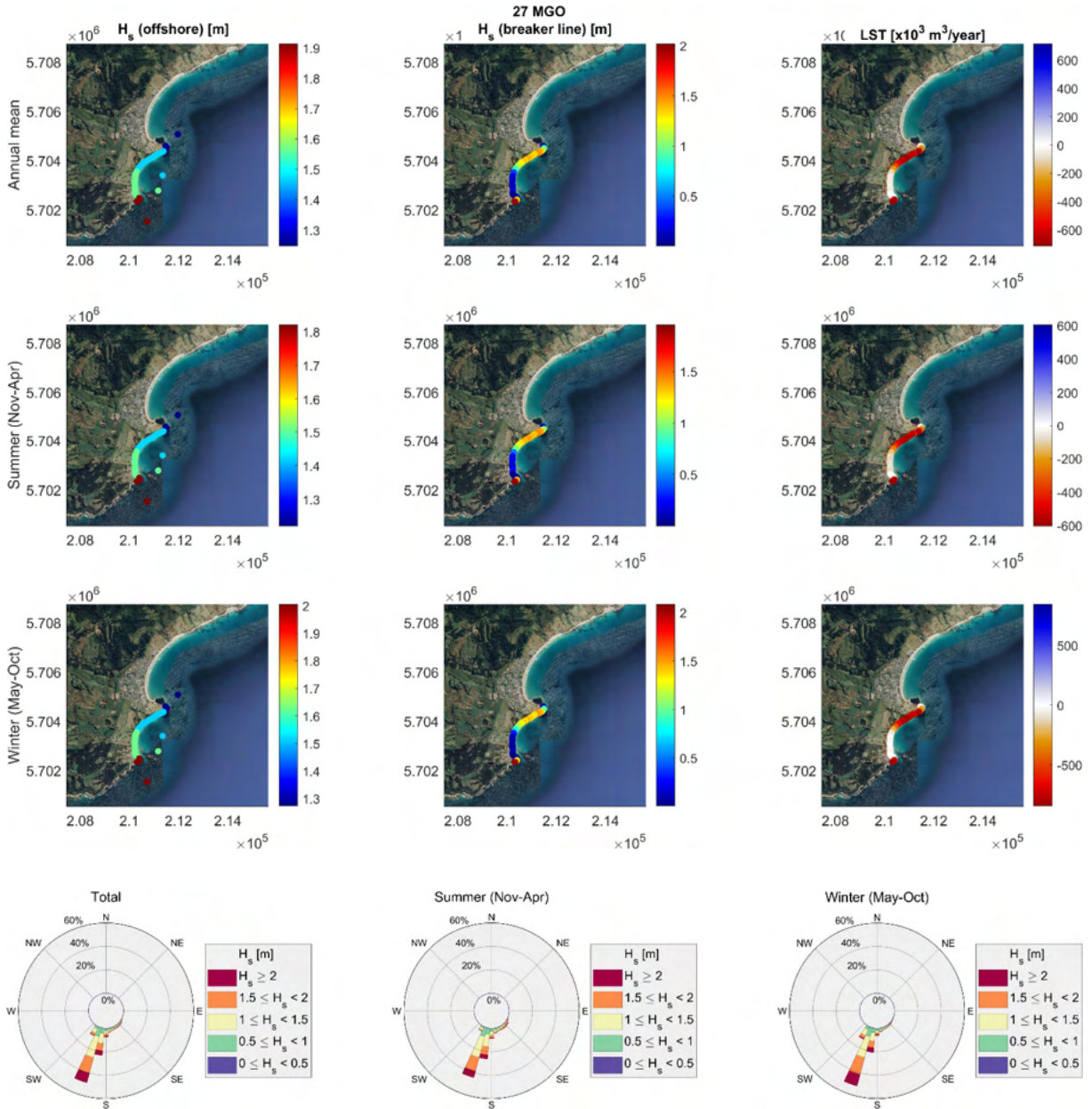
3.26 Apollo Bay (APO)

3.26.1 Model 1 – WW3



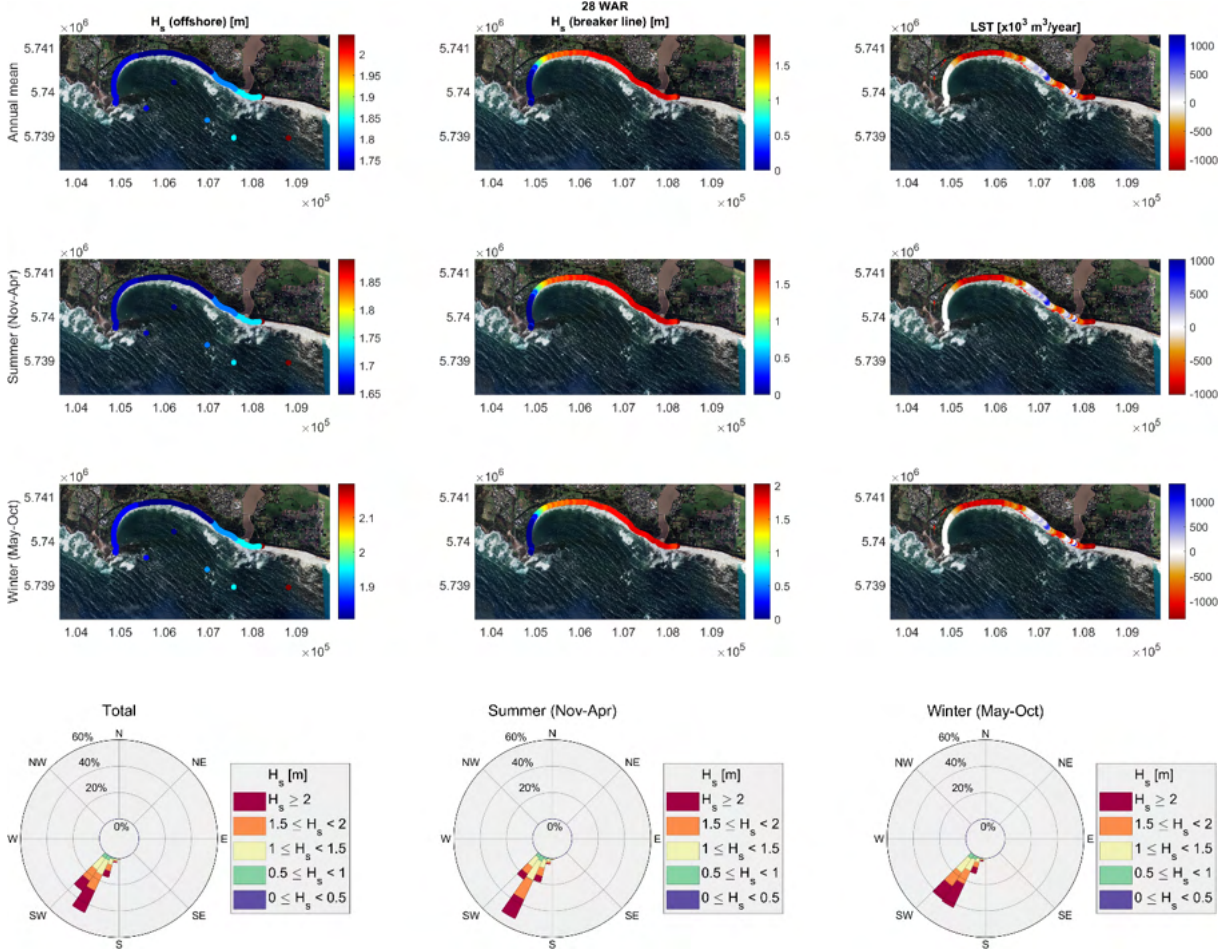
3.27 Marengo (MGO)

3.27.1 Model 1 – WW3



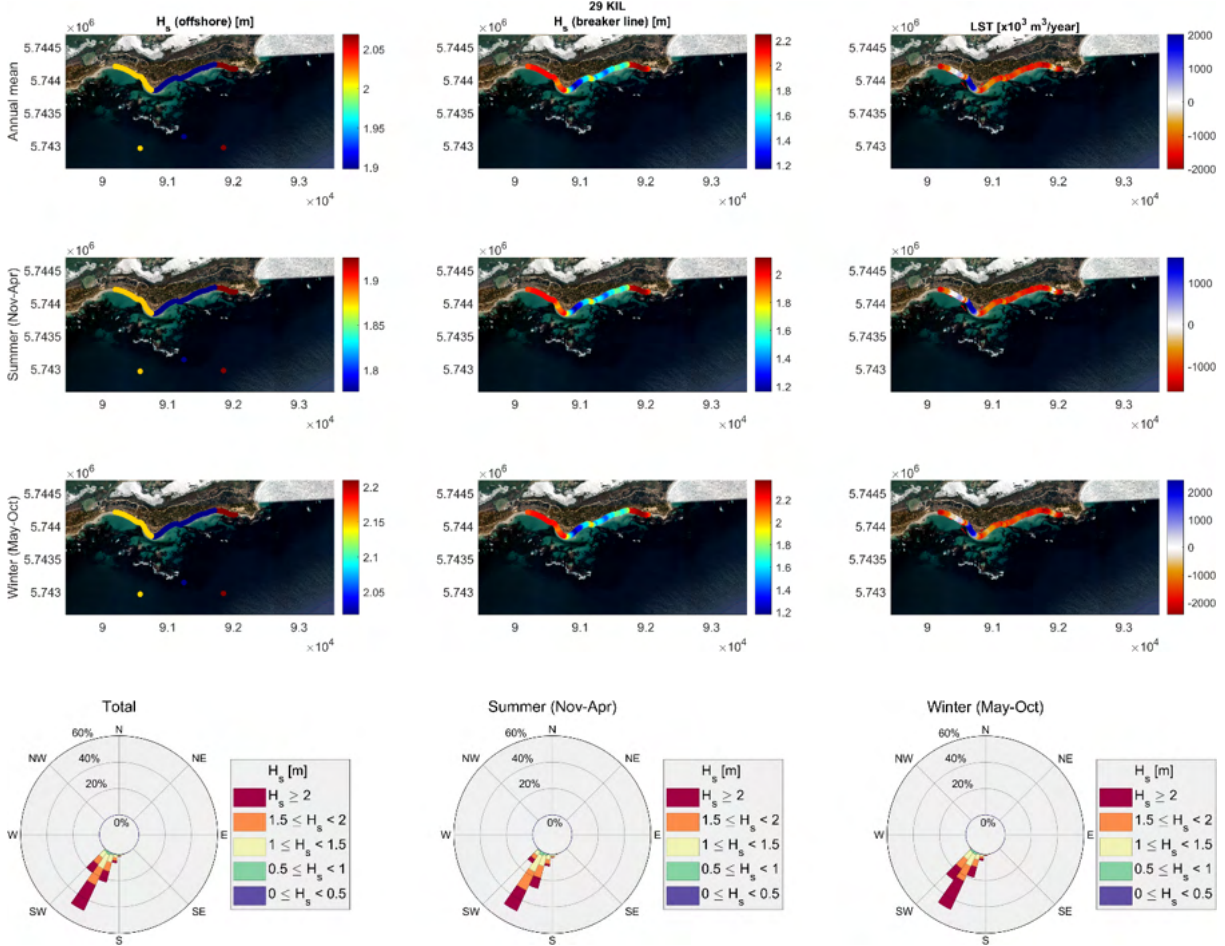
3.28 Warrnambool (WAR)

3.28.1 Model 1 – WW3



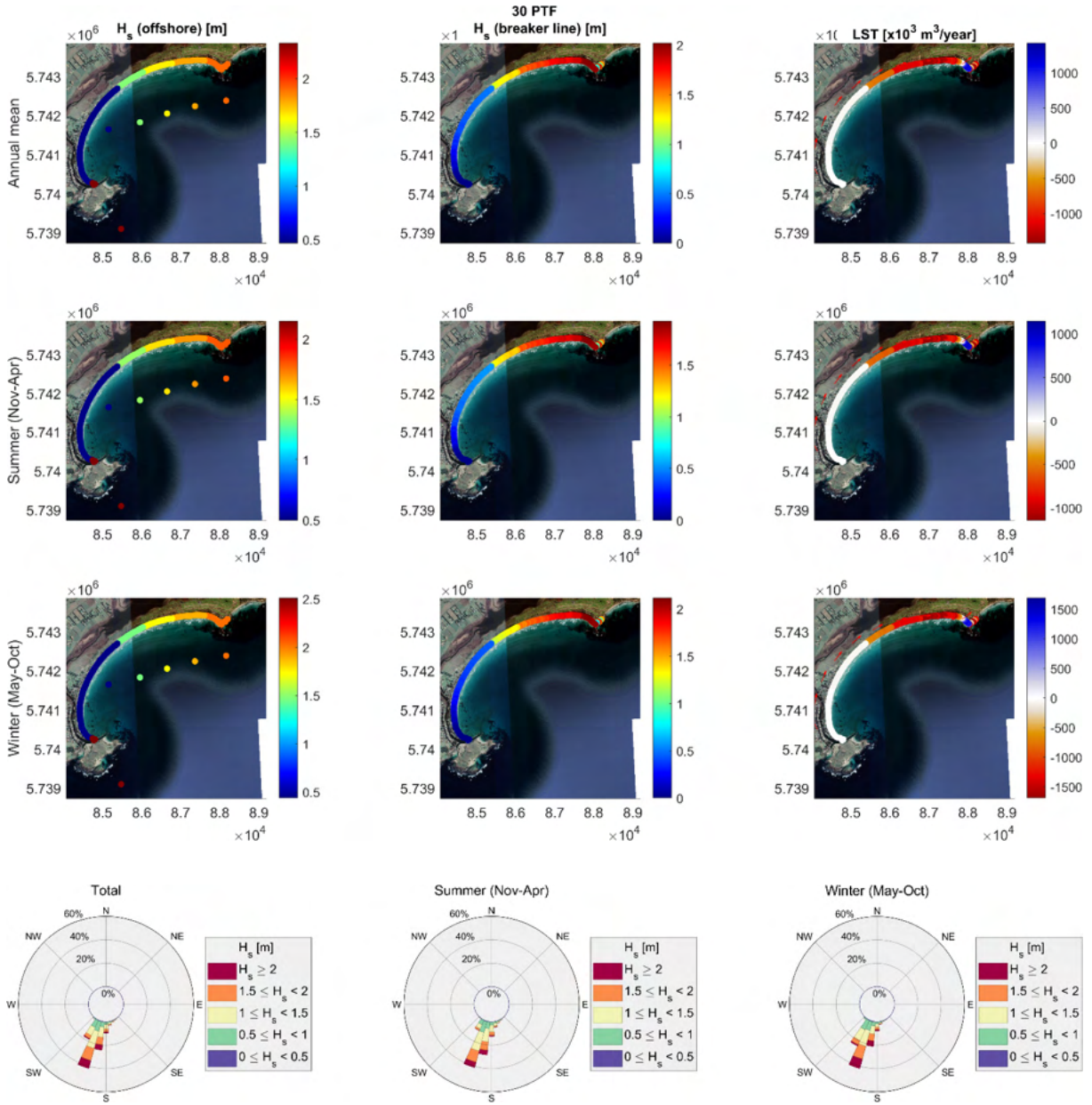
3.29 Killarney (KIL)

3.29.1 Model 1 – WW3



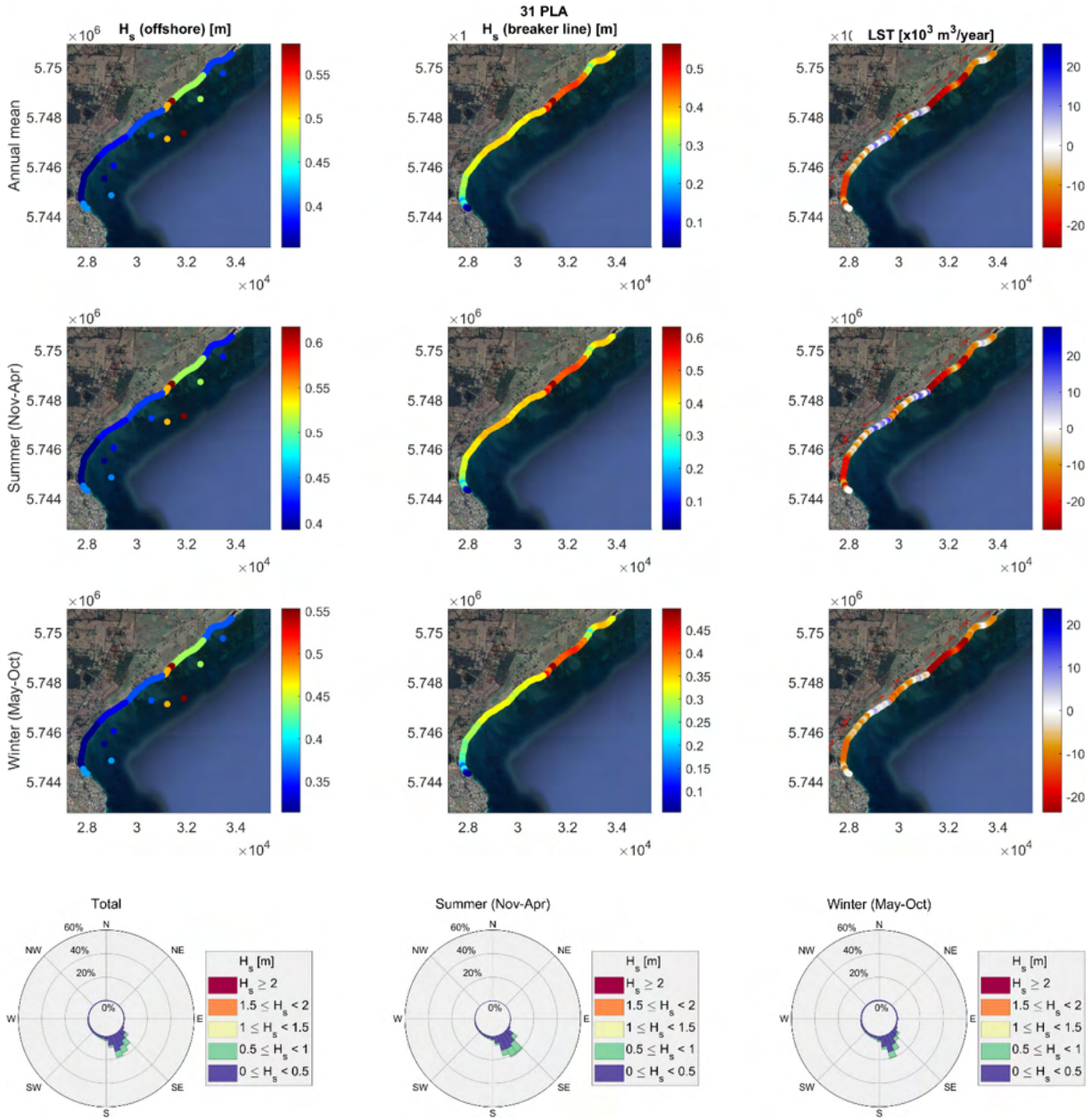
3.30 Port Fairy (PTF)

3.30.1 Model 1 – WW3



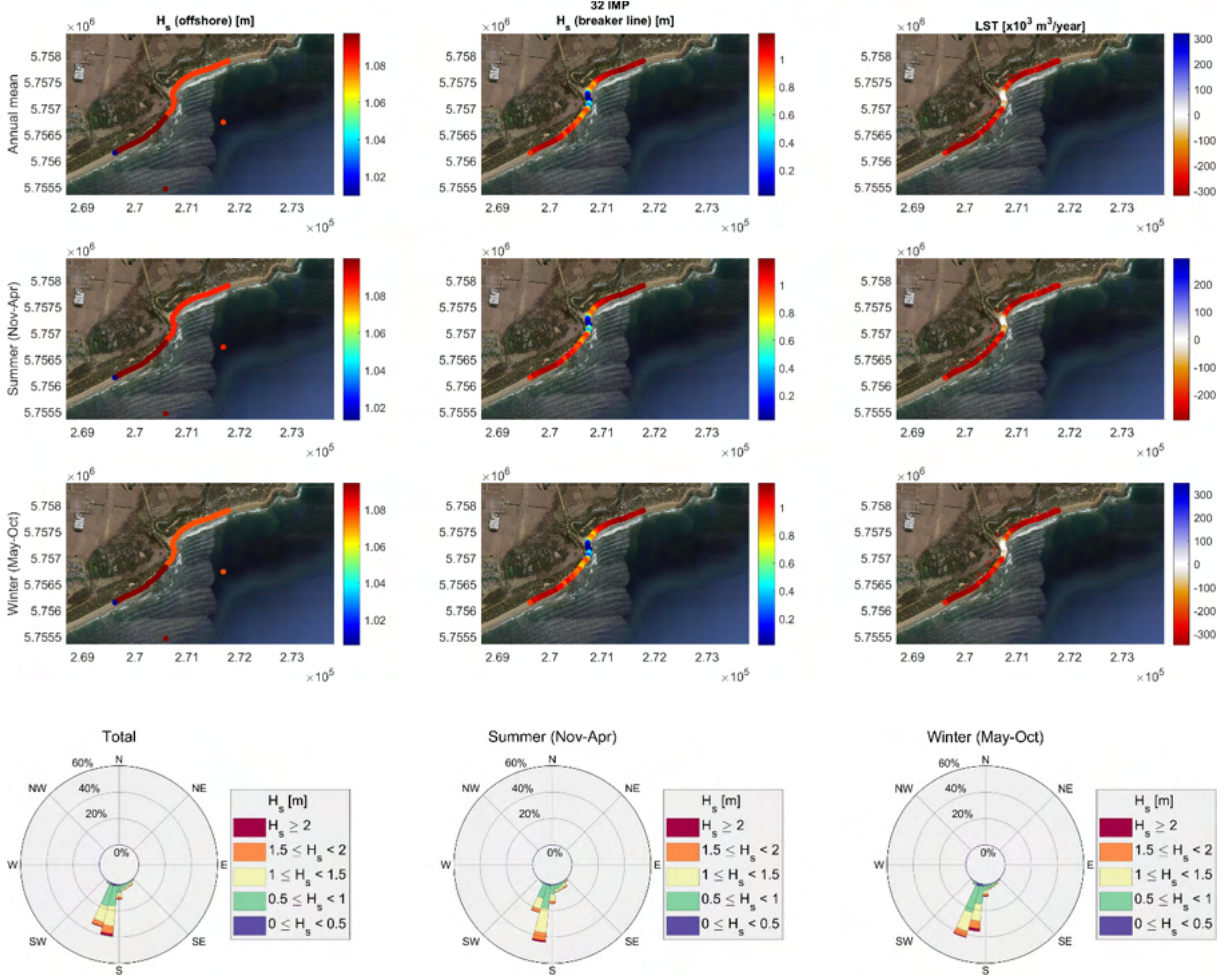
3.31 Portland (PLA)

3.31.1 Model 1 – WW3



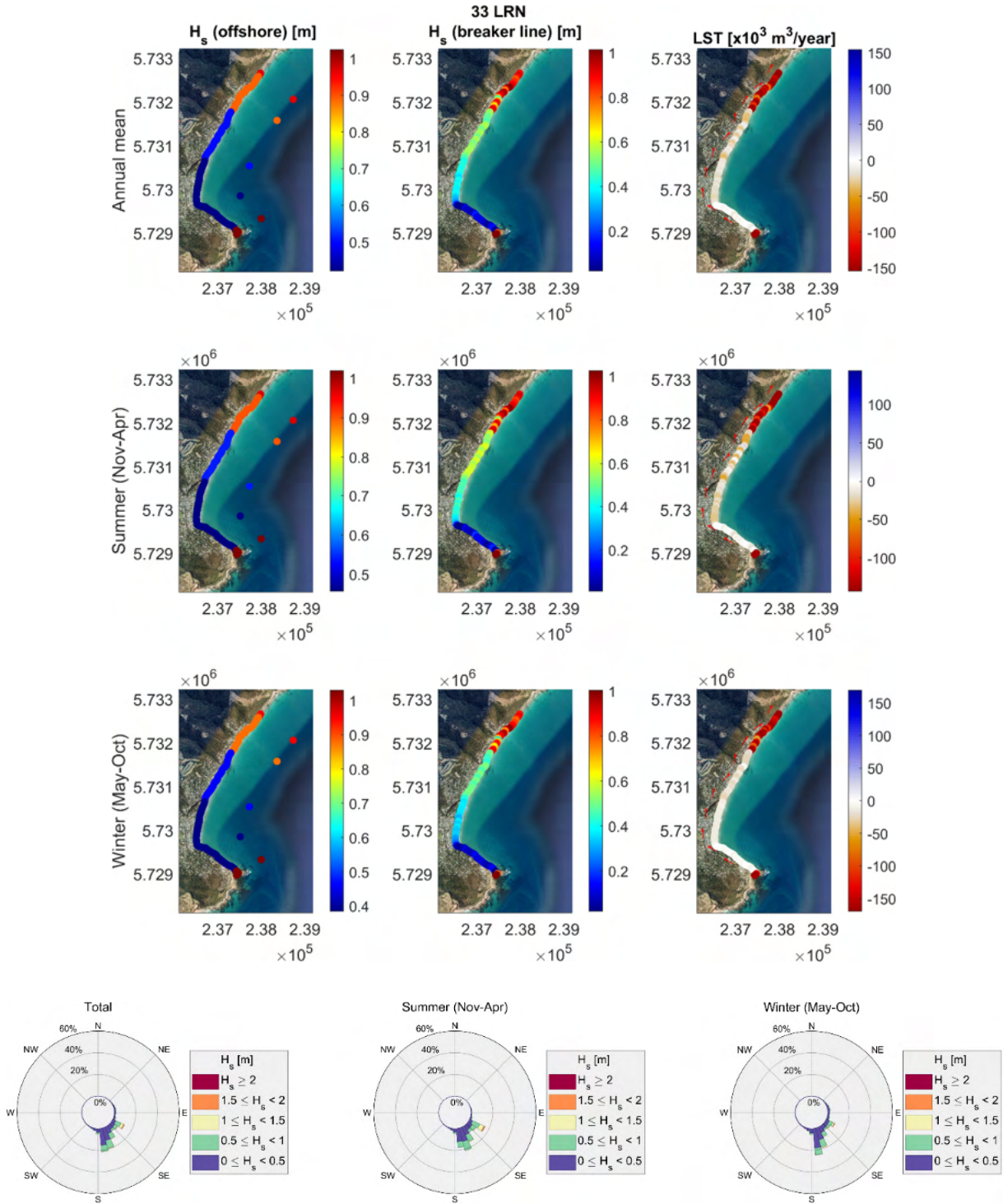
3.32 Point Impossible (IMP)

3.32.1 Model 1 – WW3



3.33 Lorne (LRN)

3.33.1 Model 1 – WW3

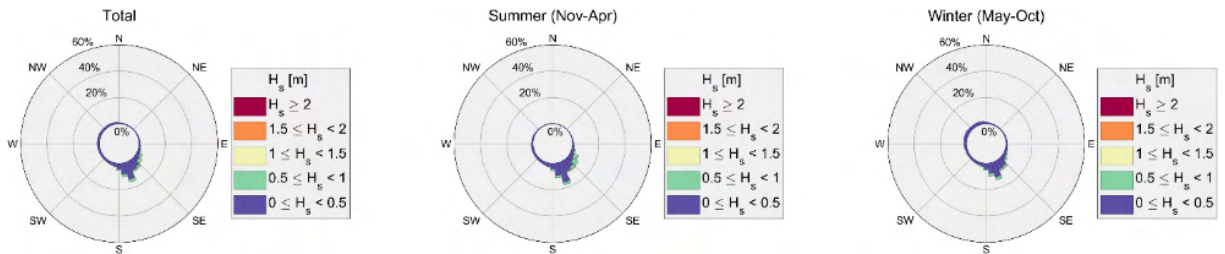
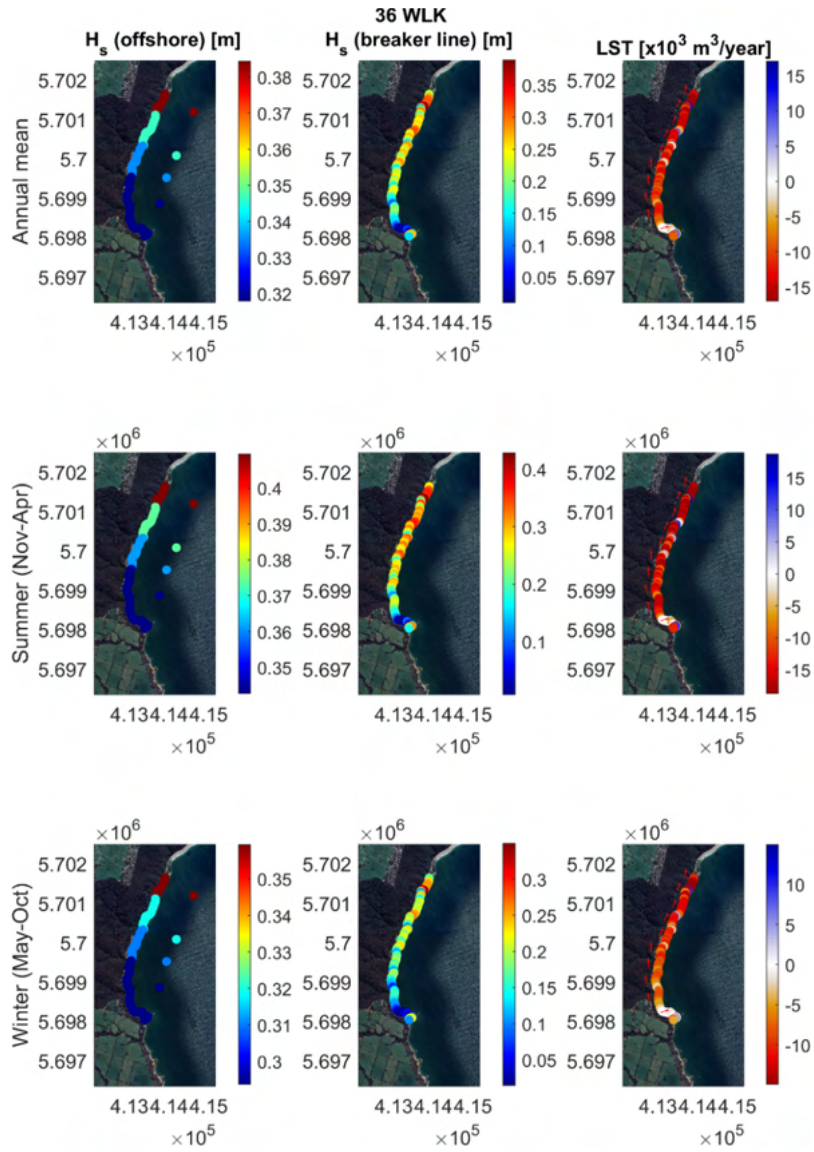


3.34 Bells Beach (LRN)

3.35 Point Addis (ADD)

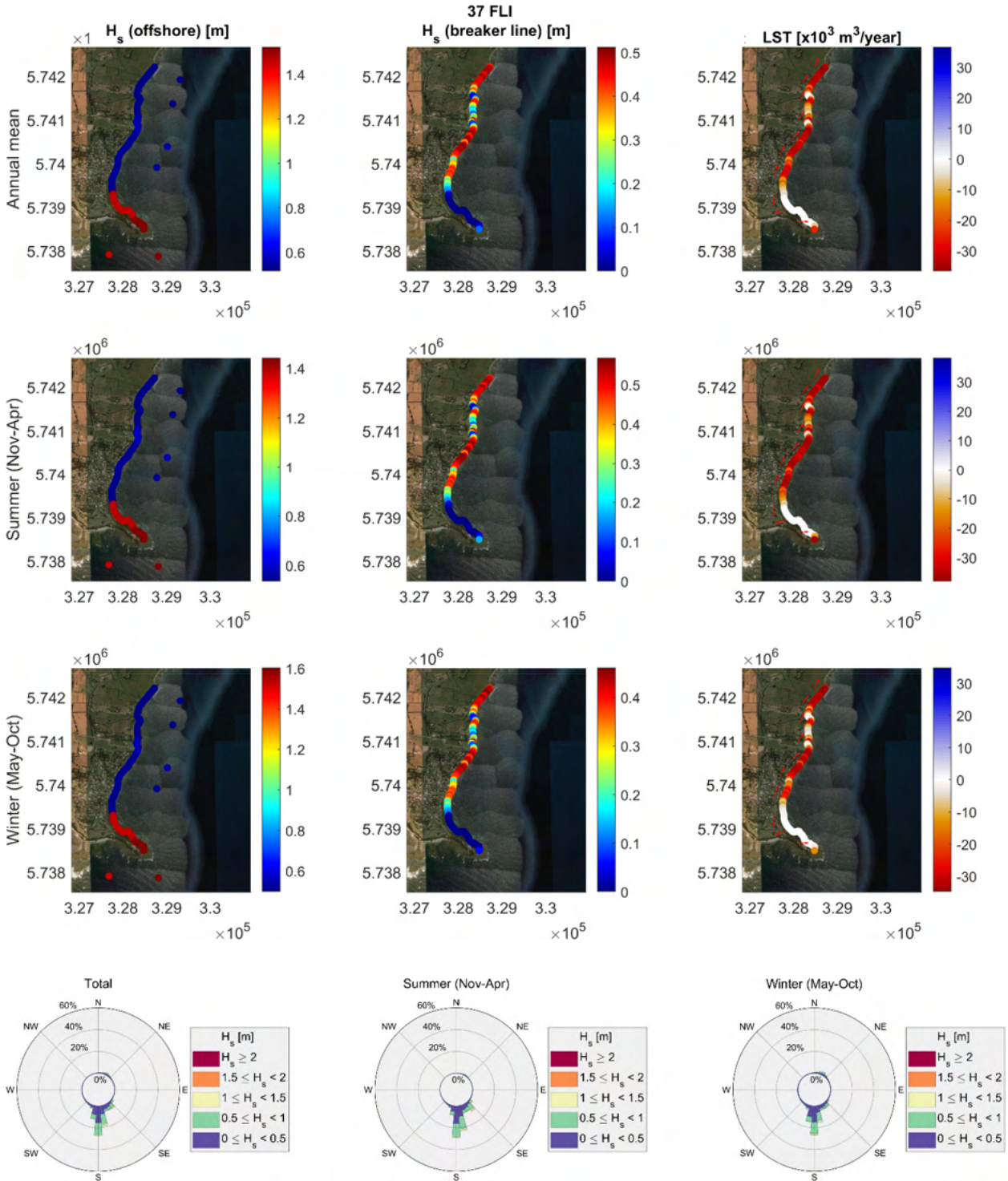
3.36 Walkerville (WLK)

3.36.1 Model 1 – WW3



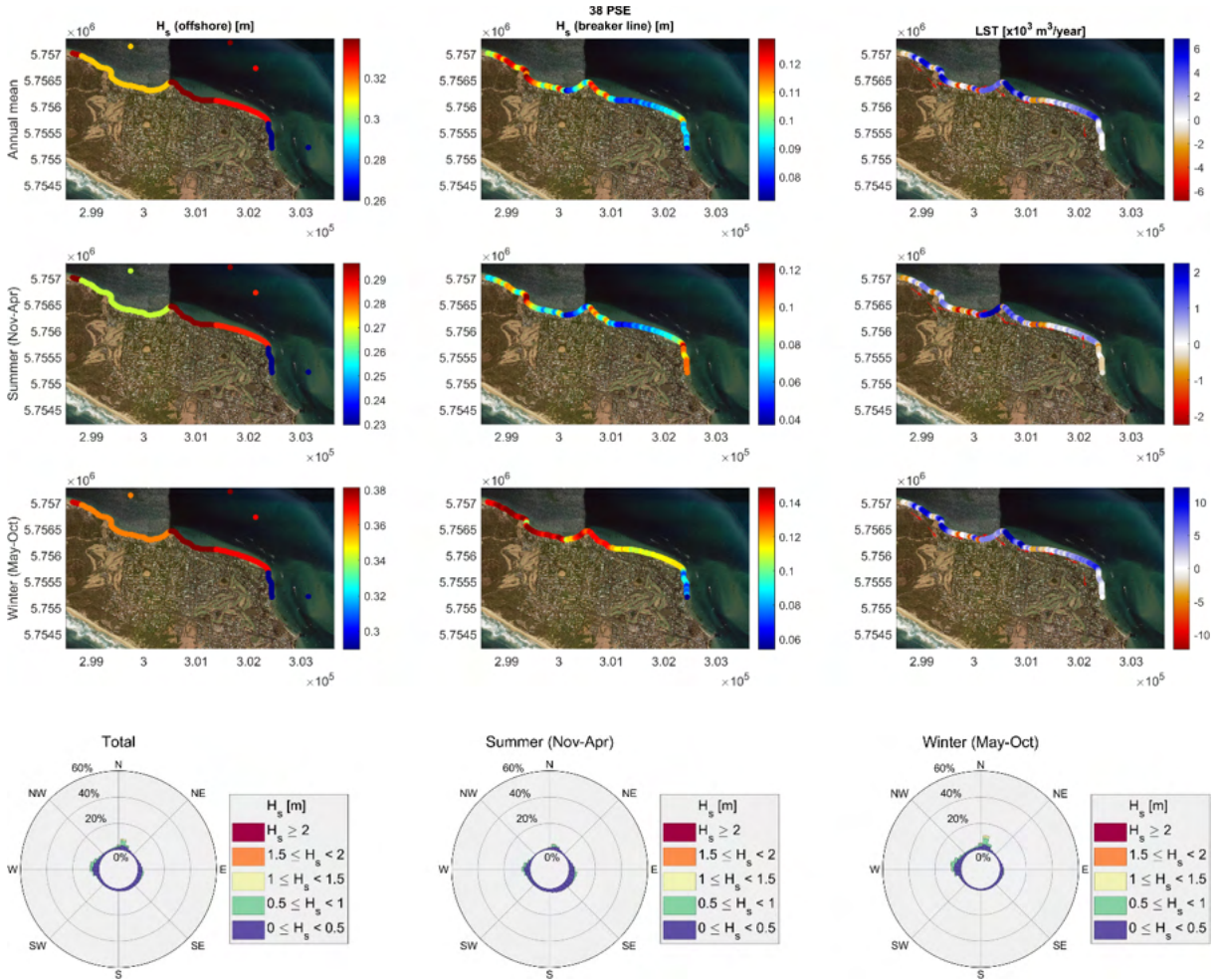
3.37 Flinders (FLI)

3.37.1 Model 1 – WW3

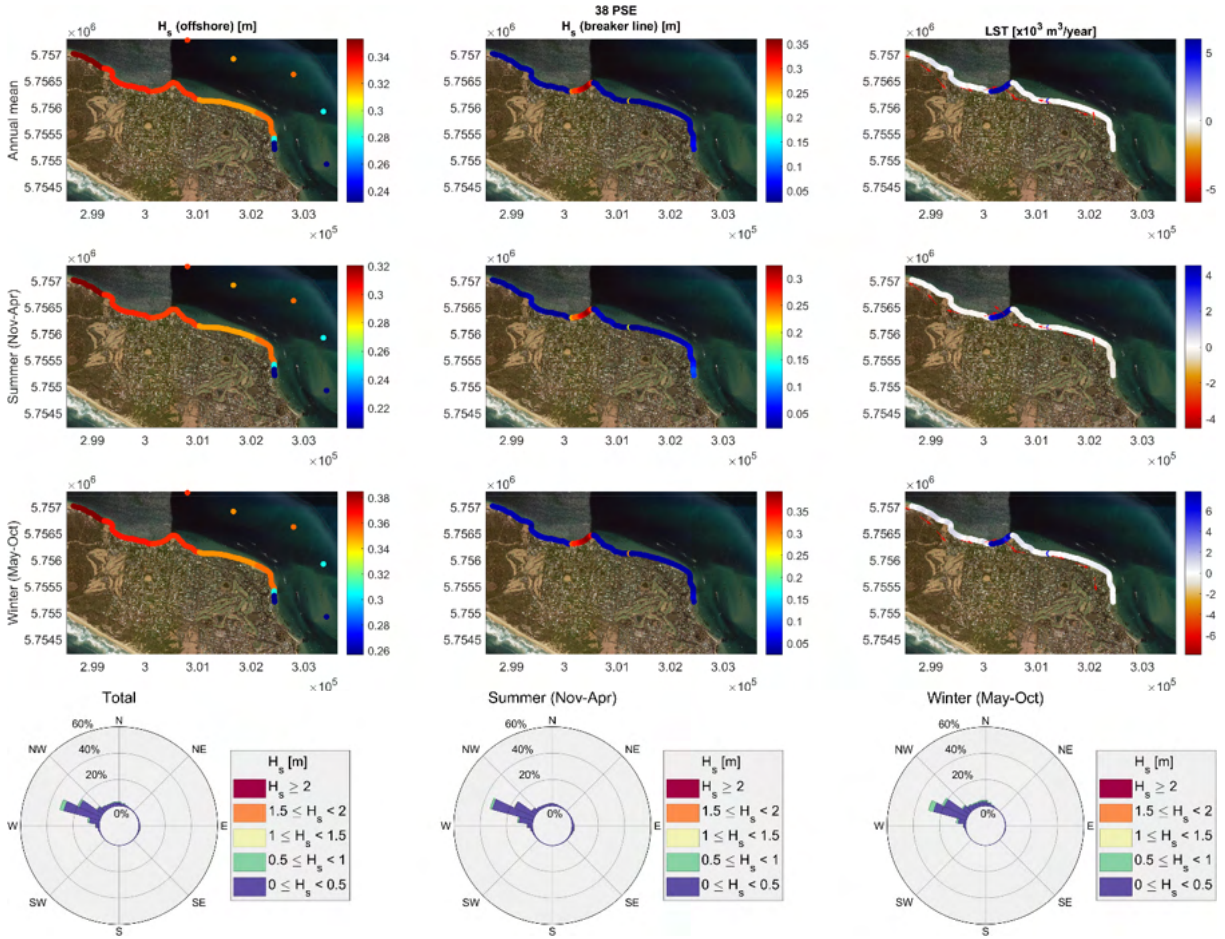


3.38 Portsea (PSE)

3.38.1 Model 1 – WW3

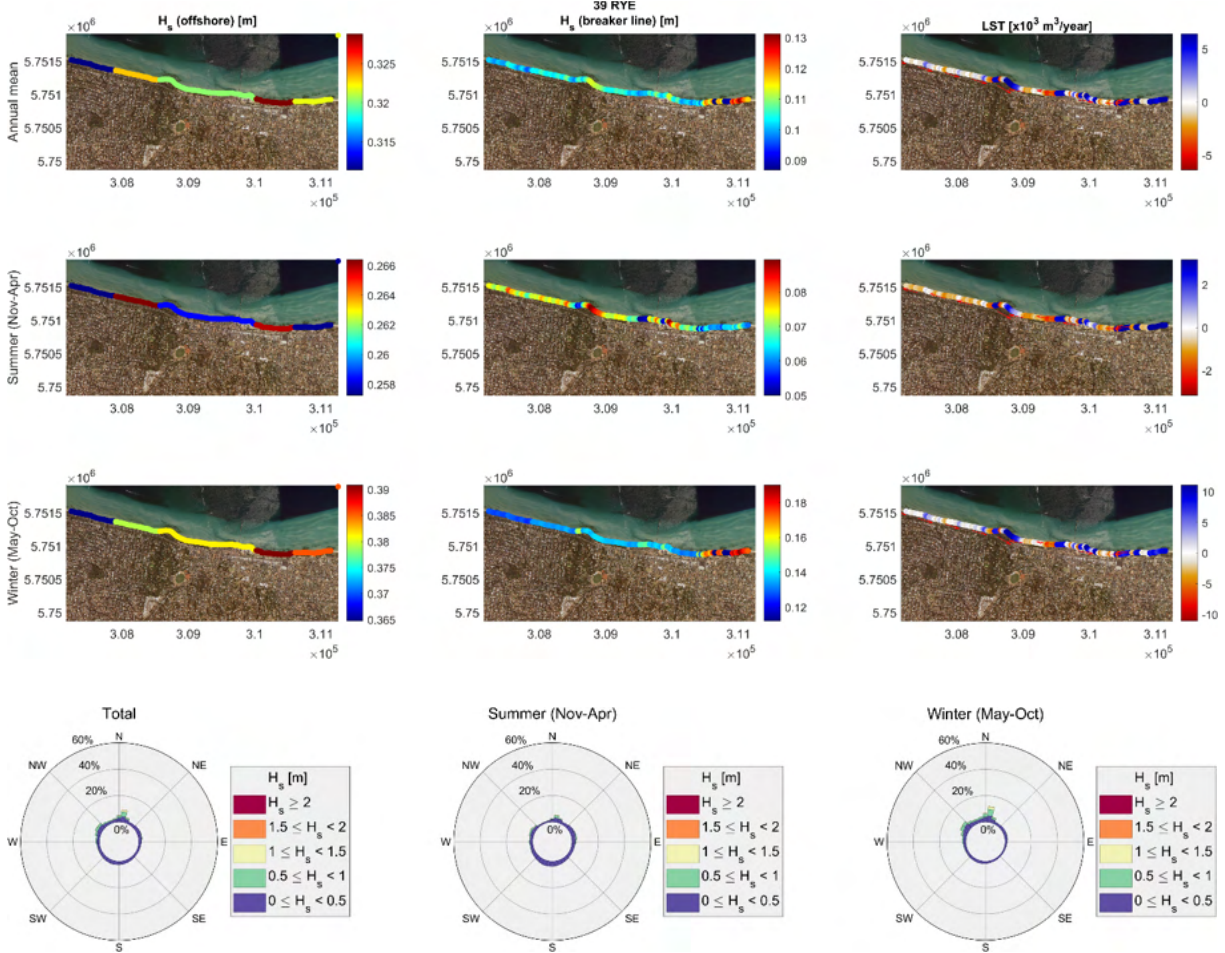


3.38.2 Model 2 – SCHISM-WWMIII

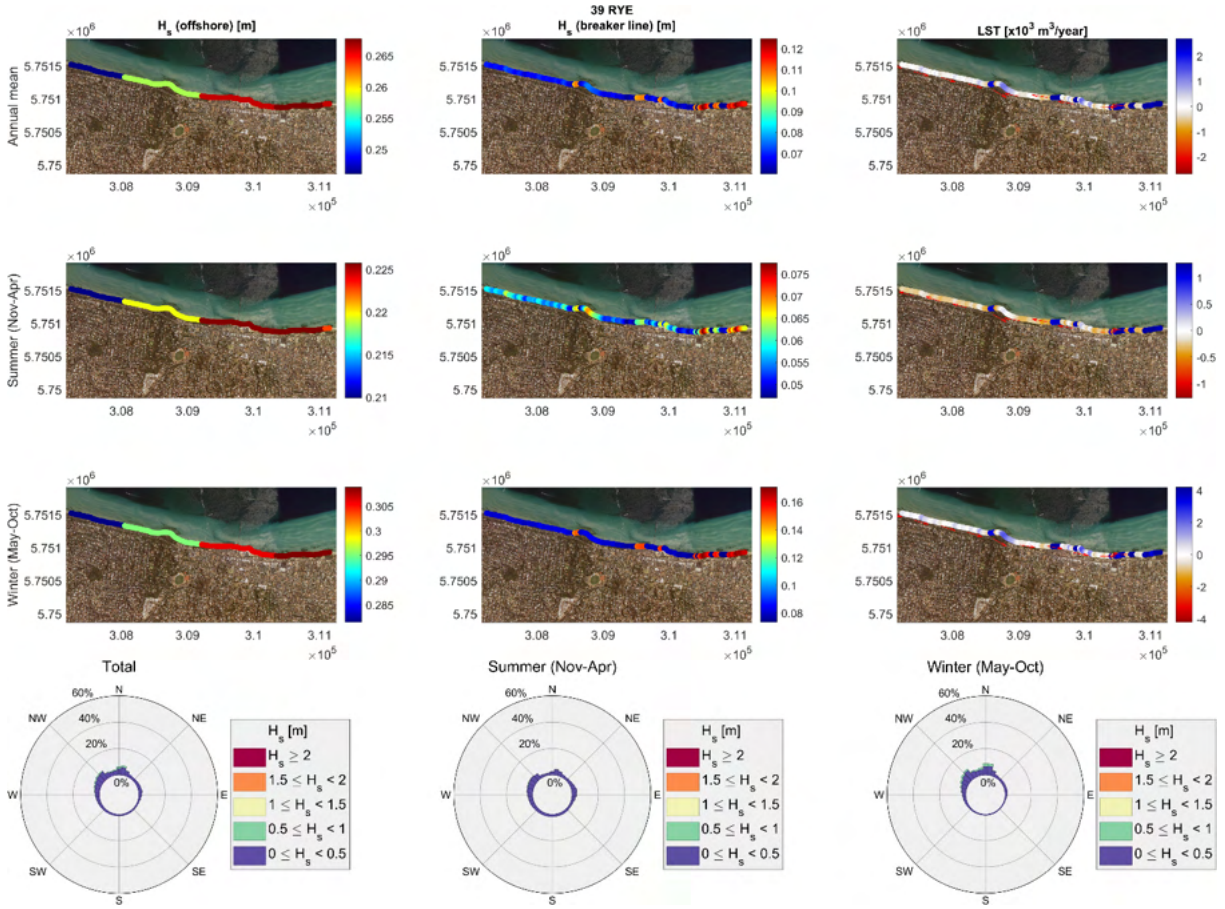


3.39 Rye (RYE)

3.39.1 Model 1 – WW3

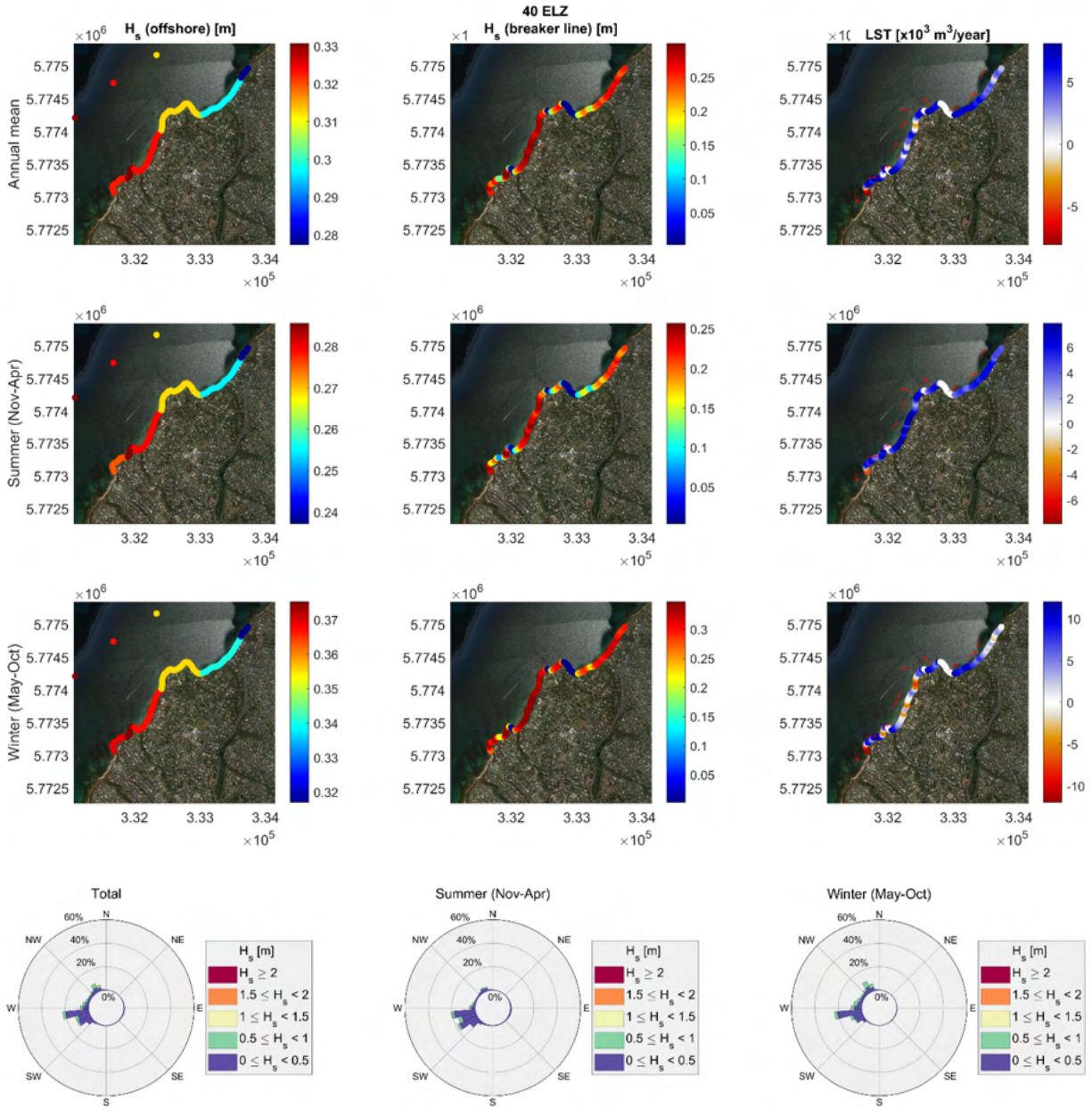


3.39.2 Model 2 – SCHISM-WWMIII

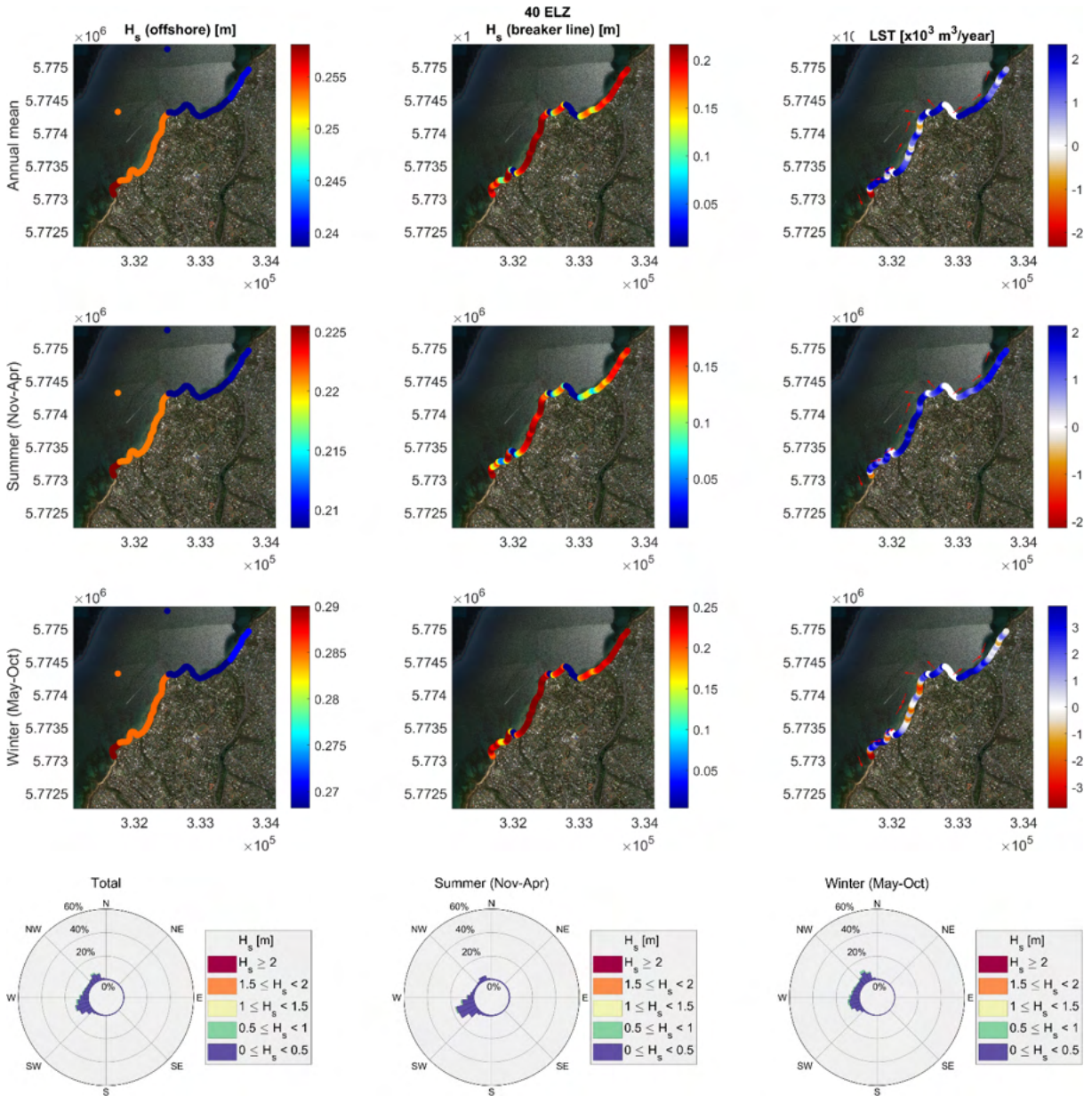


3.40 Mount Eliza (ELZ)

3.40.1 Model 1 – WW3



3.40.2 Model 2 – SCHISM-WWMIII



4 Longshore sediment transport across the Victorian coast

The longshore sediment transport across the Victorian coast and Port Phillip Bay have also been evaluated following the approach in Section 2. Figure 4.1 and Figure 4.2 show the wave conditions and LST across the Victorian coast and Phillip Bay, respectively. The results indicate powerful ocean waves approaching the western Victorian coast and inducing robust longshore sediment transport. The semi-closed Port Phillip Bay and well-protected eastern Victorian coast, however, show relatively small amplitudes in H_s and longshore sediment transport.

Seasonal values of wave conditions at 1 km offshore and the breaker line are indicated in Figures 4.1 and 4.2. The results are consistent with the facts of energetic waves in winter and relatively calm wave conditions in summer (Liu et al., 2022a).

4.1 Model 1 - WW3 (full Victoria extent)

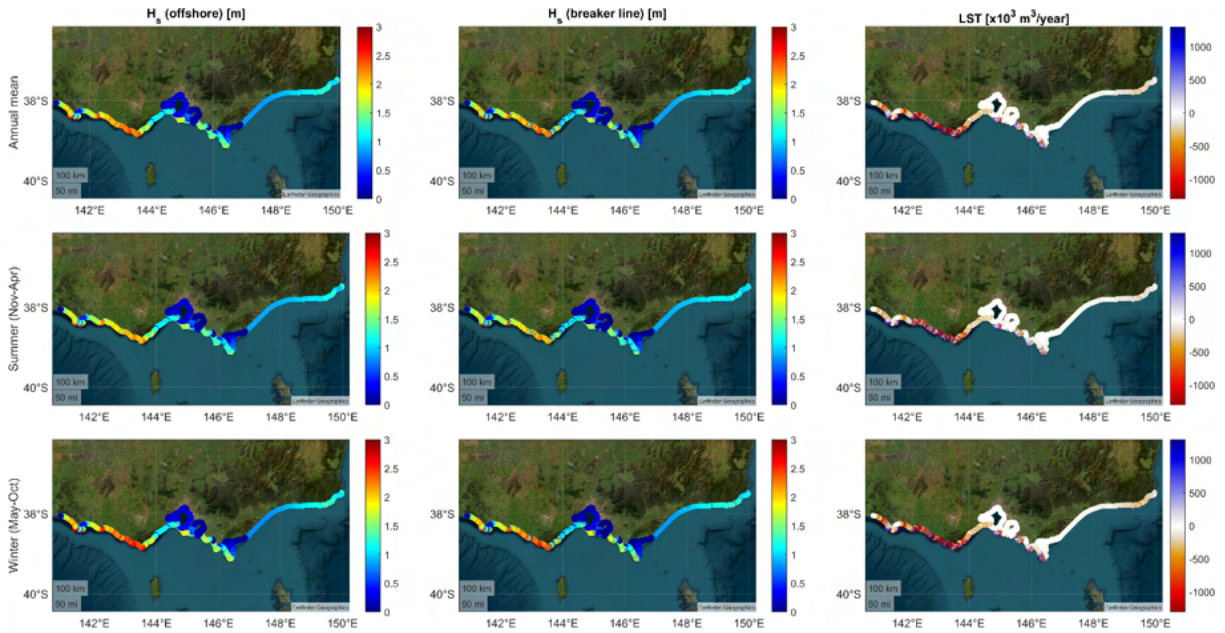


Figure 4.1: WW3-based annual mean and seasonal values of 1 km offshore H_s (left column), H_s at the breaker line (middle column) and longshore sediment transport based on the Van Rijn (2014) approach (right column) over the period 1981-2020 across the Victorian coast.

4.2 Model 2 - SCHISM-WWMIII (full Port Phillip Bay extent)

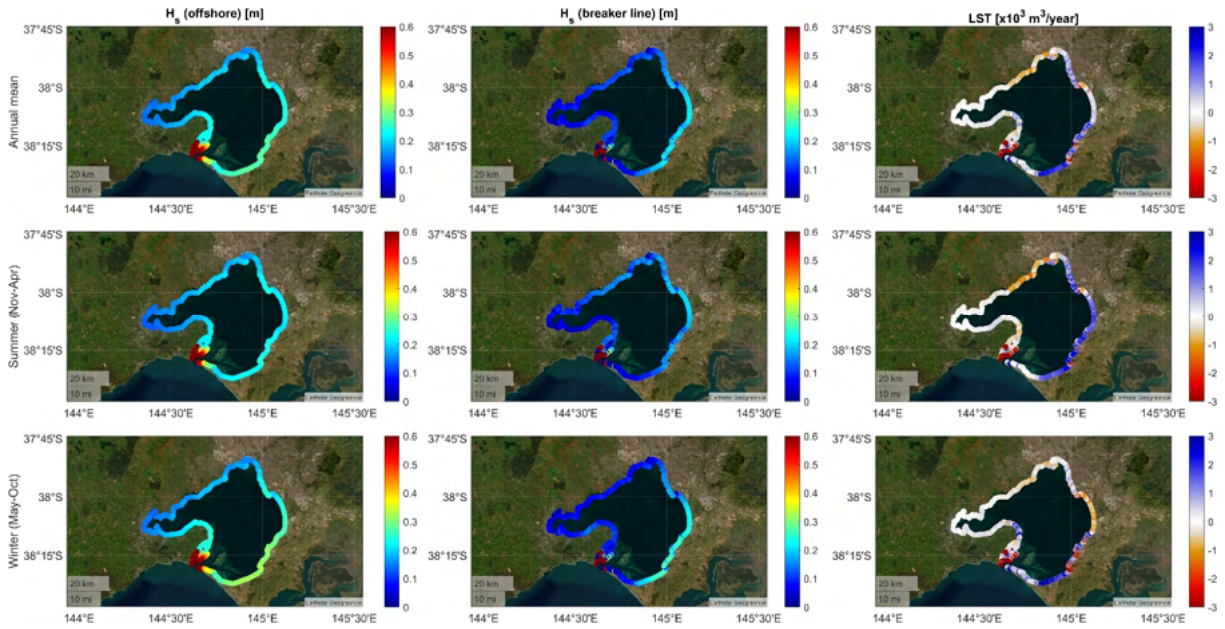


Figure 4.2: Same as Figure 4.1 but for Port Phillip Bay (SCHISM-WWMIII).

5 Data outputs, variables and access to data

We have generated the longshore sediment transport-related parameters at VCMP sites and the whole Victorian coast/Port Phillip Bay, i.e., offshore and breaking wave conditions and longshore sediment transport based on CERC and Van Rijn (2014) approaches. The properties of the variables are shown in Table 5.1. The metadata is available by contacting vcmp@delwp.vic.gov.au.

Table 5.1: available variables. WM=wave model (WW3 or SCHISM-WWMIII), LST=longshore sediment transport.

	Symbols	Variables
WM (1km offshore)	wm.lon	longitude
	wm.lat	latitude
	wm.x	x
	wm.y	y
	wm.dir	mean wave direction
	wm.wia	wave incidence angle
	wm.time	time stamp
	wm.hs_mean	annual mean significant wave height
	wm.wia_mean	annual mean wave incidence angle
	wm.depth	water depth
	wm.hs_s	seasonal significant wave height (autumn, winter, spring, summer)
	wm.wia_s	seasonal wave incidence angle
Breaker line	br.lon	longitude
	br.lat	latitude
	br.x	x
	br.y	y
	br.uid	universal identifier
	br.hs	significant wave height
	br.wia	wave incidence angle
	br.hs_mean	annual mean significant wave height
	br.dir	shoreline (omniline) direction
	br.wia_mean	annual mean wave incidence angle
	br.depth_mean	annual mean water depth
	br.hs_s	seasonal significant wave height
	br.wia_s	seasonal wave incidence angle
	br.depth_s	seasonal water depth
LST	lst.rijn	LST (Rijn 2014)
	lst.cerc	mean LST (CERC 1984)
	lst.rijn_mean	annual mean LST (Rijn 2014)

	lst.cerc_mean	annual mean LST (CERC 1984)
	lst.rijn_s	seasonal LST (Rijn 2014)
	lsr.cerc_s	seasonal mean LST (CERC 1984)

6 Conclusions

In this study, we estimated the longshore sediment transports at VCMP sites and the whole Victorian coast based on the offshore and breaking wave conditions. This study fills the knowledge gap in the field of the longshore transport of Victoria/Port Phillip Bay. The key findings are indicated below.

- The breaking H_s and longshore sediment transports behind the capes are generally reduced quickly.
- Western Victoria and Great Ocean Road are receiving long-period energetic Southern Ocean swell, which introduces big amplitudes of H_s and longshore sediment transports.
- The seasonal longshore sediment transports of Apollo Bay are always towards the east, which didn't capture the feature of beach rotation in this region. This is presumably caused by the identical seasonal mean wave direction simulated by the model, the limitation of the model resolution, etc.
- The offshore and breaking H_s and longshore sediment transport in eastern Victoria are smaller than in western Victoria and Great Ocean Road due to the sheltering effects of Tasmania and King Island. Longshore sediment transport of eastern Victoria shows large seasonality due to the changes of seasonal wave directions.
- Port Phillip Bay is a semi-closed region. Offshore and breaking H_s at Port Phillip Bay is generally below 0.5 m, which caused much smaller longshore sediment transports than in western Victoria.
- The beach rotation that occurred at Patterson River of eastern Port Phillip Bay is mainly caused by the seasonal changes in mean wave direction. Thus, annual mean longshore transport in this region shows a relatively small amplitude due to the compensation effects of seasonal changes.

References

- Bayram, A., Larson, M., & Hanson, H. (2007), A new formula for the total longshore sediment transport rate. *Coastal Engineering*, 54(9), 700-710. <https://doi.org/10.1016/j.coastaleng.2007.04.001>.
- BMT (2022), Apollo Bay Coastal processes study - stage 1 Rep.
- Bosboom, J., & Stive, M. J. (2021), Coastal dynamics.
- Liu, J., Meucci, A., Liu, Q., Babanin, A. V., Ierodiaconou, D., Xu, X., & Young, I. R. (2023a), A high-resolution wave energy assessment of south-east Australia based on a 40-year hindcast. *Renewable Energy*, 215, 118943. <https://doi.org/10.1016/j.renene.2023.118943>.
- Liu, J., Meucci, A., Liu, Q., Babanin, A. V., Ierodiaconou, D., & Young, I. R. (2022a), The wave climate of Bass Strait and south-east Australia. *Ocean Modelling*, 172, 101980. <https://doi.org/10.1016/j.ocemod.2022.101980>.
- Liu, J., Meucci, A., & Young, I. R. (2022b), Projected wave climate of Bass Strait and south-east Australia by the end of the twenty-first century. *Climate Dynamics*, 60, 393–407. <https://doi.org/10.1007/s00382-022-06310-4>.
- Liu, J., Meucci, A., & Young, I. R. (2023b), Projected 21st century wind-wave climate of Bass Strait and south-east Australia: Comparison of EC-Earth3 and ACCESS-CM2 climate model forcing. *Journal of Geophysical Research: Oceans*, 128(4), e2022JC018996. <https://doi.org/10.1029/2022JC018996>.
- Liu, Q., Babanin, A. V., Rogers, W. E., Zieger, S., Young, I. R., Bidlot, J.-R., et al. (2021), Global wave hindcasts using the observation-based source terms: Description and validation. *Journal of Advances in Modeling Earth Systems*, 13(8). <https://doi.org/10.1029/2021MS002493>.
- McCarroll, R., Masselink, G., Wiggins, M., Scott, T., Billson, O., Conley, D., & Valiente, N. (2019), High-efficiency gravel longshore sediment transport and headland bypassing over an extreme wave event. *Earth Surface Processes and Landforms*, 44(13), 2720-2727. <https://doi.org/10.1002/esp.4692>.
- O'Grady, J., Babanin, A., & McInnes, K. (2019), Downscaling future longshore sediment transport in south eastern Australia. *Journal of Marine Science and Engineering*, 7(9), 289. <https://doi.org/10.3390/jmse7090289>.
- Shore Protection Manual (1984), CERC, Waterways Experiment Station, Vicksburg, USA.
- Smith, E. R., Wang, P., Ebersole, B. A., & Zhang, J. (2009), Dependence of total longshore sediment transport rates on incident wave parameters and breaker type. *Journal of Coastal Research*, 25(3), 675-683. <https://doi.org/10.2112/07-0919.1>.
- Tran, H. Q., Provis, D., & Babanin, A. V. (2021), Hydrodynamic climate of Port Phillip Bay. *Journal of Marine Science and Engineering*, 9(8), 898. <https://doi.org/10.3390/jmse9080898>.
- Van Rijn, L. C. (2014), A simple general expression for longshore transport of sand, gravel and shingle. *Coastal Engineering*, 90, 23-39. <https://doi.org/10.1016/j.coastaleng.2014.04.008>.

